Bivariate Gaussian random fields: models, simulation, and inference

Inauguraldissertation zur Erlangung des akademischen Grades eines Doktors der Naturwissenschaften der Universität Mannheim

vorgelegt von

Olga Moreva
aus Moskau, Russland

Mannheim, 2018

Dekan: Dr. Bernd Lübcke, Universität Mannheim
Referent: Prof. Dr. Martin Schlather, Universität Mannheim
Korreferent: Prof. Dr. Tilmann Gneiting, Karlsruher Institut für Technologie

Tag der mündlichen Prüfung: 22. Juni 2018

Abstract

Spatial data with several components, such as observations of air temperature and pressure in a certain geographical region or the content of two metals in a geological deposit, require models which can capture the spatial dependence structure of individual components and the relationship between them. In a wealth of applications, multivariate Gaussian random fields are sensible models for multivariate spatial data and their second order structure specifies the marginal correlations and the cross-correlations between the components. In this thesis we focus on covariance models and simulation techniques for bivariate fields.

In Chapter 2 we summarize some definitions and facts from univariate and multivariate Geostatistics which are essential for the subsequent chapters.

Chapter 3 introduces two novel bivariate parametric covariance models, the powered exponential (or stable) covariance model and the generalized Cauchy covariance model. Both models allow for flexible smoothness, variance, scale, and cross-correlation parameters. The smoothness parameter is in $(0, 1]$. Additionally, the bivariate generalized Cauchy model allows for distinct long range parameters. The results are based on general sufficient conditions for the positive definiteness of 2×2-matrix valued functions. These conditions are easy to check, since they require only computing the derivatives of a bivariate covariance function and calculating an infimum of a function of one variable. We also show that the univariate spherical model can be generalized to the bivariate case with spherical marginal and cross-covariance functions only in a trivial way.

Circulant embedding is a powerful algorithm for fast simulation of stationary Gaussian random fields on a rectangular grid in $\mathbb{R}^n$, which works perfectly for compactly supported covariance functions. Cut-off circulant embedding techniques have been developed for univariate random fields for dimensions up to $\mathbb{R}^3$ and rely on the modification of a covariance function outside the simulation window, such that the modified covariance function is compactly supported. In Chapter 4 we propose extensions of the cut-off approach for bivariate Gaussian random fields. In particular, we provide a method for simulating bivariate fields with a bivariate powered exponential covariance model and the full bivariate Matérn covariance model for certain sets of parameters. On the way we extend the cut-off circulant embedding method even for univariate models.

In Chapter 5 we illustrate the use of the bivariate powered exponential model for a data example.

Zusammenfassung

Räumliche Daten mit mehreren Komponenten, wie Beobachtungen von Lufttemperatur und Atmosphärendruck in einer bestimmten geographischen Region oder der Gehalt von zwei Metallen in einer geologischen Lagerstätte, erfordern Modelle, die die räumliche Abhängigkeitsstruktur einzelner Komponenten und die Beziehungen zwischen ihnen erfassen. In einer Vielzahl von Anwendungen sind multivariate Gauß'sche Zufallsfelder sinnvolle Modelle für multivariate räumliche Daten und ihre Struktur zweiter Ordnung spezifiziert die marginalen Korrelationen und die Kreuzkorrelationen zwischen den Komponenten. Diese Arbeit konzentriert sich auf Kovarianzmodelle und Simulationstechniken für bivariate Felder.

Kapitel 2 fasst einige Definitionen und Fakten der univariaten und der multivariaten Geostatistik zusammen, die grundlegend für die folgenden Kapitel sind.

Kapitel 3 stellt zwei neuartige bivariate parametrische Kovarianzmodelle vor, das potenzexponentielle (oder stabile) Kovarianzmodell und das verallgemeinerte Cauchy-Kovarianzmodell. Beide Modelle ermöglichen flexible Glättungs-, Varianz-, Skalierungs- und Kreuzkorrelationsparameter. Der Glättungsparameter ist in $(0, 1]$. Zusätzlich erlaubt das bivariate verallgemeinerte Cauchy-Modell verschiedene Langzeitparameter. Die Ergebnisse basieren auf hinreichenden Bedingungen für die positiv Definitheit von 2×2-Matrix-wertigen Funktionen. Diese Bedingungen sind einfach zu überprüfen, da nur die Ableitungen einer bivariaten Kovarianzfunktion berechnet werden müssen, und das Infimum einer Funktion von einer Variablen zu bestimmen ist. Zudem wird gezeigt, dass das univariate sphärische Modell nur auf triviale Weise auf den bivariaten Fall mit sphärischen marginalen und Kreuzkovarianzfunktionen verallgemeinert werden kann.

Circulant Embedding ist ein leistungsfähiger Algorithmus zur schnellen Simulation von stationären Gauß'schen Zufallsfeldern auf einem rechteckigen Gitter in $\mathbb{R}^n$, der perfekt für Kovarianzfunktionen mit kompaktem Träger funktioniert. Cut-off circulant Embedding Techniken wurden für univariate Zufallsfelder für Dimensionen bis zu $\mathbb{R}^3$ entwickelt und basieren auf der Modifikation einer Kovarianzfunktion außerhalb des Simulationsfensters, sodass die modifizierte Kovarianzfunktion einen kompakten Träger hat. In Kapitel 4 werden Erweiterungen des Cut-off-Ansatzes für bivariate Gauß'sche Zufallsfelder vorgeschlagt. Insbesondere wird eine Methode zur Simulation von bivariaten Feldern mit einem bivariaten exponentiellen Kovarianzmodell und dem vollständigen bivariaten Matérn-Kovarianzmodell für bestimmte Parametersätze bereitgestellt. Dabei wird die Cut-off circulant Embedding-Methode auch für univariate Modelle erweitert.

Kapitel 5 illustriert die Verwendung des bivariaten potenzexponentiellen Modells anhand eines Datenbeispiels.

Acknowledgements

I am indebted to my advisor Prof. Dr. Martin Schlather, whose solid support and guidance made my thesis work possible. I owe a lot of gratitude to him for always being there for me and I really appreciate his willingness to meet me at short notice even in busy times. His ability to explain difficult things clearly helped me many times to establish the direction of my research. I would like to thank Prof. Dr. Tilmann Gneiting for being a great second dissertation advisor. I am especially grateful for his valuable and extremely prompt feedback on my papers. Workshops in HITS organized by Prof. Dr. Tilmann Gneiting broadened my mathematical horizon and provided inspiration for my research. I also thank Prof. Dr. Sebastian Engelke for orginizing my stay at École Polytechnique Fédérale de Lausanne in the end of 2016.

I am grateful to all my colleagues for many interesting discussions during seminars and workshops at the RTG 1953. My special thank goes to Elias Stehle, Alexander Kalinin and Artem Makarov for their help during my first months in Mannheim. I would like to express my sincere gratitude to Dr. Kirstin Strokorb, Dr. Eva Lübcke and Stefan Schnabel for their extensive support. Many thanks to Lena Reichmann for cheerful conversations and pleasant lunch times. I am immensely grateful to Dr. Martin Dirrler for the attentive proofreading of my thesis, his useful comments, and the constant encouragement.

Financial support by the Deutsche Forschungsgemeinschaft (DFG) through the Research Training Group RTG 1953 'Statistical Modeling of Complex Systems and Processes' and by Mannheim University through the dissertation completion grant is also gratefully acknowledged.

Finally, I have no words to express my gratitude to my family and my boyfriend Nikolaj for their continuous support, unconditional love and unshakable faith in me.

Contents

1 Introduction

Multivariate data measured in space arise in a variety of disciplines including soil science (Lark and Papritz, 2003), ecology (Pelletier et al., 2009), mining (Zawadzki et al., 2013), geology (Mery et al., 2017) and meteorology (Hewer et al., 2017). Air temperature and pressure in a certain geographical region or the content of two metals in a geological deposit are the examples of spatial processes with two components. Spatial dependence within and between the components is exploited in particular when the component of interest is not exhaustively sampled, whereas the measurement of other components can be easily carried out, e.g. in soil sciences (Goovaerts (1999) and Atkinson et al. (1992)). An appropriate multivariate spatial covariance model gives more sensible results for spatial interpolation than univariate models, see for example Cressie and Zammit-Mangion (2016). In environmental and climate sciences it is important to model spatial meteorological data jointly in order to reflect spatial dependence within and between components adequately (see the discussions in Feldmann et al. (2015), Berrocal et al. (2007), and Gel et al. (2004)); otherwise the obtained results might be unsound.

Multivariate Gaussian random fields, characterized by their mean and covariance functions, are the basis for modeling spatial data in these areas. Classical textbooks on univariate and multivariate geostatistics include Cressie (1993), Chilès and Delfiner (1999), Lantuejoul (2001), Wackernagel (2003), and Goovaerts and Goovaerts (1997). For simplicity, in the theoretical part of the thesis we consider zero mean random fields. Then a covariance function describes the properties of the corresponding Gaussian random field. Consider, for example, a realization of a Gaussian random field with two components shown in two upper plots in Figure 1.1. This field has the bivariate Matérn covariance model (Gneiting et al., 2010), which is plotted under the realizations. The functions ψ_{11} and ψ_{22}, called marginal covariances, describe the properties of the first and the second field respectively. The behavior of the covariance function at the origin largely reflects the smoothness of the corresponding field (Gneiting, 2002). In the bivariate Matérn model the smoothness of each field is controlled by the corresponding parameter $\nu_{ii} > 0$, $i = 1, 2$. In Figure 1.1, $\nu_{22} > \nu_{11}$ and therefore the realization on the right hand side is smoother than the one on the left hand sight. The scale parameter $s_{ii} > 0$, $i = 1, 2$, controls the decay of the marginal correlation with the distance. For example, the correlation of any two observations of the first field for the larger distance is higher than the correlation of any two observations of the second field, therefore the upper left plot is more colorful than the upper right one. The middle picture in the lower panel of Figure 1.1 is the graph of the cross-covariance function ψ_{12}, which describes the covariance structure between the two components. The scale parameter s_{12} controls the correlation decay between the components. Thus, the correlation between the observation of the first field and the observation of the second field is maximum at zero distance and it decreases as the distance increases. While the maximum of a marginal covariance function is always at the origin, the maximum of the cross-covariance function (assuming positive correlation between a given variable pair) may be shifted away from the origin, which is typical when one component affects another component with some delay (Wackernagel (2003), Hansen (2018)). However, we focus on covariance functions which

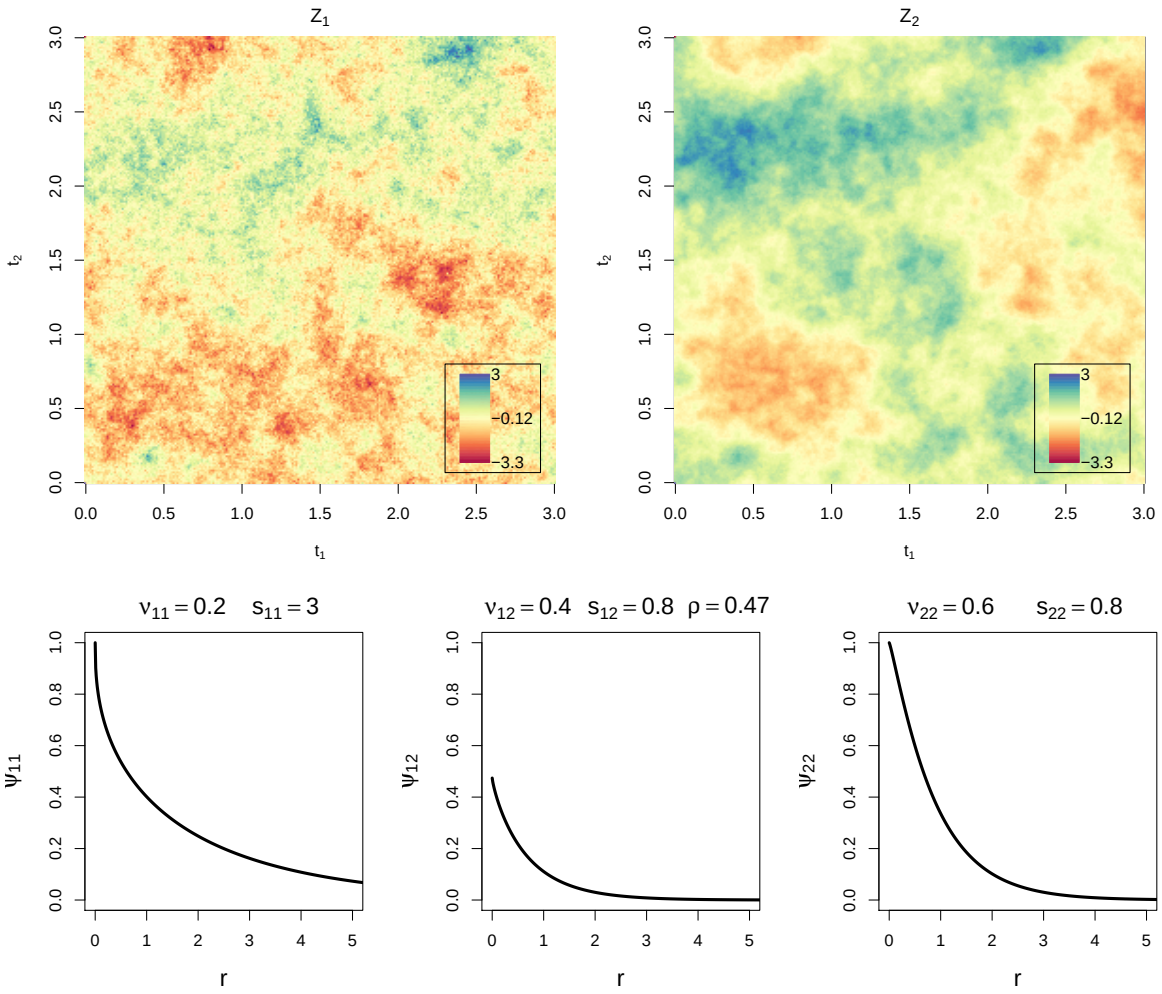

Figure 1.1: A realization of a bivariate Gaussian random field (upper two plots) with the bivariate Matérn covariance model (lower three plots). The stationary and isotropic covariance function depends on the distance r between the locations. The lower left and the right plots show the marginal covariance functions ψ_{11} and ψ_{22}, respectively.

depend only on the distance between observations, i.e. they are invariant with respect to the location of observations and the direction of the separation vector.

A covariance function must guarantee that the variance of an arbitrary linear combination of observations of any involved components, taken at arbitrary spatial locations is nonnegative. In this thesis we concentrate on constructing matrix-valued functions that satisfy this requirement, on simulation techniques which are suitable for these functions and on inference with them. In Chapter 2 we summarize some definitions and facts from univariate and multivariate Geostatistics which are crucial for the subsequent chapters.

A comprehensive overview of recent covariance functions for multivariate geostatistics is found in Genton and Kleiber (2015) and Schlather et al. (2015). Among these models is the linear model of coregionalization (LMC), see Goulard and Voltz (1992) and Wackernagel (2003). Although it is widely used by practitioners, it lacks flexibility, since all direct and cross variograms share the same set of basic structures. This means, in particularly, that the

smoothness of any component is equal to the smoothness of the roughest latent process, and, thus, the standard approach LMC does not admit individually distinct smoothness properties, unless structural zeros are imposed on the latent process coefficients (Gneiting et al. (2010) and Goovaerts and Goovaerts (1997)). Models with compact support are introduced in Du and Ma (2013), Porcu et al. (2013), Daley et al. (2015) and Schlather et al. (2017). Kleiber (2017) studies the properties of multivariate random fields in the frequency domain. Cressie and Zammit-Mangion (2016) develop a conditional approach for constructing multivariate models.

Genton and Kleiber (2015) pose the question how to characterize a parameter set of the valid multivariate powered exponential (or stable) model. In Chapter 3 we give a partial answer to this question, providing sufficient conditions for the positive definiteness of a bivariate model. In a similar way we can also formulate sufficient conditions for the positive definiteness of the bivariate generalized Cauchy model. These models are flexible, intuitive and easily interpretable: in both models three parameters characterize the smoothness of the covariances of process components and the cross-covariance. Further three parameters model the long-range behaviour in the bivariate Cauchy model. The smoothness parameters of marginal covariances in both models are restricted to values in $(0, 1]$. The results are based on general sufficient conditions for the positive definiteness of a 2×2-matrix valued functions. These conditions require only computing the derivatives of a bivariate covariance function of order two and three in $\mathbb{R}$ and in $\mathbb{R}^3$, respectively, and calculating an infimum of a function of one variable. We also show that the univariate spherical model can be generalized to the bivariate case with spherical marginal and cross-covariance functions only in a trivial way. We collect some new bivariate models, whose construction follows directly from Schoenberg's theorem.

Development of many multivariate covariance models led to the increasing interest in simulation algorithms. Cholesky decomposition is not suitable for samples with a larger number of locations, not least because the computing time of the algorithm is cubic in the number of variables. For functions possessing spectral densities with closed formulae, the spectral turning bands algorithm can be used (Arroyo and Emery (2017) and Emery et al. (2016)). The multivariate turning bands method is implemented in the R package **RandomFields** (Schlather et al., 2017). Both turning bands methods are faster than the Cholesky decomposition and can be performed for any configuration of the target locations, but they produce realizations that are only approximately Gaussian. Under certain conditions on a covariance function the multivariate version of the circulant embedding algorithm, presented in Chan and Wood (1999) and explained in detail in Helgason et al. (2011), produces Gaussian realizations. However, similarly to the univariate case, for many multivariate covariance models that do not have compact support exact simulation is not possible. Cut-off circulant embedding techniques have been developed for univariate random fields for dimensions up to $\mathbb{R}^3$ and rely on the modification of a covariance function outside the simulation window, such that the modified covariance function is compactly supported. In Chapter 4 we propose extensions of the cut-off approach for univariate and bivariate Gaussian random fields. In particular, we provide a method for simulating bivariate fields with a bivariate powered exponential covariance model and the full bivariate Matérn covariance model for certain sets of parameters on a grid.

In Chapter 5 we illustrate the use of the bivariate exponential model for a data example on the content of copper and zinc in the top soil of a 14 km^2 region in Swiss Jura. We compare the performance of bivariate powered exponential model to the traditional linear model of coregionalization and the bivariate Matérn model.

2 Preliminaries

We briefly summarize some basic definitions and facts about covariance functions and variograms of univariate and multivariate Gaussian random fields, which are necessary in the subsequent parts.

There is sometimes a confusion between the notions *multidimensional* and *multivariate* in the literature. Hereinafter we call a random field Z *univariate* if it has only one component, and *multivariate* if it has $m \geq 1$ components, i.e. $Z(x) = (Z_1(x), \ldots, Z_m(x))$, $x \in \mathbb{R}^n$. In Chapters 3 and 4 we will be concerned with *bivariate* fields, i.e. $m = 2$. The term *multidimensional* refers to the index set of Z, i.e. to the dimension of x. For example, a one dimensional univariate field is just a temporal stochastic process, a two dimensional univariate field is a 'classical' random field and a three dimensional bivariate field $Z(x) = (Z_1(x), Z_2(x))$ has two components with $x \in \mathbb{R}^3$.

The finite dimensional distributions of a multivariate Gaussian random field $Z(x)$ are multivariate normal and thus the distribution of the field is uniquely characterized by its mean and covariance function. For simplicity, we assume in the theoretical part of the thesis that the random field is centered, i.e. $\mathbb{E}Z(x) = 0$ for all $x \in \mathbb{R}^n$. We denote the covariance function by $C(x, y) = \mathrm{Cov}(Z(x), Z(y))$, $x, y \in \mathbb{R}^n$. Clearly, a covariance function C of a multivariate field is a matrix-valued function, whose diagonal elements $C_{ii}(x, y)$, $i = 1, \ldots, m$, are the marginal covariance functions and the off-diagonal elements $C_{ij}(x, y)$ are the cross-covariance functions of the components of the process $1 \leq i \neq j \leq m$. The content of the next two sections is based mostly on Wackernagel (2003), Chilès and Delfiner (1999) and Yaglom (1987).

2.1 Multivariate covariance functions

A covariance function C is called *stationary* if for any $x, h \in \mathbb{R}^n$ and $i, j = 1, \ldots, m$ it holds:

$$C_{ij}(x + h, x) = C_{ij}(h, 0) =: C_{ij}(h).$$

A stationary multivariate covariance function is not necessarily an even or odd function. In general, we have

$$C_{ij}(-h) \neq C_{ij}(h),$$

but

$$C_{ij}(h) = C_{ji}(-h).$$

C is *stationary and isotropic* if additionally $C(h_1) = C(h_2)$ whenever $\|h_1\| = \|h_2\|$, i.e. marginal covariance functions and cross-covariance functions depend only on the distance between the variables locations. Hereinafter we write $C(r)$ instead of $C(h)$ with $r = \|h\|$, whenever C is stationary and isotropic.

We denote by Φ_n the set of continuous functions $\varphi : [0, \infty) \mapsto \mathbb{R}$ such that the map $(x, y) \mapsto \varphi(||x - y||)$ is positive definite on $\mathbb{R}^n$. Analogously, Φ_n^m denotes the class of mappings $\varphi = [\varphi_{ij}(\cdot)]_{i,j=1}^m : [0, \infty) \mapsto \mathbb{R}^{m \times m}$ with each φ_{ij} being continuous, such that

$$C(x, y) = [\varphi_{ij}(||x - y||)]_{i,j=1}^m, \qquad x, y \in \mathbb{R}^n,$$

is an $m \times m$ matrix-valued covariance function on $\mathbb{R}^n$.

We recall that a covariance function must be *positive definite*, i.e. it guarantees that the variance of an arbitrary linear combination of observations of any involved components $Z_i(x)$, $i = 1, \dots, m$, taken at arbitrary spatial locations is nonnegative. That is, C is symmetric and for any $p \in \mathbb{N}$, $a_1, \dots, a_p \in \mathbb{R}^m$, and $x_1, \dots, x_p \in \mathbb{R}^n$ it must hold

$$\sum_{i=1}^{p} a_i^T C(x_i - x_j) a_j \geq 0.$$

Reversely, for each positive definite function C there exists a Gaussian random field with C being its covariance function. Thus, the terms covariance function and positive definite function are interchangeable.

Example 2.1 (Linear model of coregionalization, Goulard and Voltz (1992); Wackernagel (2003))
The basic statement of the linear model of coregionalization (LMC) is that each variable Z_i, $i = 1, \dots, m$, of a multivariate field Z is a linear combination of p independent univariate stationary random fields with unit variance $\{Y_k, k = 1, \dots, p\}$.

$$Z_i(x) = \sum_{k=1}^{p} a_{ik} Y_k(x), \qquad x \in \mathbb{R}^n.$$

The resulting multivariate covariance is

$$C_{ij}(h) = \sum_{k=1}^{p} a_{ik} a_{jk} \rho_k(h), \qquad h \in \mathbb{R}^n,$$

where $\rho_k(h)$ is a correlation function of Y_k and $A = [a_{ik}]_{i,k=1}^{m,p}$ is a $m \times p$ full rank matrix. Although this model is widely used among practitioners, it lacks flexibility and its limitations are discussed in Gneiting et al. (2010)

Example 2.2 (Convolution)
Suppose that $c_1, \dots, c_m$ are real-valued functions on $\mathbb{R}^n$ which are both integrable and square-integrable. The matrix-valued function defined by equation

$$C_{ij}(h) = (c_i * c_j)(h), \qquad h \in \mathbb{R}^n, \qquad i, j = 1, \dots, m,$$

where the asterisk $*$ denotes the convolution operator, is a matrix-valued covariance function on $\mathbb{R}^n$ (Theorem 2 in Gneiting et al. (2010)). These models are introduced in Ver Hoef and Barry (1998) and Gaspari and Cohn (1999); the multivariate parsimonious Matérn covariance model (Gneiting et al., 2010) serves as an example of this construction. Kleiber (2017) discusses the properties and limitations of this class of models.

For a better understanding of the properties of a covariance function it is often useful to examine its Fourier transform. A stationary covariance function C has the following spectral representation

$$C(h) = \int_{\mathbb{R}^n} e^{i\langle x,h\rangle} F(dx) \qquad \text{for all } h \in \mathbb{R}^n, \tag{2.1}$$

where the increments $\Delta F(x) = F(x + \Delta x) - F(x)$ of the matrix-valued function $F(x)$ are positive semidefinite matrices for all $x \in \mathbb{R}^n$ and $\Delta x \geq 0$ (componentweise). The diagonal elements $F_{ii}(x)$, $i = 1, \ldots, m$, are real, non-decreasing and bounded; the off-diagonal terms $F_{ij}(x)$, $i \neq j$, $i, j = 1, \ldots, m$, are in general complex-valued and of finite variation. Conversely, any matrix of continuous functions $C(h)$ is a matrix-valued covariance function, if the matrices of increments $\Delta F(x)$ are positive semi-definite for any $x \in \mathbb{R}^n$ and $\Delta x \geq 0$. This result is a multidimensional generalization of Cramer's theorem (Cramer, 1940), which is itself a multivariate generalization of Bochner's theorem (Bochner, 1955) and can be found in Gikhman and Skorokhod (2004), Yaglom (1987), and Wackernagel (2003).

When the C_{ij} are additionally absolutely integrable, there exists a *spectral density matrix* such that

$$C(h) = \int_{\mathbb{R}^n} e^{i\langle h,x\rangle} f(x)dx \qquad \text{for all } h \in \mathbb{R}^n$$

and $f(x)$ is a positive semi-definite matrix for all $x \in \mathbb{R}^n$, see Yaglom (1987).

If C is stationary and isotropic, the Fourier transform in (2.1) can be replaced by a Hankel transform, that is,

$$C(r) = 2^{(n-2)/2}\Gamma\left(\frac{n}{2}\right) \int_0^\infty (ru)^{-(n-2)/2} J_{(n-2)/2}(ru)dG(u), \qquad r \geq 0, \tag{2.2}$$

where G_{ij} are the functions of bounded variation having the property that the matrix $\Delta G(u) = G(u + \Delta u) - G(u)$ is positive semidefinite for all $u, \Delta u > 0$ (Yaglom, 1987). Analogous Hankel transform for the spectral density reads

$$C(r) = (2\pi)^{n/2} \int_0^\infty (ru)^{-(n-2)/2} J_{(n-2)/2}(ru) u^{n-1} f(u)du, \qquad r \geq 0,$$

where $[f(u)]_{i,j=1}^m$ is a positive semi-definite matrix for all $u \geq 0$. This result is a nultivariate generalization of Schoenberg's theorem (Schoenberg, 1938). The inversion formula for the spectral density f, which exists if $\int_0^\infty r^{n-1}|C(r)|dr < \infty$, is

$$f(u) = (2\pi)^{-n/2} \int_0^\infty (ur)^{-(n-2)/2} J_{(n-2)/2}(ur) r^{n-1} C(r)dr,$$

see for example Stein (1999). In the subsequent Chapters 3, 4 and 5 we restrict our attention to stationary and isotropic bivariate covariance models, whose components stem from the same family, i.e. to models of the form

$$C(r) = \begin{bmatrix} \sigma_1^2\psi_{11}(r) & \rho\sigma_1\sigma_2\psi_{12}(r) \\ \rho\sigma_1\sigma_2\psi_{12}(r) & \sigma_2^2\psi_{22}(r) \end{bmatrix}, \tag{2.3}$$

where $\sigma_i > 0$ is the variance of the field Z_i, $\psi_{ij}(\cdot) = \psi(\cdot|\theta_{ij}, s_{ij})$ is a continuous univariate stationary and isotropic correlation function, which depends on a scale (or range) parameter $s_{ij} > 0, i, j = 1, 2$, and another optional parameter $\theta_{ij} = (\theta_{ij}^1, ..., \theta_{ij}^k)$ with $k \in \mathbb{N}$ (e.g. smoothness, long range behaviour). Necessarily, $|\rho| \leq 1$. Note that isotropy implies $\psi_{12}(r) = \psi_{21}(r)$. Furthermore, we choose $\sigma_1 = \sigma_2 = 1$, since the general case follows immediately from the following fact:

$$C(r) = \begin{bmatrix} \sigma_1 & 0 \\ 0 & \sigma_2 \end{bmatrix} \times \begin{bmatrix} \psi_{11}(r) & \rho\psi_{12}(r) \\ \rho\psi_{12}(r) & \psi_{22}(r) \end{bmatrix} \times \begin{bmatrix} \sigma_1 & 0 \\ 0 & \sigma_2 \end{bmatrix}.$$

For instance, the multivariate Matérn model (Gneiting et al., 2010; Apanasovich et al., 2012) is a representative of this class with

$$\psi(r|\nu, s) = \frac{2^{1-\nu}}{\Gamma(\nu)}(sr)^{\nu}K_{\nu}(sr),$$

where $s > 0$ is a scale parameter, $\nu > 0$ is a smoothness parameter and K_{ν} is a modified Bessel function of the second kind. The bivariate powered exponential model (Moreva and Schlather, 2017) also belongs to the class (2.3) with

$$\psi(r|\alpha, s) = e^{-(sr)^{\alpha}},$$

where $s > 0$ is a scale parameter and $\alpha \in (0, 2]$ is a smoothness parameter.

The class given by (2.3) can be seen as a generalization of the class of separable models introduced by Mardia and Goodall (1993), where a multivariate covariance factorizes into a product of a covariance matrix R and a univariate correlation function $\psi(\cdot)$, i.e.

$$C_{ij}(r) = R_{ij}\psi(r), \qquad r \geq 0, \qquad i, j = 1, \ldots, m.$$

That is, a separable model assumes that all components share the same spatial correlation structure and differ only in their variances. In particular, the scale parameter is the same for both marginal and cross-covariances. The class (2.3) is more flexible allowing each field to have distinct smoothness, scale, and variance parameters and admitting flexible cross-correlation between the fields. Given a univariate correlation function ψ, our goal in Chapter 3 is to find the parameter sets for which the function C in (2.3) is a valid covariance function. Clearly, if the components are uncorrelated, i.e. $\rho = 0$, then C is always a bivariate covariance function. Thus, we are interested in the cases when $|\rho| > 0$.

2.2 Variograms

In Section 4.3 we focus on intrinsically stationary univariate random fields. Intrinsic stationarity is a weaker assumption than stationarity. A random field Z with $\mathbb{E}(Z(x) - Z(y))^2 < \infty$, $x, y \in \mathbb{R}^n$ is called *intrinsically stationary* if $\mathbb{E}(Z(x + h) - Z(x))$ and $\mathbb{E}(Z(x + h) - Z(x))^2$ do not depend on x for all $h \in \mathbb{R}^n$. Then we define the *variogram*

$$\gamma(h) = \frac{1}{2}\mathbb{E}(Z(x + h) - Z(x))^2.$$

We recall that a function $\gamma : \mathbb{R}^n \mapsto \mathbb{R}$ is *negative definite*, if for any $p \in \mathbb{N}$, $x_1, \ldots, x_p \in \mathbb{R}^n$, and $a_1, \ldots, a_p \in \mathbb{R}$, such that $\sum_{i=1}^{p} a_i = 0$, the following inequality holds

$$\sum_{i=1}^{p}\sum_{j=1}^{p} a_i\gamma(x_i - x_j)a_j \leq 0.$$

Theorem 2.3 (Gneiting et al. (2001))
If γ is a real symmetric function in $\mathbb{R}^n$ satisfying $\gamma(0) = 0$, the following properties are equivalent.

(i) There exists an intrinsically stationary Gaussian random field Z with variogram $\gamma(\cdot)$.

(ii) The function γ is negative definite.

(iii) For all $a > 0$, $\exp(-a\gamma(\cdot))$ is a covariance function.

The equivalence of (i) and (ii) mimics the characterization of covariances as positive definite functions. Theorem 2.3 extends known result (see the references in Gneiting et al. (2001)) by removing the additional assumption of continuity of γ.

A stationary random field is always intrinsically stationary, but the converse is not true: the Wiener process is a counterexample. A stationary field has a bounded variogram γ which is linked with the covariance function C by the relation

$$\gamma(h) = C_0 - C(h), \qquad h \in \mathbb{R}^n, \tag{2.4}$$

where $C_0 = C(0)$. If the variogram $\gamma(h)$ of an intrinsically stationary random field is bounded, there exists a constant $C_0 > 0$ such that $C(h) = C_0 - \gamma(h)$ is a covariance function. The minimal value of C_0 is of great interest because higher variances can always be achieved by adding a spatially constant, independent Gaussian random variable to a random field. Gneiting et al. (2001) give the minimal value of C_0 for bounded variograms. If γ is unbounded, then (2.4) can hold locally, i.e. for $|h| \leq r$ and some $r > 0$. The existence and minimum value of C_0 in (2.4) is discussed in Gneiting et al. (2001).

Finally, the rate with which a variogram $\gamma(h)$ of a centered field can increase to infinity is constrained by

$$\lim_{\|h\| \to \infty} \frac{\gamma(h)}{\|h\|^2} = 0, \qquad h \in \mathbb{R}^n.$$

3 Bivariate covariance models

We discuss a sufficient condition and a necessary condition for the positive definiteness of models from the class (2.3). We consider some examples of this class and introduce novel bivariate models, built on Schoenberg's theorem and on the sufficient condition. This chapter is partially based on Moreva and Schlather (2017).

3.1 Models obtained by spectral approach

We collect some new examples of the class (2.3). The proof of positive definiteness (or the contrary) of these models is based on Schoenberg's theorem. Hereinafter we denote by f_{ij} the spectral density of a correlation function ψ_{ij}, $i, j = 1, 2$. By Schoenberg's theorem, a matrix-valued function C in (2.3) is positive definite if and only if

$$f_{11}(r)f_{22}(r) - \rho^2 f_{12}^2(r) \geq 0 \tag{3.1}$$

for all $r > 0$.

Surprisingly, not all univariate models can be generalized to the multivariate case in a non-trivial way. For example, the univariate spherical model, $\psi(r|s) = \left(1 - \frac{3}{2}sr + \frac{1}{2}(sr)^3\right)_+$, $r \geq 0$, $s > 0$, is widely used in geostatistics, but its bivariate generalization, defined by (2.3) is not a covariance function unless the components are independent or the model is separable. To prove this fact, we first need the following auxiliary results.

Lemma 3.1
Let $(u_k)_{k\in\mathbb{N}}$ be a sequence such that $u_k - ak \uparrow b$ for some $a > b > 0$ as k tends to infinity. Then for any $s < 1$, there exists a $k_0 \in \mathbb{N}$ such that $u_{k_0}/s \neq u_k$ for all $k \in \mathbb{N}$.

Proof. We prove the lemma by contradiction. Suppose that there exists an $s < 1$ such that for all $k \in \mathbb{N}$ there is $l_k \in \mathbb{N}$ with $u_k/s = u_{l_k}$. First note that there exists $N \in \mathbb{N}$ such that for every $k \geq N$ the corresponding u_k lies inside the interval $(b + a(k-1), b + ak)$ and there exists a decreasing sequence $\varepsilon_k \downarrow 0$, $\varepsilon_k \in (0, a)$, such that

$$u_k = b + ak - \varepsilon_k.$$

For any $s < 1$, there is $n \in \mathbb{N}$ and $0 \leq c < 1$ such that $a/s = an - ac$.

Consider the following cases.

(i) $c = 0$. There exist $n_b \in \mathbb{N}$ and $c_b \in [0, 1)$ such that $b/s = b + a(n_b - c_b)$. Then we have

$$u_{l_k} = \frac{u_k}{s} = \frac{b + ak - \varepsilon_k}{s} = b + a(n_b - c_b) + ank - \frac{\varepsilon_k}{s} = b + a(n_b + nk) - \left(ac_b + \frac{\varepsilon_k}{s}\right).$$

We choose k large enough so that $0 < ac_b + \frac{\varepsilon_k}{s} < a$. Since

$$b + a(n_b + n - 1) < u_{l_k} < b + a(n_b + n),$$

we get $l_k = n_b + n$ and $\varepsilon_{n_b+n} = ac_b + \varepsilon_k/s$. But then it follows that $\varepsilon_{l_k} > \varepsilon_k$, which cannot be true, since $(\varepsilon_k)_{k\in\mathbb{N}}$ is a decreasing sequence.

(ii) $c > 0$. By our assumption, for u_{k+1} there exists $l_{k+1} > k+1$, such that $\frac{u_{k+1}}{s} = u_{l_{k+1}}$. We obtain

$$\begin{aligned}\frac{u_{k+1}}{s} &= \frac{u_k + a - (\varepsilon_{k+1} - \varepsilon_k)}{s} \\ &= \frac{u_k}{s} + \frac{a}{s} - \frac{\varepsilon_{k+1} - \varepsilon_k}{s} \\ &= u_{l_k} + an - ac - \frac{\varepsilon_{k+1} - \varepsilon_k}{s} \\ &= b + al_k - \varepsilon_{l_k} + an - ac - \frac{\varepsilon_{k+1} - \varepsilon_k}{s} \\ &= b + a(l_k + n) - \left(ac + \varepsilon_{l_k} + \frac{\varepsilon_{k+1} - \varepsilon_k}{s} \right)\end{aligned}$$

Choose k large enough, so that $0 < ac + \varepsilon_{l_k} + \frac{\varepsilon_{k+1} - \varepsilon_k}{s} < a$. Then $l_{k+1} = l_k + n$ and $\varepsilon_{l_k+n} = ac + \varepsilon_{l_k} + \frac{\varepsilon_{k+1} - \varepsilon_k}{s}$. Note that $\varepsilon_{l_k+n} \to ac$ when $k \to \infty$, which is a contradiction, since $c > 0$.

□

Lemma 3.2
Let C be an m-variate continuous covariance function. Then the set of roots of f_{ij} is a superset of the roots of f_{ii} and the roots of f_{jj} for any $i, j = 1, \ldots, m$.

Proof. The lemma follows directly from Schoenberg's theorem. □

Theorem 3.3
Let C be stationary and isotropic covariance function from class (2.3) with $\psi_{ij}(r) = \psi(r/s_{ij})$, $r \geq 0$, $s_{ij} > 0$, $i, j = 1, 2$, and let f be the spectral density of ψ. Suppose that there exists a positive strictly increasing sequence $(u_k)_{k\in\mathbb{N}}$ such that the following properties hold:

(i) for any $s < 1$, there is a $k_0 \in \mathbb{N}$ with $u_{k_0}/s \neq u_k$ for all $k \in \mathbb{N}$,

(ii) the elements of the sequence $(u_k)_{k\in\mathbb{N}}$ constitute all positive roots of f.

Then either $\rho = 0$ or $s_{11} = s_{12} = s_{22}$.

Proof. Without loss of generality we assume $s_{11} \leq s_{22}$. First note that the positive roots of f_{ij} form the sequence $(s_{ij}u_k)_{k\in\mathbb{N}}$ and we denote by A_{ij} the set of positive roots of f_{ij}, i.e. $A_{ij} = \{s_{ij}u_k,\ k \in \mathbb{N}\}$, $i, j = 1, 2$. We consider three cases:

- $s_{12} > s_{11}$, then $s_{11}u_1 \notin A_{12}$ and by Lemma 3.2, the function C cannot be positive definite.
- $s_{12} < s_{11}$, then by condition (i) there exists k_0 such that $\frac{s_{11}}{s_{12}}u_{k_0} \neq u_k$ for all $k \in \mathbb{N}$ and therefore $s_{11}u_{k_0} \notin A_{12}$. By condition (ii) $s_{11}u_{k_0} \in A_{11}$. Then by Lemma 3.2, the function C cannot be positive definite.
- $s_{12} = s_{11} < s_{22}$. This case is treated analogously to the previous one.

□

The generalization of Theorem 3.3 to a multivariate covariance function C follows immediately from the properties of positive definite matrices.

Corollary 3.4
Let C be stationary and isotropic multivariate covariance function C with $C_{ii}(r) = \psi(r/s_{ii})$, $C_{ij}(r) = \rho_{ij}\psi(r/s_{ij})$, $s_{ij} > 0$, $|\rho_{ij}| \leq 1$, $i, j = 1, \ldots, m$, $i \neq j$, and let f be the spectral density of ψ. Suppose that there exists a positive strictly increasing sequence $(u_k)_{k\in\mathbb{N}}$ such the conditions (i) and (ii) of Theorem 3.3 hold. Then for all $i, j = 1, \ldots, m$ either $\rho_{ij} = 0$ or $s_{ij} = s$ for some $s > 0$.

Theorem 3.5
The bivariate spherical model

$$\begin{bmatrix} \left(1 - \frac{3}{2}s_{11}r + \frac{1}{2}(s_{11}r)^3\right)_+ & \rho\left(1 - \frac{3}{2}s_{12}r + \frac{1}{2}(s_{12}r)^3\right)_+ \\ \rho\left(1 - \frac{3}{2}s_{12}r + \frac{1}{2}(s_{12}r)^3\right)_+ & \left(1 - \frac{3}{2}s_{22}r + \frac{1}{2}(s_{22}r)^3\right)_+ \end{bmatrix},$$

with $r \geq 0$, $s_{ij} > 0$, $|\rho| \leq 1$, $i, j = 1, 2$, belongs to the class Φ_3^2 if and only if $\rho = 0$ or $s_{11} = s_{12} = s_{22}$.

Proof. The spectral density of the univariate spherical correlation functions is

$$f(u) = \frac{3s}{\pi^2 u^6}(u\cos(u/2s) - 2s\sin(u/2s))^2$$

Clearly, f is pseudo periodic and takes infinitely many zeros on $u > 0$. We denote by u_k, $k \in \mathbb{N}$, the roots of the function $\tilde{f}(u) = u - \tan(u)$ on $u > 0$. Then the roots of the spectral density f_{ij} are $2s_{ij}u_k$, $k \in \mathbb{N}$, $i, j = 1, 2$. Noting that $u_k \uparrow \frac{\pi}{2} + \pi k$ as $k \to \infty$, we apply Lemma 3.1 and Theorem 3.3 and prove the theorem. □

Remark 3.6
It is possible to construct a bivariate covariance model with the spherical marginal covariance functions using the convolution approach, see Example 2.2 and Du and Ma (2013). In Example 2.2 in $\mathbb{R}^3$ we take

$$c_1(x) = \mathbb{1}_{\{\|x\| \leq a/2\}},$$
$$c_2(x) = \mathbb{1}_{\{\|x\| \leq b/2\}},$$

where $x \in \mathbb{R}^3$, $a, b > 0$. We assume without loss of generality that $a > b$. Then the marginal covariance functions C_{11}, C_{22} are

$$C_{11}(r) = \int_{\mathbb{R}^3} \mathbb{1}_{\{\|x-y\| \leq a/2\}}\mathbb{1}_{\{\|y\| \leq a/2\}}dy = \frac{\pi a^3}{6}\left(1 - \frac{3}{2}\frac{r}{a} + \frac{1}{2}\left(\frac{r}{a}\right)^3\right)_+$$
$$C_{22}(r) = \int_{\mathbb{R}^3} \mathbb{1}_{\{\|x-y\| \leq b/2\}}\mathbb{1}_{\{\|y\| \leq b/2\}}dy = \frac{\pi b^3}{6}\left(1 - \frac{3}{2}\frac{r}{b} + \frac{1}{2}\left(\frac{r}{b}\right)^3\right)_+,$$

and the cross-covariance function is

$$\begin{aligned} C_{12}(r) = C_{21}(r) &= \int_{\mathbb{R}^3} \mathbb{1}_{\{\|x-y\| \leq a/2\}}\mathbb{1}_{\{\|y\| \leq b/2\}}dy \\ &= \begin{cases} \frac{\pi b^3}{6}, & r \leq \frac{a-b}{2} \\ \frac{\pi}{12r}\left(\frac{a+b}{2} - r\right)^2\left(r^2 - \frac{3}{4}(a-b)^2 + r(a+b)\right), & \frac{a-b}{2} \leq r \leq \frac{a+b}{2}, \\ 0, & r \geq \frac{a+b}{2}. \end{cases} \end{aligned}$$

where $r = \|x\|$.

Theorem 3.7 (Bessel I model)
The bivariate Bessel I model

$$2^{\frac{n-2}{2}}\Gamma\left(\frac{n}{2}\right)\begin{bmatrix} J_{\frac{n-2}{2}}(s_{11}r)(s_{11}r)^{-\frac{n-2}{2}} & \rho J_{\frac{n-2}{2}}(s_{12}r)(s_{12}r)^{-\frac{n-2}{2}} \\ \rho J_{\frac{n-2}{2}}(s_{12}r)(s_{12}r)^{-\frac{n-2}{2}} & J_{\frac{n-2}{2}}(s_{22}r)(s_{22}r)^{-\frac{n-2}{2}} \end{bmatrix}, \tag{3.2}$$

where $s_{ij} > 0$, $i, j = 1, 2$, belongs to the class Φ_n^2 if and only if $\rho = 0$ or $s_{11} = s_{12} = s_{22}$.

Proof. Similarly to Theorem 3.5, if $\rho = 0$ or $s_{11} = s_{12} = s_{22}$ the function defined by (3.2) belongs to Φ_n^2. In remains to show that for other parameter values (3.2) is not in Φ_n^2. The function $\psi(r) = 2^{\frac{n-2}{2}}\Gamma(\frac{n}{2})(sr)^{-\frac{n-2}{2}}J_{\frac{n-2}{2}}(sr)$, $r \geq 0$, $s > 0$, has the spectral representation (2.2) with spectral distrubution function

$$G_s(u) = \begin{cases} 0, & u \leq s, \\ 1, & u > s \end{cases}$$

By Schoenberg's theorem the function (3.2) is positive definite if and only if the matrix

$$\Delta G(u) = \begin{bmatrix} G_{s_{11}}(u+\Delta u) & \rho G_{s_{12}}(u+\Delta u) \\ \rho G_{s_{12}}(u+\Delta u) & G_{s_{22}}(u+\Delta u) \end{bmatrix} - \begin{bmatrix} G_{s_{11}}(u) & \rho G_{s_{12}}(u) \\ \rho G_{s_{12}}(u) & G_{s_{22}}(u) \end{bmatrix}$$

is positive definite for any $u \geq 0$ and $\Delta u \geq 0$. First, consider the case $s_{11} = s_{22}$. This case splits into two subcases.

- $s_{11} = s_{22}$, $s_{12} > s_{11}$. Choose u and $u+\Delta u$ such that $s_{11} < u < s_{12} < u+\Delta u$ and observe that the matrix

  $$\Delta G(u) = \begin{bmatrix} 1 & \rho \\ \rho & 1 \end{bmatrix} - \begin{bmatrix} 1 & 0 \\ 0 & 1 \end{bmatrix} = \begin{bmatrix} 0 & \rho \\ \rho & 0 \end{bmatrix}$$

  is not positive definite.

- $s_{11} = s_{22}$, $s_{12} < s_{11}$. Choose u and $u+\Delta u$ such that $u < s_{12} < u+\Delta u < s_{11}$ and observe that the matrix

  $$\Delta G(u) = \begin{bmatrix} 0 & \rho \\ \rho & 0 \end{bmatrix}$$

  is not positive definite.

If $s_{11} \neq s_{22}$, we assume without loss of generality that $s_{11} < s_{22}$. Then the following cases are possible.

- $s_{11} \leq s_{12} < s_{22}$. Choose u and $u + \Delta u$ such that $u < s_{11} \leq s_{12} < u + \Delta u < s_{22}$. Then we get

  $$\Delta G(u) = \begin{bmatrix} 1 & \rho \\ \rho & 0 \end{bmatrix}$$

  is not positive definite.

- $s_{11} < s_{22} \leq s_{12}$. Choose u and $u + \Delta u$ such that $s_{11} < u < s_{22} \leq s_{12} < u + \Delta u$. Then we obtain that the matrix

$$\Delta G(u) = \begin{bmatrix} 1 & \rho \\ \rho & 1 \end{bmatrix} - \begin{bmatrix} 1 & 0 \\ 0 & 0 \end{bmatrix} = \begin{bmatrix} 0 & \rho \\ \rho & 1 \end{bmatrix}$$

  is not positive definite.

- $s_{12} < s_{11} < s_{22}$. Choose u and $u + \Delta u$ such that $u < s_{12} < u + \Delta u < s_{11} < s_{22}$.

$$\Delta G(u) = \begin{bmatrix} 0 & \rho \\ \rho & 0 \end{bmatrix}$$

  is not positive definite

□

Remark 3.8 (Cardinal sine model)
A special case of the Bessel model with $n = 3$ is a cardinal sine. Theorem 3.7 asserts that the following model

$$\begin{bmatrix} \frac{\sin(s_{11}r)}{s_{11}r} & \rho\frac{\sin(s_{12}r)}{s_{12}r} \\ \rho\frac{\sin(s_{12}r)}{s_{12}r} & \frac{\sin(s_{12}r)}{s_{12}r} \end{bmatrix},$$

where $s_{ij} > 0, i, j = 1, 2$, belongs to the class Φ_3^2 if and only if $\rho = 0$ or if $s_{11} = s_{12} = s_{22}$.

From Schoenberg's theorem it follows the Bessel I model cannot be generalized to fields with a number of components higher than two, unless the components are independent or the model is separable.

If we replace $\frac{n-2}{2}$ by $\nu_{ij} > \frac{n-2}{2}$, $i, j = 1, 2$, in the Bessel I model (3.2) then the resulting model is valid for some parameter set, which is described by the following theorem.

Theorem 3.9 (Bessel II model)
The bivariate Bessel II model

$$\varphi(r) = \begin{bmatrix} 2^{\nu_{11}}\Gamma(\nu_{11}+1)\frac{J_{\nu_{11}}(s_{11}r)}{(s_{11}r)^{\nu_{11}}} & \rho 2^{\nu_{12}}\Gamma(\nu_{12}+1)\frac{J_{\nu_{12}}(s_{12}r)}{(s_{12}r)^{\nu_{12}}} \\ \rho 2^{\nu_{12}}\Gamma(\nu_{12}+1)\frac{J_{\nu_{12}}(s_{12}r)}{(s_{12}r)^{\nu_{12}}} & 2^{\nu_{22}}\Gamma(\nu_{22}+1)\frac{J_{\nu_{22}}(s_{22}r)}{(s_{22}r)^{\nu_{22}}} \end{bmatrix}, \tag{3.3}$$

where $\nu_{ij} > (n-2)/2$, $s_{ij} > 0$, $i, j = 1, 2$, and J_ν is a Bessel function of the first kind, belongs to the class Φ_n^2 if and only if $s_{12} \leq \min\{s_{11}, s_{22}\}$ and its cross-correlation parameter ρ satisfies the following inequality.

$$\rho^2 \leq \frac{\Gamma(\nu_{11}+1)\Gamma(\nu_{22}+1)}{\Gamma(\nu_{12}+1)^2}\frac{\Gamma(\nu_{12}-\frac{n-2}{2})^2}{\Gamma(\nu_{11}-\frac{n-2}{2})\Gamma(\nu_{22}-\frac{n-2}{2})}\frac{s_{12}^{4\nu_{12}}}{s_{11}^{2\nu_{11}}s_{22}^{2\nu_{22}}}2^{2\nu_{12}-\nu_{11}-\nu_{22}}\times \inf_{0<u<s_{12}^2}\frac{(s_{11}^2-u)^{\nu_{11}-n/2}(s_{22}^2-u)^{\nu_{22}-n/2}}{(s_{12}^2-u)^{2\nu_{12}-n}}. \tag{3.4}$$

In particular, this can be written as one of the following cases:

(i) if $\frac{n}{2} - 1 < \nu_{12} < \frac{n}{2}$, the bivariate Bessel II model is in Φ_n^2 if and only if $\rho = 0$,

(ii) if $\nu_{12} = n/2$, $\nu_{11} \geq n/2$, $\nu_{22} \geq n/2$, the bivariate Bessel II model is in Φ_n^2 if and only if

$$\rho^2 \leq \frac{1}{\Gamma(\frac{n}{2}+1)^2} \frac{\Gamma(\nu_{11}+1)\Gamma(\nu_{22}+1)}{\Gamma(\nu_{11}+1-\frac{n}{2})\Gamma(\nu_{22}+1-\frac{n}{2})} \frac{s_{12}^{2n}}{s_{11}^{2\nu_{11}} s_{22}^{2\nu_{22}}} 2^{n-\nu_{11}-\nu_{22}} \times (s_{11}^2 - s_{12}^2)^{\nu_{11}-n/2} (s_{22}^2 - s_{12}^2)^{\nu_{22}-n/2},$$

(iii) if $\nu_{12} = n/2$, $(n-2)/2 < \nu_{11} \leq n/2$, $(n-2)/2 < \nu_{22} \leq n/2$, the bivariate Bessel II model is in Φ_n^2 if and only if

$$\rho^2 \leq \frac{1}{\Gamma(\frac{n}{2}+1)^2} \frac{\Gamma(\nu_{11}+1)\Gamma(\nu_{22}+1)}{\Gamma(\nu_{11}+1-\frac{n}{2})\Gamma(\nu_{22}+1-\frac{n}{2})} \frac{s_{12}^{2n}}{s_{11}^{n} s_{22}^{n}} 2^{n-\nu_{11}-\nu_{22}},$$

(iv) if $\nu_{12} = n/2$, and ν_{11}, ν_{22} are not as in (ii)-(iii), the infimum in (3.4) is attained either at $u = 0$ or $u = s_{12}^2$ or at

$$u = \left((n/2-\nu_{11})s_{22}^2 + (n/2-\nu_{22})s_{11}^2\right)/(n-\nu_{11}+\nu_{22}),$$

(v) if ν_{11}, $\nu_{22} > (n-2)/2$ and $\nu_{12} > n/2$ the infimum is attained either if $u = 0$, or if $u \in (0, s_{12})$ is a solution of the quadratic equation,

$$\begin{aligned} &(\nu_{11}+\nu_{22}-2\nu_{12})u^2 \\ &+ (n-\nu_{11}-\nu_{22})s_{12}^2 u + (2\nu_{12} - \frac{n}{2})(s_{22}^2 + s_{11}^2)u - (\nu_{22}s_{11}^2 + \nu_{11}s_{22}^2)u \\ &+ (\nu_{11} - \frac{n}{2})s_{22}^2 s_{12}^2 + (\nu_{22} - \frac{n}{2})s_{11}^2 s_{12}^2 + (n-2\nu_{12})s_{11}^2 s_{22}^2 = 0. \end{aligned} \tag{3.5}$$

Proof. The spectral density of the Bessel covariance function $\psi(r) = 2^\nu \Gamma(\nu+1)(sr)^{-\nu} J_\nu(sr)$, $r \geq 0$, $s > 0$, $\nu > (n-1)/2$, in $\mathbb{R}^n$ is

$$f(u) = \begin{cases} \frac{u^{-\frac{n-2}{2}}}{\pi^{\frac{n}{2}}} \frac{\Gamma(\nu+1)}{s^{2\nu}2^\nu\Gamma(\nu+1-\frac{n}{2})} \left(s^2-u^2\right)^{\nu-\frac{n}{2}}, & u \leq s, \\ 0, & u > s, \end{cases}$$

see for example Chapter 22.2 in Yaglom (1987). Clearly, by Schoenberg's theorem the function (3.3) cannot be positive definite if $s_{12} > \min\{s_{11}, s_{22}\}$. Assume now that $s_{12} \leq \min\{s_{11}, s_{22}\}$. Then the function (3.3) is positive definite if and only if inequality (3.4) holds true. Let us examine the function under infimum

$$w(u) = \frac{(s_{11}^2-u)^{\nu_{11}-n/2}(s_{22}^2-u)^{\nu_{22}-n/2}}{(s_{12}^2-u)^{2\nu_{12}-n}},$$

where $u \in [0, s_{12}^2]$. Consider the following cases.

(i) $\frac{n}{2} - 1 \leq \nu_{12} < \frac{n}{2}$, then $w(s_{12}) = 0$.

(ii) - (iv) $\nu_{12} = n/2$, then $w(u) = (s_{11}^2-u)^{\nu_{11}-n/2}(s_{22}^2-u)^{\nu_{22}-n/2}$. The derivative of $w(u)$ is

$$w'(u) = -(s_{11}^2-u)^{\nu_{11}-n/2-1}(s_{22}^2-u)^{\nu_{22}-n/2-1} \times [(\nu_{11}-n/2)(s_{22}^2-u) + (\nu_{22}-n/2)(s_{11}^2-u)].$$

The first two factors in the round brackets are positive for $u \in [0, s_{12}^2]$. If $\nu_{11} \geq n/2$ and $\nu_{22} \geq n/2$, then the term in square brackets is nonnegative and the derivative is nonpositive. Therefore, $w(u)$ is nonincreasing and the minimum is reached at $u = s_{12}$. If $\nu_{11} \leq n/2$ and $\nu_{22} \leq n/2$, the term in square brackets is nonpositive and the derivative is nonnegative. Therefore, $w(u)$ is nondecreasing and the minimum is reached at $u = 0$. For other values of ν_{11} and ν_{22} the minimum of $w(u)$ on $[0, s_{12}^2]$ is attained either at $u = 0$ or $u = s_{12}$ or at

$$u = \left((n/2 - \nu_{11})s_{22}^2 + (n/2 - \nu_{22})s_{11}^2\right)/(n - \nu_{11} + \nu_{22}).$$

(v) If $\nu_{11}, \nu_{22} > (n-2)/2$ and $\nu_{12} > n/2$ we analyze the derivative of $w(u)$,

$$\begin{aligned}
w'(u) = &- (\nu_{11} - n/2)(s_{11}^2 - u)^{\nu_{11}-n/2-1}(s_{22}^2 - u)^{\nu_{22}-n/2}(s_{12}^2 - u)^{n-2\nu_{12}} \\
&- (\nu_{22} - n/2)(s_{11}^2 - u)^{\nu_{11}-n/2}(s_{22}^2 - u)^{\nu_{22}-n/2-1}(s_{12}^2 - u)^{n-2\nu_{12}} \\
&- (n - 2\nu_{12})(s_{11}^2 - u)^{\nu_{11}-n/2}(s_{22}^2 - u)^{\nu_{22}-n/2}(s_{12}^2 - u)^{n-2\nu_{12}-1} \\
= &- (s_{11}^2 - u)^{\nu_{11}-n/2-1}(s_{22}^2 - u)^{\nu_{22}-n/2-1}(s_{12}^2 - u)^{n-2\nu_{12}-1} \\
&\times [(\nu_{11} - n/2)(s_{22}^2 - u)(s_{12}^2 - u) + (\nu_{22} - n/2)(s_{11}^2 - u)(s_{12}^2 - u) \\
&\quad + (n - 2\nu_{12})(s_{11}^2 - u)(s_{22}^2 - u)].
\end{aligned}$$

The first three factors are positive for $u \in [0, s_{12}^2]$. The term in square brackets is quadratic in u and equals to

$$\begin{aligned}
&(\nu_{11} + \nu_{22} - 2\nu_{12})u^2 \\
&+ (n - \nu_{11} - \nu_{22})s_{12}^2 u + (2\nu_{12} - \frac{n}{2})(s_{22}^2 + s_{11}^2)u - (\nu_{22}s_{11}^2 + \nu_{11}s_{22}^2)u \\
&+ (\nu_{11} - \frac{n}{2})s_{22}^2 s_{12}^2 + (\nu_{22} - \frac{n}{2})s_{11}^2 s_{12}^2 + (n - 2\nu_{12})s_{11}^2 s_{22}^2.
\end{aligned}$$

Thus, $w(u)$ attains its minimum either at $u = 0$ or if u is a solution of (3.5) that is in $[0, s_{12}^2]$.

□

Corollary 3.10
If in Theorem 3.9 $s_{11} = s_{12} = s_{22} = s$, $s > 0$, then the two following cases are possible:

1. *$\nu_{12} < (\nu_{11} + \nu_{22})/2$, then the Bessel II model is in Φ_n^2 if and only if $\rho = 0$,*
2. *$\nu_{12} \geq (\nu_{11} + \nu_{22})/2$, then the Bessel II model is in Φ_n^2 if and only if*

$$\rho^2 \leq \frac{\Gamma(\nu_{11}+1)\Gamma(\nu_{22}+1)}{\Gamma(\nu_{12}+1)^2} \frac{\Gamma(\nu_{12} - \frac{n-2}{2})^2}{\Gamma(\nu_{11} - \frac{n-2}{2})\Gamma(\nu_{22} - \frac{n-2}{2})}.$$

Although Schoenberg's theorem provides necessary and sufficient conditions for a matrix-valued function to be positive definite, for many covariance models there exists no closed formulae for their spectral densities. But even if there are analytical formulae, Schoenberg's theorem often leads to cumbersome expressions, which are impossible to calculate analytically and very hard to minimize numerically. Consider, for example the Hole effect model.

Theorem 3.11 (Hole effect model)
The bivariate Hole effect model

$$\begin{bmatrix} e^{-s_{11}r}\cos(b_{11}r) & \rho e^{-s_{12}r}\cos(b_{12}r) \\ \rho e^{-s_{12}r}\cos(b_{12}r) & e^{-s_{22}r}\cos(b_{22}r) \end{bmatrix}, \tag{3.6}$$

where $s_{ii} \geq \sqrt{3}b_{ii}$, $s_{ij} > 0$, $b_{ij} > 0$, $i = 1, 2$, *belongs to the class* Φ_3^2 *if and only if*

$$\begin{aligned} \rho^2 \leq \inf_{u\geq 0} \frac{s_{11}s_{22}}{s_{12}^2} &\left[\frac{u^2 + 2(s_{11}^2 + b_{11}^2)u + (s_{11}^2 + b_{11}^2)(s_{11}^2 - 3b_{11}^2)}{(u^2 + 2u(s_{11}^2 - b_{11}^2) + (s_{11}^2 + b_{11}^2)^2)^2}\right] \times \\ &\left[\frac{u^2 + 2(s_{22}^2 + b_{22}^2)u + (s_{22}^2 + b_{22}^2)(s_{22}^2 - 3b_{22}^2)}{(u^2 + 2u(s_{22}^2 - b_{22}^2) + (s_{22}^2 + b_{22}^2)^2)^2}\right] \times \\ &\left[\frac{(u^2 + 2u(s_{12}^2 - b_{12}^2) + (s_{12}^2 + b_{12}^2)^2)^4}{(u^2 + 2(s_{12}^2 + b_{12}^2)u + (s_{12}^2 + b_{12}^2)(s_{12}^2 - 3b_{12}^2))^2}\right]. \end{aligned} \tag{3.7}$$

Proof. The spectral density of $\psi(r) = e^{-sr}\cos(br)$, $r \geq 0$, $s > 0$, $b > 0$, is

$$\begin{aligned} f(u) &= \frac{1}{2\pi^2 u}\int_0^\infty re^{-sr}\sin(ur)\cos(br)dr \\ &= \frac{1}{4\pi^2 u}\int_0^\infty re^{-sr}(\sin(r(u+b)) + \sin(r(u-b)))dr \\ &= \frac{1}{4\pi^2 u}\left[\int_0^\infty re^{-sr}\sin(r(u+b))dr + \int_0^\infty re^{-sr}\sin(r(u-b))dr\right] \\ &= \frac{1}{4\pi^2 u}\left[\frac{2s(u+b)}{(s^2+(u+b)^2)^2} + \frac{2s(u-b)}{(s^2+(u-b)^2)^2}\right] \\ &= \frac{s}{2\pi^2 u}\left[\frac{u+b}{(s^2+(u+b)^2)^2} + \frac{u-b}{(s^2+(u-b)^2)^2}\right] \\ &= \frac{s}{2\pi^2 u}\left[\frac{2u(s^4 - 2s^2b^2 + 2s^2u^2 - 3b^4 + 2b^2u^2 + u^4)}{(s^2+(u+b)^2)^2(s^2+(u-b)^2)^2}\right] \\ &= \frac{s}{\pi^2}\left[\frac{u^4 + 2(s^2+b^2)u^2 + s^4 - 2s^2b^2 - 3b^4}{(s^2+(u+b)^2)^2(s^2+(u-b)^2)^2}\right] \\ &= \frac{s}{\pi^2}\left[\frac{u^4 + 2(s^2+b^2)u^2 + (s^2+b^2)(s^2-3b^2)}{(u^4 + 2u^2(s^2-b^2) + (s^2+b^2)^2)^2}\right]. \end{aligned}$$

By the inequality (3.1) the function (3.6) is positive definite if and only if the inequality (3.7) holds true. □

3.2 Necessary condition for positive definiteness

The condition $\nu_{12} < (\nu_{11} + \nu_{22})/2$ in the bivariate Matérn model (Gneiting et al., 2010) necessarily leads to the independence of the components. In the forth section of their article, the authors only very briefly discuss the origin of this condition. Similar restrictions are imposed on smoothness parameters in the bivariate powered exponential model and the bivariate generalized Cauchy model in Sections 3.4 and 3.5. Since this kind of constrains is common for many models of type (2.3) we look at it in detail and explain additionally similar conditions on long-range parameters in the bivariate generalized Cauchy model.

These constraints come from the multivariate version of Schoenberg's theorem and the Tauberian theorems (Bingham, 1972; Leonenko, 1999). Tauberian theorems link the properties of a univariate correlation function with those of its spectral measure. We first need the notion of slow variation.

A function $L : (0, \infty) \mapsto [0, \infty)$ is said to be *slowly varying* at infinity (at zero), if for every $\lambda > 0$, it holds

$$\frac{L(\lambda r)}{L(r)} \to 1 \text{ as } r \to \infty \, (r \to 0).$$

We write $f \dot{\sim} g$ as $t \to t_0$, $t_0 \in [0, \infty]$, for two functions f and g on $[0, \infty)$, if f is asymptotically proportional to g, i.e. $f(t)/g(t) \to A$, $A > 0$, as $t \to t_0$.

Theorem 3.12 (Abelian and Tauberian theorems)
Let F be a spectral measure on $[0, \infty)$ of a stationary and isotropic univariate correlation function ψ in $\mathbb{R}^n$ and let L be a function varying slowly at infinity.

- *If $0 < \alpha < 2$, then*
$$1 - \psi(r) \dot{\sim} r^{\alpha} L(1/r) \qquad \text{as } r \to 0+ \tag{3.8}$$
if and only if
$$1 - F(u) \dot{\sim} \frac{L(u)}{u^{\alpha}} \qquad \text{as } u \to \infty. \tag{3.9}$$
If $\alpha = 2$, relation (3.8) is equivalent to
$$\int_0^r u[1 - F(u)]du \dot{\sim} L(r) \text{ as } r \to \infty$$
or to
$$\int_0^r u^2 F(du) \dot{\sim} L(r) \text{ as } r \to \infty.$$
If $\alpha = 0$, the relation (3.8) implies the asymptotic equivalence (3.9). Conversely, (3.9) implies (3.8) with $\alpha = 0$ if $[1 - F(u)]$ is convex for u sufficiently large, but not in general.

- *Let $0 < \beta < n$. If*
$$\psi(r) \dot{\sim} L(r) r^{-\beta} \text{ as } r \to \infty,$$
then
$$F(u) \dot{\sim} L\left(\frac{1}{u}\right) u^{\beta} \text{ as } u \to 0 + .$$

Corollary 3.13
Let the spectral densities f_{ij} of a matrix-valued function C in (2.3) be decreasing. Let $\theta_{ij} = (\alpha_{ij}, \beta_{ij})$ in equation (2.3) parametrize the behaviour of $\psi(r|\theta_{ij}, s_{ij})$ at the origin and at infinity respectively, i.e.

$$1 - \psi(r|\theta_{ij}) \dot{\sim} r^{\alpha_{ij}} \text{ as } r \to 0+,$$
$$\psi(r|\theta_{ij}) \dot{\sim} r^{-\beta_{ij}} \text{ as } r \to \infty,$$

$\alpha_{ij} \in (0, 2)$, $\beta_{ij} \in (0, n)$, $i, j = 1, 2$. Then C in (2.3) with $\alpha_{12} < (\alpha_{11} + \alpha_{22})/2$ or $\beta_{12} < (\beta_{11} + \beta_{22})/2$ cannot be positive definite unless $\rho = 0$.

Proof. Theorem 3.12 implies that the spectral densities f_{ij} admit the following relations

$$\begin{aligned} f_{ij}(r) &\dot{\sim} r^{-\alpha_{ij}-n} \text{ as } r \to \infty, \\ f_{ij}(r) &\dot{\sim} r^{\beta_{ij}-n} \text{ as } r \to 0+. \end{aligned} \tag{3.10}$$

Combining (3.10) and (3.1) gives the assertion of the corollary. □

In Corollary 3.13 we assumed for simplicity that $s_{ij} = 1$, $i, j = 1, 2$, because distinct scales would not change the asymptotics. Additionally, we chose $L(1/r)$ to be equal to some constant, which is indeed the case for the examples below.

Example 3.14 (Powered exponential correlation function)
Let $\psi(r) = e^{-r^\alpha}$, $r > 0$, $\alpha \in (0, 2)$, then observe that $1 - \psi(r) \dot{\sim} r^\alpha$ as $r \to 0+$ and $L(r) = 1$. The corresponding measure F varies at infinity as follows

$$1 - F(u) \dot{\sim} u^{-\alpha} \text{ as } u \to \infty.$$

Since the function ψ decreases rapidly enough at infinity, the density f of F exists and

$$f(u) \dot{\sim} u^{-\alpha-n} \text{ as } u \to \infty.$$

The latter matches with the series representation of f in Nolan (2005). Thus, by Corollary 3.13, the bivariate powered exponential model of the form (2.3) requires necessarily $\alpha_{12} \geq (\alpha_{11} + \alpha_{22})/2$ unless $\rho = 0$.

Example 3.15 (Generalized Cauchy correlation function)
Let $\psi(r) = (1 + r^\alpha)^{-\beta/\alpha}$, $r, \beta > 0$, $\beta < n$, $\alpha \in (0, 2)$. Then $1 - \psi(r) \dot{\sim} \frac{\beta}{\alpha} r^\alpha$ as $r \to 0+$, so in this case $L(r) = \frac{\beta}{\alpha}$. The spectral density f of ψ decays at infinity as follows

$$f(u) \dot{\sim} u^{-\alpha-n} \text{ as } u \to \infty.$$

This matches the series representation for the spectral density of the Cauchy covariance in Lim and Teo (2009). Analogously, the spectral density f behaves at the origin as

$$f(u) \dot{\sim} u^{\beta-n} \text{ as } u \to 0.$$

Thus, by Corollary 3.13, the bivariate generalized Cauchy model of the form (2.3) requires necessarily $\alpha_{12} \geq (\alpha_{11} + \alpha_{22})/2$ and $\beta_{12} \geq (\beta_{11} + \beta_{22})/2$ unless $\rho = 0$.

3.3 Sufficient condition for positive definiteness

Porcu and Zastavnyi (2011) provide the following construction principle for multivariate covariance models.

Theorem 3.16 *A. Let $(\Omega, \mathcal{F}, \mu)$ be a measure space and E be a linear space. Assume that the family of matrix-valued functions $A(x, u) = [A_{ij}(x, u)] : E \times \Omega \mapsto \mathbb{R}^{m \times m}$ satisfies the following conditions:*

(a) for every $i, j = 1, \ldots, m$ and $x \in E$, the functions $A_{ij}(x, \cdot)$ belong to $L_1(\Omega, \mathcal{F}, \mu)$;

(b) $A(\cdot, u)$ is a positive definite matrix-valued function for μ-almost every $u \in \Omega$.

Let

$$C(x) := \int_\Omega A(x,u)d\mu(u) = \left[\int_\Omega A_{ij}(x,u)d\mu(u)\right]_{i,j=1}^{m}, \qquad x \in E.$$

Then C is a positive definite matrix-valued function in E.

B. *Conditions (a) and (b) in part A are satisfied when $A(x,u) = k(x,u)g(x,u)$, where the maps $k(x,u) : E \times \Omega \mapsto \mathbb{R}$ and $g(x,u) = [g_{ij}(x,u)]_{i,j=1}^{m} : E \times \Omega \mapsto \mathbb{R}^{m\times m}$ satisfy the following conditions:*

   a) *for every $i,j = 1,\dots,m$ and $x \in E$, the functions $k(x,\cdot)g_{ij}(x,\cdot)$ belong to $L_1(\Omega,\mathcal{F},\mu)$;*

   b) *$k(\cdot,u)$ is positive definite for μ-almost every $u \in \Omega$;*

   c) *$g(\cdot,u)$ is a positive definite matrix-valued function or $g(\cdot,u) = g(u)$ is a positive semidefinite matrix for μ-almost every $u \in \Omega$.*

Starting from known functions k and g_{ij}, Porcu et al. (2013) and Daley et al. (2015), see also Schlather et al. (2017), construct new compactly supported multivariate covariance functions. Our approach inspired by Gneiting (1999) and Sironvalle (1980) is different; we consider the model (2.3) as a candidate for a multivariate covariance function and then find the corresponding g_{ij}, which depend on parameters s_{ij}, θ_{ij}, and the parameter set which guarantees its positive definiteness.

The following theorem provides sufficient conditions for positive definiteness of a bivariate model C in (2.3).

Theorem 3.17
A matrix-valued function C defined by equation (2.3) belongs

a) *to the class Φ_1^2 if $\psi_{ij}(r), i,j = 1,2$, is continuously differentiable in $(0,\infty)$ with piecewise existing second derivative in $(0,\infty)$ and the following conditions hold:*

   (i) $r\psi'_{ij}(r) \to 0$ *as* $r \to \infty$ *and* $r\psi'_{ij}(r) \to 0$ *as* $r \to 0$,

   (ii) $\psi'_{ij}(r)$ *is integrable in* $(0,\infty)$, $i,j = 1,2$,

   (iii) the matrix

$$\begin{bmatrix} \psi''_{11}(r) & \rho\psi''_{12}(r) \\ \rho\psi''_{12}(r) & \psi''_{22}(r) \end{bmatrix} \tag{3.11}$$

   is positive definite for almost all $r \geq 0$.

b) *to the class Φ_3^2 if $\psi_{ij}(r)$, $i,j = 1,2$ is twice continuously differentiable in $(0,\infty)$ with piecewise existing third derivative in $(0,\infty)$ and the following conditions hold:*

   (i) $r\psi'_{ij}(r) \to 0$, $r^2\psi''_{ij}(r) \to 0$ *as* $r \to \infty$ *and* $r\psi'_{ij}(r) \to 0$, $r^2\psi''_{ij}(r) \to 0$ *as* $r \to 0$,

   (ii) $\psi'_{ij}(r)$, $r\psi''_{ij}(r)$ *are integrable in* $(0,\infty)$, $i,j = 1,2$,

   (iii) the matrix

$$\begin{bmatrix} \psi''_{11}(r) - r\psi'''_{11}(r) & \rho(\psi''_{12}(r) - r\psi'''_{12}(r)) \\ \rho(\psi''_{12}(r) - r\psi'''_{12}(r)) & \psi''_{11}(r) - r\psi'''_{11}(r) \end{bmatrix} \tag{3.12}$$

   is positive semidefinite for almost all $r \geq 0$.

Proof. In Theorem 3.16 B we take a Euclidean space $\mathbb{R}^n$, $n \in \{1, 3\}$, as E and the Lebesgue measure as μ. We first prove the assertion in $\mathbb{R}$. We take $k(r,u) = \left(1 - \frac{r}{u}\right)_+$, $g_{ii}(u) = u\psi''_{ii}(u)$, $i = 1, 2$, and $g_{12}(u) = g_{21}(u) = \rho u\psi''_{12}(u)$ for $r \geq 0$, $u > 0$ and such that $\psi''_{ij}(u)$ are defined. We check the conditions of Theorem 3.16 B consequently. Conditions (i) and (ii) allow us to apply integration by parts in the following integral, see for example Chapter 10.13 in Apostol (1974),

$$\int_0^\infty u\psi''_{ij}(u)du = u\psi'_{ij}(u)|_0^\infty - \int_0^\infty \psi'_{ij}(u)du = \psi_{ij}(0) < \infty. \tag{3.13}$$

From equation (3.13) follows the condition a) in Theorem 3.16.B. Clearly, $k(\cdot, u)$ is a positive definite function in $\mathbb{R}$ for $u > 0$ and therefore in Theorem 3.16 holds. Condition c) in Theorem 3.16.B is satisfied due to condition (iii). Then the following matrix-valued function is positive definite

$$\begin{bmatrix} \int_0^\infty \left(1 - \frac{r}{u}\right)_+ u\psi''_{11}(u)du & \rho\int_0^\infty \left(1 - \frac{r}{u}\right)_+ u\psi''_{12}(u)du \\ \rho\int_0^\infty \left(1 - \frac{r}{u}\right)_+ u\psi''_{12}(u)du & \int_0^\infty \left(1 - \frac{r}{u}\right)_+ u\psi''_{22}(u)du \end{bmatrix}. \tag{3.14}$$

To simplify function (3.14) we apply integration by parts again. For $r \geq 0$ we have

$$\begin{aligned} \int_0^\infty \left(1 - \frac{r}{u}\right)_+ u\psi''_{ij}(u)du &= \int_r^\infty (u - r)\psi''_{ij}(u)du \\ &= \int_r^\infty (u - r)d\psi'_{ij}(u) \\ &= (u - r)\psi'_{ij}(u)\big|_r^\infty - \int_r^\infty \psi'_{ij}(u)du \\ &= \psi_{ij}(r). \end{aligned}$$

Thus, (3.14) and (2.3) are the same matrices.

The proof for $\mathbb{R}^3$ is analogous with $k(r,u) = \left(1 - \frac{r}{u}\right)_+ - \frac{r}{2u}\left(1 - \frac{r^2}{u^2}\right)_+$ and $g_{ii}(u) = \frac{1}{3}(u\psi''_{ii}(u) - u^2\psi'''_{ii}(u))$, $i = 1, 2$, $g_{12}(u) = \frac{1}{3}\rho(u\psi''_{12}(u) - u^2\psi'''_{12}(u))$, $r \geq 0$, $u > 0$ and such that $\psi_{ij}(u)'''$, $i, j = 1, 2$, are defined. Applying again integration by parts we obtain

$$\begin{aligned} &\int_0^\infty \left[\left(1 - \frac{r}{u}\right)_+ - \frac{r}{2u}\left(1 - \frac{r^2}{u^2}\right)_+\right](u\psi''_{ij}(u) - u^2\psi'''_{ij}(u))du \\ &= \int_r^\infty \left[1 - \frac{3r}{2u} + \frac{r^3}{2u^3}\right](u\psi''_{ij}(u) - u^2\psi'''_{ij}(u))du \\ &= \int_r^\infty \left(u - \frac{3r}{2} + \frac{r^3}{2u^2}\right)(\psi''_{ij}(u) - u\psi'''_{ij}(u))du \\ &= \int_r^\infty \left(u - \frac{3r}{2} + \frac{r^3}{2u^2}\right)\psi''_{ij}(u)du - \int_r^\infty \left(u^2 - \frac{3ru}{2} + \frac{r^3}{2u}\right)\psi'''_{ij}(u)du \\ &= \int_r^\infty \left(u - \frac{3r}{2} + \frac{r^3}{2u^2}\right)\psi''_{ij}(u)du - \int_r^\infty \left(u^2 - \frac{3ru}{2} + \frac{r^3}{2u}\right)d\psi''_{ij}(u) \\ &= \int_r^\infty \left(u - \frac{3r}{2} + \frac{r^3}{2u^2}\right)\psi''_{ij}(u)du \\ &\quad - \left(u^2 - \frac{3ru}{2} + \frac{r^3}{2u}\right)\psi''_{ij}(u)\Big|_r^\infty + \int_r^\infty \left(2u - \frac{3r}{2} - \frac{r^3}{2u^2}\right)\psi''_{ij}(u)du \end{aligned}$$

$$
\begin{aligned}
&= \int_r^\infty 3\,(u-r)\,\psi_{ij}''(u)du \\
&= 3\int_r^\infty (u-r)\,d\psi_{ij}'(u) \\
&= 3\,(u-r)\,\psi_{ij}'(u)\big|_r^\infty - 3\int_r^\infty \psi_{ij}'(u)du \\
&= 3\psi_{ij}(r).
\end{aligned}
$$

□

Remark 3.18
Two following conditions are sufficient for condition (iii) in Theorem 3.17, part a):

$$\psi_{ii}''(r) \geq 0, \qquad i = 1, 2,\ r \in A, \tag{3.15}$$

and

$$\rho^2 \leq \inf_{r\in A} \frac{\psi_{11}''(r)\psi_{22}''(r)}{\psi_{12}''(r)^2}, \tag{3.16}$$

where $A = \{r \geq 0 : \psi_{ij}''(r), i, j = 1, 2,\ exist\}$.

Two following conditions are sufficient for condition (iii) in Theorem 3.17, part b):

$$\psi_{ii}''(r) - r\psi_{ii}'''(r) \geq 0, \qquad i = 1, 2,\ r \in B, \tag{3.17}$$

and

$$\rho^2 \leq \inf_{r\in B} \frac{(\psi_{11}''(r) - r\psi_{11}'''(r))(\psi_{22}''(r) - r\psi_{22}'''(r))}{(\psi_{12}''(r) - r\psi_{12}'''(r))^2}, \tag{3.18}$$

where $B = \{r \geq 0 : \psi_{ij}'''(r), i, j = 1, 2,\ exist\}$. *The infimum in inequalities* (3.16) *and* (3.18) *is taken over all* $r > 0$ *with* $\psi_{12}''(r) \neq 0$ *and* $\psi_{12}''(r) - r\psi_{12}'''(r) \neq 0$ *respectively. Note that the inequalities* (3.15) *and* (3.17) *must hold only for marginal covariance functions, but not for the cross-covariance functions, This allows* α_{12} *to take values in* $(0, 2]$ *in the bivariate powered exponential model and the bivariate generalized Cauchy model.*

The functions $k(r, u)$ are equal to the Euclid's hat functions, $k(r, u) = h_n(r/u), n = 1, 3$, (Gneiting, 1999). Thus, Theorem 3.17 can be generalized to higher dimensions with the corresponding functions h_n, but it requires the calculation of higher order derivatives.

Let the following function C be a covariance function of a stationary and isotropic m-variate Gaussian random field,

$$C(r) = \begin{bmatrix} {}^2\psi_{11}(r) & \rho_{12}\psi_{12}(r) & \dots & \rho_{1m}\sigma_m\psi_{1m}(r) \\ \sigma_2\rho_{12}\psi_{12}(r) & {}^2\psi_{22}(r) & \dots & \rho_{2m}\sigma_m\psi_{2m}(r) \\ \vdots & \vdots & \ddots & \vdots \\ \rho_{1m}\sigma_m\psi_{1n}(r) & \rho_{2n}\sigma_m\psi_{2m}(r) & \dots & \sigma_m^2\psi_{mm}(r) \end{bmatrix}, \tag{3.19}$$

where ψ_{ij}, $i, j = 1, \dots, m$, as in (2.3). Then Theorem 3.17 can be generalized in the following way.

Theorem 3.19
A matrix-valued function C *defined by equation* (3.19) *belongs*

a) to the class Φ_1^2 *if* $\psi_{ij}(r), i,j = 1,\dots,m$, *is continuously differentiable in* $(0,\infty)$ *with piecewise existing second derivative in* $(0,\infty)$ *and the following conditions holds*

(i) $r\psi'_{ij}(r) \to 0$ *as* $r \to \infty$ *and* $r\psi'_{ij}(r) \to 0$ *as* $r \to 0$, $i,j = 1,\dots,m$,

(ii) $\psi'_{ij}(r)$ *is integrable in* $(0,\infty)$, $i,j = 1,\dots,m$,

(iii) the matrix

$$\begin{bmatrix} \psi''_{11}(r) & \rho_{12}\psi''_{12}(r) & \dots & \rho_{1m}\psi''_{1m}(r) \\ \rho_{12}\psi''_{12}(r) & \psi''_{22}(r) & \dots & \rho_{2m}\psi''_{1m}(r) \\ \vdots & \vdots & \ddots & \vdots \\ \rho_{1m}\psi''_{12}(r) & \rho_{2m}\psi''_{2m}(r) & \dots & \psi''_{mm}(r) \end{bmatrix}$$

is positive semidefinite for almost all $r \geq 0$.

b) to the class Φ_3^2 *if* $\psi_{ij}(r)$, $i,j = 1,\dots,m$, *is twice continuously differentiable in* $(0,\infty)$ *with piecewise existing third derivative in* $(0,\infty)$ *and the following conditions holds*

(i) $r\psi'_{ij}(r) \to 0$, $r^2\psi''_{ij}(r) \to 0$ *as* $r \to \infty$ *and* $r\psi'_{ij}(r) \to 0$, $r^2\psi''_{ij}(r) \to 0$ *as* $r \to 0$, $i,j = 1,\dots,m$,

(ii) $\psi'_{ij}(r)$, $r\psi''_{ij}(r)$ *are integrable in* $(0,\infty)$, $i,j = 1,\dots,m$,

(iii) the matrix

$$\begin{bmatrix} \psi''_{11}(r) - r\psi'''_{11}(r) & \rho_{12}(\psi''_{12}(r) - r\psi'''_{12}(r)) & \dots & \rho_{1m}(\psi''_{1m}(r) - r\psi'''_{1m}(r)) \\ \rho_{12}(\psi''_{12}(r) - r\psi'''_{12}(r)) & (\psi''_{22}(r) - r\psi'''_{22}(r)) & \dots & \rho_{2m}(\psi''_{2m}(r) - r\psi'''_{2m}(r)) \\ \vdots & \vdots & \ddots & \vdots \\ \rho_{1m}(\psi''_{1m}(r) - r\psi'''_{1m}(r)) & \rho_{2m}(\psi''_{2m}(r) - r\psi'''_{2m}(r)) & \dots & (\psi''_{mm}(r) - r\psi'''_{mm}(r)) \end{bmatrix}$$

is positive semidefinite for almost all $r \geq 0$.

3.4 Bivariate powered exponential model

The univariate powered exponential correlation function

$$\psi(r|\alpha, s) = \exp(-(sr)^\alpha),$$

$s > 0$, $\alpha \in (0,2]$, generalizes the exponential correlation function ($\alpha = 1$) and the Gaussian correlation function ($\alpha = 2$). It permits the full range of allowable values for the fractal dimension (Gneiting, 2002). Unlike the Matérn model, the univariate powered exponential correlation function does not allow for a smooth parametrization of the differentiability of the field paths. Indeed, the paths are continuous and non-differentiable for $\alpha < 2$ and infinitely often differentiable for $\alpha = 2$. Nevertheless, the powered exponential covariance may be a good alternative for non-differentiable fields, as it is easy to calculate. Univariate powered exponential covariance is used in Rundel et al. (2013), Guillot and Santos (2009), Henderson et al. (2002), and Kent and Wood (1997), for example.

Each marginal covariance functions of the bivariate powered exponential model,

$$C_{ii}(r) = \exp(-(s_{ii}r)^{\alpha_i}), \tag{3.20}$$

are of powered exponential type with smoothness parameter $\alpha_{ii} \in (0,2]$ and scale parameter $s_{ii} > 0$, $i = 1,2$. The cross covariance functions,

$$C_{12}(r) = C_{21}(r) = \rho \exp(-(s_{12}r)^{\alpha_{12}}), \tag{3.21}$$

are also a powered exponential function with colocated correlation ρ, smoothness parameter $\alpha_{12} \in (0,2]$ and scale parameter $s_{12} > 0$.

To describe a parameter space, for which the matrix-valued function (3.20) and (3.21) is a covariance function, we define auxiliary functions $q^{(n)}_{\alpha,s}(r)$, $n \in \{1,3\}$, by

$$\begin{aligned} q^{(1)}_{\alpha,s}(r) &= \alpha(sr)^{\alpha} - \alpha + 1, \\ q^{(3)}_{\alpha,s}(r) &= \alpha^2(sr)^{2\alpha} - 3\alpha^2(sr)^{\alpha} + 4\alpha(sr)^{\alpha} + \alpha^2 - 4\alpha + 3. \end{aligned}$$

Theorem 3.20
A matrix-valued function C given by equations (3.20) *and* (3.21) *with $\alpha_{ii} \in (0,1]$, $i = 1,2$, and $\alpha_{12} \in (0,2]$, belongs to the class Φ^2_n, $n \in \{1,3\}$, if*

$$\begin{aligned} \rho^2 \leq \frac{\alpha_{11}\alpha_{22}s_{11}^{\alpha_{11}}s_{22}^{\alpha_{22}}}{\alpha_{12}^2 s_{12}^{2\alpha_{12}}} \inf_{r>0} \Bigg[& r^{\alpha_{11}+\alpha_{22}-2\alpha_{12}} e^{2(s_{12}r)^{\alpha_{12}} - (s_{11}r)^{\alpha_{11}} - (s_{22}r)^{\alpha_{22}}} \\ & \times \frac{q^{(n)}_{\alpha_{11},s_{11}}(r) q^{(n)}_{\alpha_{22},s_{22}}(r)}{(q^{(n)}_{\alpha_{12},s_{12}}(r))^2} \Bigg]. \end{aligned} \tag{3.22}$$

In particular, the infimum in (3.22) *is positive if and only if one of the following conditions is satisfied*

(i) $\alpha_{12} = \alpha_{11} = \alpha_{22}$ *and* $s_{12}^{\alpha_{11}} \geq \frac{s_{11}^{\alpha_{11}} + s_{22}^{\alpha_{11}}}{2}$,

(ii) $\alpha_{12} = \alpha_{11} > \alpha_{22}$ *and* $s_{12} > 2^{-1/\alpha_{11}} s_{11}$,

(iii) $\alpha_{12} = \alpha_{22} > \alpha_{11}$ *and* $s_{12} > 2^{-1/\alpha_{22}} s_{22}$,

(iv) $\alpha_{12} > \max\{\alpha_{11}, \alpha_{22}\}$.

Moreover, if $\alpha_{12} < (\alpha_{11} + \alpha_{22})/2$ is in Φ^2_n, $n \in \mathbb{N}$, if and only if $\rho = 0$.

Proof. Functions $\psi_{ij}(r|\alpha_{ij}, s_{ij})$, $i,j = 1,2$, of the bivariate powered exponential model satisfy the requirements of Theorem 3.17. The derivatives of $\psi_{ij}(r|\alpha_{ij}, s_{ij})$ are

$$\begin{aligned} \psi'(r|\alpha_{ij}, s_{ij}) &= -\alpha_{ij} s_{ij}^{\alpha_{ij}} r^{\alpha_{ij}-1} e^{-(s_{ij}r)^{\alpha_{ij}}}, \\ \psi''(r|\alpha_{ij}, s_{ij}) &= \alpha_{ij} s_{ij}^{\alpha_{ij}} r^{\alpha_{ij}-2} e^{-(s_{ij}r)^{\alpha_{ij}}} (\alpha_{ij}(s_{ij}r)^{\alpha_{ij}} - \alpha_{ij} + 1), \\ \psi'''(r|\alpha_{ij}, s_{ij}) &= -\alpha_{ij} s_{ij}^{\alpha_{ij}} r^{\alpha_{ij}-3} e^{-(s_{ij}r)^{\alpha_{ij}}} \\ &\quad \times (3\alpha_{ij}((s_{ij}r)^{\alpha_{ij}} - 1) + \alpha_{ij}^2((s_{ij}r)^{2\alpha_{ij}} - 3(s_{ij}r)^{\alpha_{ij}} + 1) + 2). \end{aligned}$$

- in $\mathbb{R}$ we plug in the derivatives into inequality (3.16). Then we get

$$\begin{aligned} \rho^2 &\leq \inf_{r>0} \frac{\psi''(r|\alpha_{11}, s_{11})\psi''(r|\alpha_{22}, s_{22})}{(\psi''(r|\alpha_{12}, s_{12}))^2} \\ &= \frac{\alpha_{11}\alpha_{22}}{\alpha_{12}^2} \frac{s_{11}^{\alpha_{11}} s_{22}^{\alpha_{22}}}{s_{12}^{2\alpha_{12}}} \inf_{r>0} \Big[r^{\alpha_{11}+\alpha_{22}-2\alpha_{12}} e^{2(s_{12}r)^{\alpha_{12}} - (s_{11}r)^{\alpha_{11}} - (s_{22}r)^{\alpha_{22}}} \\ &\quad \times \frac{(\alpha_{11}(s_{11}r)^{\alpha_{11}} - \alpha_{11} + 1)(\alpha_{22}(s_{22}r)^{\alpha_{22}} - \alpha_{22} + 1)}{((\alpha_{12}(s_{12}r)^{\alpha_{12}} - \alpha_{12} + 1))^2} \Big]. \end{aligned}$$

- in $\mathbb{R}^3$ we first calculate

$$\begin{aligned}
&\psi''(r|\alpha_{ij}, s_{11}) - r\psi'''(r|\alpha_{ij}, s_{ij}) \\
&= \alpha_{ij} s_{ij}^{\alpha_{ij}} r^{\alpha_{ij}-2} e^{-(s_{ij}r)^{\alpha_{ij}}} (\alpha_{ij}(s_{ij}r)^{\alpha_{ij}} - \alpha_{ij} + 1) \\
&+ \alpha_{ij} s_{ij}^{\alpha_{ij}} r^{\alpha_{ij}-2} e^{-(s_{ij}r)^{\alpha_{ij}}} (3\alpha_{ij}((s_{ij}r)^{\alpha_{ij}} - 1) + \alpha_{ij}^2((s_{ij}r)^{2\alpha_{ij}} - 3(s_{ij}r)^{\alpha_{ij}} + 1) + 2) \\
&= \alpha_{ij} s_{ij}^{\alpha_{ij}} r^{\alpha_{ij}-2} e^{-(s_{ij}r)^{\alpha_{ij}}} [\alpha_{ij}(s_{ij}r)^{\alpha_{ij}} - \alpha_{ij} + 1 + 3\alpha_{ij}(s_{ij}r)^{\alpha_{ij}} - 3\alpha_{ij} \\
&+ \alpha_{ij}^2(s_{ij}r)^{2\alpha_{ij}} - 3\alpha_{ij}^2(s_{ij}r)^{\alpha_{ij}} + \alpha_{ij}^2 + 2] \\
&= \alpha_{ij} s_{ij}^{\alpha_{ij}} r^{\alpha_{ij}-2} e^{-(s_{ij}r)^{\alpha_{ij}}} \left[\alpha_{ij}^2(s_{ij}r)^{2\alpha_{ij}} - 3\alpha_{ij}^2(s_{ij}r)^{\alpha_{ij}} + 4\alpha_{ij}(s_{ij}r)^{\alpha_{ij}} + \alpha_{ij}^2 \right. \\
&\left. - 4\alpha_{ij} + 3\right].
\end{aligned} \tag{3.23}$$

  Analogously to the previous case, we plug in (3.23) into inequality (3.18) and obtain the desired inequality (3.22).

All factors of the right-hand side of (3.22) are positive for $r > 0$ meaning that the infimum can be zero only at $r = 0$ or $r = \infty$. Clearly, the infimum is positive for the parameter values given in $(i) - (iv)$ and it is zero otherwise. The case $\alpha_{12} < \frac{\alpha_{11}+\alpha_{22}}{2}$ is discussed in Section 3.2. □

Since inequality (3.22) provides only a sufficient but not a necessary condition for the positive definiteness, a zero infimum in inequality (3.22) does not imply that the model defined by (3.20) and (3.21) is not a valid covariance model. Consider, for example, a bivariate exponential model, i.e. a model with $\alpha_{11} = \alpha_{12} = \alpha_{22} = 1$ in (3.20) and (3.21). It is a special case of the bivariate Matérn model and a necessary and sufficient condition for its positive definiteness can be calculated from Theorem 3 in Gneiting et al. (2010).

Corollary 3.21
The bivariate exponential model belongs to the class Φ_n^2, $n \in \mathbb{N}$, if and only if

$$\rho^2 \leq \frac{s_{11}s_{22}}{s_{12}^2} \inf_{r>0} \frac{(s_{12}^2 + r^2)^{1+n}}{(s_1^2 + r^2)^{1/2+n/2}(s_2^2 + r^2)^{1/2+n/2}}. \tag{3.24}$$

In particular, this can be written as one of the following cases:

1. *if $s_{12} \leq \min\{s_{11}, s_{22}\}$ the bivariate exponential model is in Φ_n^2, $n \in \mathbb{N}$, if and only if*

$$\rho^2 \leq \left(\frac{s_{12}^2}{s_{11}s_{22}}\right)^n$$

2. *if $\min\{s_{11}, s_{22}\} \leq s_{12} \leq \max\{s_{11}, s_{22}\}$ the infimum in (3.24) is attained either if $r = 0$, or in the limit as $r \to \infty$ or if*

$$r^2 = \frac{s_{11}^2 s_{12}^2 + s_{12}^2 s_{22}^2 - 2s_{11}^2 s_{22}^2}{s_{11}^2 + s_{22}^2 - 2s_{12}^2}.$$

3. *if $s_{12} \geq \max\{s_{11}, s_{22}\}$ the bivariate exponential model is in Φ_n^2, $n \in \mathbb{N}$, if and only if*

$$\rho^2 \leq \frac{s_{11}s_{22}}{s_{12}^2}.$$

We compare Corollary 3.21 with the sufficient condition from Theorem 3.20 in $\mathbb{R}$. The corresponding inequality for ρ is the following

$$\rho^2 \leq \frac{s_{11}^2 s_{22}^2}{s_{12}^4} \inf_{r>0} e^{(2s_{12}-s_{11}-s_{22})r}. \tag{3.25}$$

In particular,

1. if $2s_{12} - s_{11} - s_{22} \geq 0$ the bivariate exponential model is valid in $\mathbb{R}$ if
$$\rho^2 \leq \frac{s_{11}^2 s_{22}^2}{s_{12}^4}$$
2. if $2s_{12} - s_{11} - s_{22} < 0$ the infimum in (3.25) is zero and attained in the limit as $r \to \infty$ and therefore $\rho = 0$.

Thus, the sufficient condition for the bivariate exponential model (3.25) is more restrictive than the criterion in Corollary 3.21.

The bivariate Gaussian model is a special case of the bivariate powered exponential model with $\alpha_{ij} = 2$, $i, j = 1, 2$. The spectral density of model admits the closed-form expression and therefore the following criterion for positive definiteness can be formulated.

Theorem 3.22
The bivariate Gaussian model

$$\begin{bmatrix} e^{-(s_{11}r)^2} & \rho e^{-(s_{12}r)^2} \\ \rho e^{-(s_{12}r)^2} & e^{-(s_{22}r)^2} \end{bmatrix}, \tag{3.26}$$

with $s_{ij} > 0$, $|\rho| \leq 1$, $i, j = 1, 2$, belongs to the class Φ_n^2 if and only if

(i) $s_{12}^2 \leq 2s_{11}^2 s_{22}^2/(s_{11}^2 + s_{22}^2)$ *and* $\rho^2 \leq (s_{12}^2/(s_{11}s_{22}))^n$
or

(ii) $s_{12}^2 > 2s_{11}^2 s_{22}^2/(s_{11}^2 + s_{22}^2)$ *and* $\rho = 0$.

Proof. The Gaussian correlation function $\psi = e^{-(sr)^2}$, $r \geq 0$, $s > 0$, has the spectral density

$$f_s(u) = \frac{1}{2^n \pi^{n/2} s^n} e^{-\frac{u^2}{4s^2}}, \qquad u \geq 0.$$

By Schoenberg's theorem, function (3.26) is positive definite if and only if

$$\rho^2 \leq \frac{s_{12}^{2n}}{s_{11}^n s_{22}^n} \inf_{r>0} e^{-\frac{r^2}{4s_{11}^2} - \frac{r^2}{4s_{22}^2} + 2\frac{r^2}{4s_{12}^2}} = \frac{s_{12}^{2n}}{s_{11}^n s_{22}^n} \inf_{r>0} e^{\frac{r^2}{4s_{11}^2 s_{22}^2 s_{12}^2}(2s_{11}^2 s_{22}^2 - s_{12}^2 s_{11}^2 - s_{12}^2 s_{22}^2)} \tag{3.27}$$

Consider the following cases:

1. $s_{12}^2 \leq 2s_{11}^2 s_{22}^2/(s_{11}^2 + s_{22}^2)$, then the exponent in (3.27) is increasing in r, the infimum is attained at zero and $\rho^2 \leq (s_{12}^2/(s_{11}s_{22}))^n$.
2. $s_{12}^2 > 2s_{11}^2 s_{22}^2/(s_{11}^2 + s_{22}^2)$, then the exponent in (3.27) is decreasing in r, the infimum at attained at infinity and $\rho = 0$.

□

The bivariate powered exponential model is implemented in the R package **RandomFields** (Schlather et al., 2017). Figure 3.1 provides an example of the maximum attainable $|\rho|$ in inequality (3.22) that have been found numerically. For details on implementation see Section 5.2.

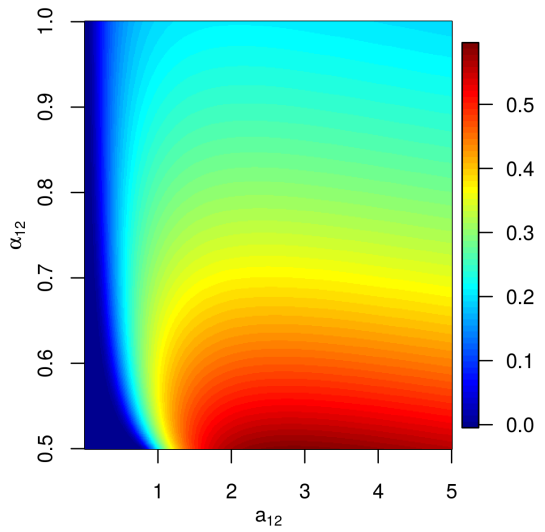

Figure 3.1: The maximum attainable $|\rho|$ in inequality (3.22) for the bivariate powered exponential covariance model in $\mathbb{R}$. The parameters are $\alpha_{11} = 0.2$, $\alpha_{22} = 0.5$, $s_{11} = 2$, $s_{22} = 3$.

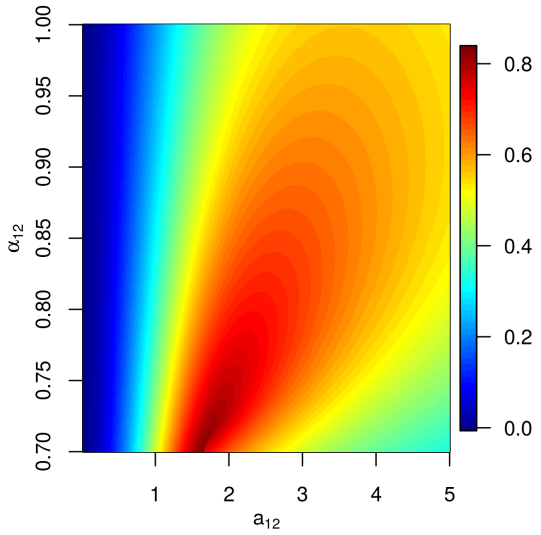

Figure 3.2: The maximum attainable $|\rho|$ in inequality (3.30) for the bivariate Cauchy covariance model in $\mathbb{R}$. The parameters are $\alpha_{11} = 0.5$, $\alpha_{22} = 0.9$, $\beta_{11} = 2$, $\beta_{12} = 2.5$, $\beta_{22} = 2.1$, $s_{11} = 2$, $s_{22} = 2.5$.

3.5 Bivariate generalized Cauchy model

The univariate generalized Cauchy model,

$$\psi(r|\alpha, \beta, s) = (1 + (sr)^{\alpha})^{-\beta/\alpha},$$

has been introduced in Gneiting (2000); Gneiting and Schlather (2004). Here $s > 0$ is a scale parameter, $\alpha \in (0, 2]$ is a smoothness parameter and $\beta > 0$ controls the long range behaviour of the field. The model was applied to many fields of science and technology, including network traffic (Li and Lim, 2008), hydrology (Koutsoyiannis, 2005) and medicine (Muniandy and Stanslas, 2008).

Each marginal covariances of the bivariate generalized Cauchy model,

$$C_{ii}(r) = \sigma_1^2(1 + (s_{ii}r)^{\alpha_{ii}})^{-\beta_{ii}/\alpha_{ii}}, \tag{3.28}$$

is of generalized Cauchy type with variance parameter σ_i, smoothness parameter $\alpha_{ii} \in (0, 2]$, long range parameter $\beta_{ii} > 0$ and scale parameter $s_{ii} > 0$, $i = 1, 2$. Each cross covariance,

$$C_{12}(r) = C_{21}(r) = \rho\sigma_1\sigma_2(1 + (s_{12}r)^{\alpha_{12}})^{-\beta_{12}/\alpha_{12}}, \tag{3.29}$$

is also of generalized Cauchy type with the colocated correlation coefficient ρ, smoothness parameter $\alpha_{12} \in (0, 2]$, long range parameter $\beta_{12} > 0$ and scale parameter $s_{12} > 0$.

To describe a parameter space, for which the matrix-valued function (3.20) and (3.21) is a covariance function, we define the auxiliary functions $p^{(n)}_{\alpha,\beta,s}(r)$, $n \in \{1,3\}$,

$$p^{(1)}_{\alpha,\beta,s}(r) = \frac{(\beta+1)(sr)^\alpha - \alpha + 1}{(1+(sr)^\alpha)^{\beta/\alpha+2}}$$
$$p^{(3)}_{\alpha,\beta,s}(r) = \frac{(\beta+1)(\beta+3)(sr)^{2\alpha} + (sr)^\alpha(4\beta+5-3\alpha-3\beta\alpha-\alpha^2) + (\alpha-1)(\alpha-3)}{(1+(sr)^\alpha)^{\beta/\alpha+3}}$$

Theorem 3.23
A matrix-valued function C given by equations (3.28) *and* (3.29) *with $\alpha_{ii} \in (0,1]$, $\alpha_{12} \in (0,2]$ and $\beta_{ij} > 0$, $i,j = 1,2$, is positive definite in $\mathbb{R}^n$, $n \in \{1,3\}$ if*

$$\rho^2 \le \frac{\beta_{11}\beta_{22}}{\beta_{12}^2} \frac{s_{11}^{\alpha_{11}} s_{22}^{\alpha_{22}}}{s_{12}^{2\alpha_{12}}} \inf_{r>0} r^{\alpha_{11}+\alpha_{22}-2\alpha_{12}} \frac{p^{(n)}_{\alpha_{11},\beta_{11},s_{11}}(r) p^{(n)}_{\alpha_{22},\beta_{22},s_{22}}(r)}{(p^{(n)}_{\alpha_{12},\beta_{12},s_{12}}(r))^2} \tag{3.30}$$

In particular,

(i) if $\alpha_{12} \ge (\alpha_{11}+\alpha_{22})/2$ and $\beta_{12} \ge (\beta_{11}+\beta_{22})/2$ the infimum in inequality (3.30) *is positive.*

(ii) if $\alpha_{12} < (\alpha_{11}+\alpha_{22})/2$ the model is valid only for $\rho = 0$,

(iii) if $\beta_{12} < (\beta_{11}+\beta_{22})/2$ and $\beta_{ij} < n$, $i,j = 1,2$, the model is valid if and only if $\rho = 0$,

(iv) if $2\beta_{12} < \beta_{ii} + n$, $\beta_{ii} < n$ and $\beta_{jj} > n$ for $i \ne j$, the model is valid if and only if $\rho = 0$,

(v) if $\beta_{12} < (\beta_{11}+\beta_{22})/2$, the infimum in inequality (3.30) *is zero.*

Proof. Analogously to the bivariate powered exponential model, functions $\psi_{ij}(r|\alpha_{ij},\beta_{ij},s_{ij})$, $i,j = 1,2$ of the bivariate generalized Cauchy model satisfy the requirements of Theorem 3.17. Their derivatives are

$$\psi'(r|\alpha_{ij},\beta_{ij},s_{ij}) = -\beta_{ij} s_{ij}^{\alpha_{ij}} r^{\alpha_{ij}-1}(1+(s_{ij}r)^{\alpha_{ij}})^{-\beta_{ij}/\alpha_{ij}-1},$$
$$\psi''(r|\alpha_{ij},\beta_{ij},s_{ij}) = \beta_{ij} s_{ij}^{\alpha_{ij}}(1+(s_{ij}r)^{\alpha_{ij}})^{-\beta_{ij}/\alpha_{ij}-2} r^{\alpha_{ij}-2}((\beta_{ij}+1)(s_{ij}r)^{\alpha_{ij}} - \alpha_{ij} + 1),$$
$$\psi'''(r|\alpha_{ij},\beta_{ij},s_{ij}) = -\beta_{ij} s_{ij}^{\alpha_{ij}}(1+(s_{ij}r)^{\alpha_{ij}})^{-\beta_{ij}/\alpha_{ij}-3} r^{\alpha_{ij}-3} \left[(s_{ij}r)^{2\alpha_{ij}}(\beta_{ij}+1)(\beta_{ij}+2)\right.$$
$$\left. -(s_{ij}r)^{\alpha_{ij}}(\alpha_{ij}-1)(3\beta_{ij}+\alpha_{ij}+4) + (\alpha_{ij}-1)(\alpha_{ij}-2))\right].$$

- In $\mathbb{R}$ we plug in the derivatives into the inequality 3.16. Then we get

$$\rho^2 \le \inf_{r>0} \frac{\psi''(r|\alpha_{11},\beta_{11},s_{11})\psi''(r|\alpha_{22},\beta_{22},s_{22})}{(\psi''(r|\alpha_{12},\beta_{12},s_{12}))^2}$$
$$= \frac{\beta_{11}\beta_{22}}{\beta_{12}^2} \frac{s_{11}^{\alpha_{11}} s_{22}^{\alpha_{22}}}{s_{12}^{2\alpha_{12}}} \inf_{r>0} \left[r^{\alpha_{11}+\alpha_{22}-2\alpha_{12}} \right.$$
$$\times \frac{(1+(s_{12}r)^{\alpha_{12}})^{2\beta_{12}/\alpha_{12}+4}}{(1+(s_{11}r)^{\alpha_{11}})^{\beta_{11}/\alpha_{11}+2}(1+(s_{22}r)^{\alpha_{22}})^{\beta_{22}/\alpha_{22}+2}}$$
$$\left. \times \frac{((\beta_{11}+1)(s_{11}r)^{\alpha_{11}} - \alpha_{11} + 1)((\beta_{22}+1)(s_{22}r)^{\alpha_{22}} - \alpha_{22} + 1)}{((\beta_{12}+1)(s_{12}r)^{\alpha_{12}} - \alpha_{12} + 1)^2} \right].$$

- In $\mathbb{R}^3$ we first calculate

$$\begin{aligned}
&\psi''(r|\alpha_{ij},\beta_{ij},s_{ij}) - r\psi'''(r|\alpha_{ij},\beta_{ij},s_{ij}) \\
&= \beta_{ij}s_{ij}^{\alpha_{ij}}(1+(s_{ij}r)^{\alpha_{ij}})^{-\beta_{ij}/\alpha_{ij}-2}r^{\alpha_{ij}-2}((\beta_{ij}+1)(s_{ij}r)^{\alpha_{ij}} - \alpha_{ij}+1) \\
&\quad + \beta_{ij}s_{ij}^{\alpha_{ij}}(1+(s_{ij}r)^{\alpha_{ij}})^{-\beta_{ij}/\alpha_{ij}-3}r^{\alpha_{ij}-2}\left[(s_{ij}r)^{2\alpha_{ij}}(\beta_{ij}+1)(\beta_{ij}+2)\right. \\
&\quad\quad \left. -(s_{ij}r)^{\alpha_{ij}}(\alpha_{ij}-1)(3\beta_{ij}+\alpha_{ij}+4) + (\alpha_{ij}-1)(\alpha_{ij}-2)\right] \\
&= \beta_{ij}s_{ij}^{\alpha_{ij}}(1+(s_{ij}r)^{\alpha_{ij}})^{-\beta_{ij}/\alpha_{ij}-2}r^{\alpha_{ij}-2}\Big[(\beta_{ij}+1)(\beta_{ij}+2)(s_{ij}r)^{2\alpha_{ij}} \\
&\quad + (s_{ij}r)^{\alpha_{ij}}(\beta_{ij}+1-3\beta_{ij}\alpha_{ij}-\alpha_{ij}^2-4\alpha_{ij}+3\beta_{ij}+\alpha_{ij}+4) + (\alpha_{ij}-1)(\alpha_{ij}-3)\Big] \\
&= \beta_{ij}s_{ij}^{\alpha_{ij}}(1+(s_{ij}r)^{\alpha_{ij}})^{-\beta_{ij}/\alpha_{ij}-2}r^{\alpha_{ij}-2}\Big[(\beta_{ij}+1)(\beta_{ij}+2)(s_{ij}r)^{2\alpha_{ij}} \\
&\quad + (s_{ij}r)^{\alpha_{ij}}(4\beta_{ij}-3\beta_{ij}\alpha_{ij}-\alpha_{ij}^2-3\alpha_{ij}+5) + (\alpha_{ij}-1)(\alpha_{ij}-3)\Big].
\end{aligned} \tag{3.31}$$

  Then we plug in (3.31) into (3.18) and obtain the desired inequality (3.30).

Similarly to the bivariate powered exponential model, all factors of the right-hand side of inequality (3.30) are positive for $r > 0$. This means that the infimum can be zero only at $r = 0$ or $r = \infty$. Clearly, for the parameter values given in (v) the infimum is zero at infinity, and positive for parameters in (i). The cases (ii) and (iii) are discussed in Section 3.2. The assertion in (iv) follows from the inequality (3.1) and the fact that $f_{12}(r) \dot{\sim} r^{\beta_{12}-n}$, $f_{ii}(r) \dot{\sim} r^{\beta_{ii}-n}$ as $r \to 0$ and $f_{jj}(r) \dot{\sim} C$ for some $C > 0$ as $r \to 0$, $i \neq j$. The assertions in (v) and (i) follows directly from the inequality (3.30).

□

Analogously to the powered exponential model, inequality (3.30) is only a sufficient but not a necessary condition for positive definiteness. Figure 3.2 provides an example of the maximum attainable $|\rho|$ in inequality (3.30) that have been found numerically.

Theorem 3.24
A matrix-valued function C given by equations (3.28) *and* (3.29) *with $\alpha_{11} = \alpha_{22} = \alpha_{12} = 2$ the model belongs to the class Φ_n^2, $n \in \mathbb{N}$ if and only if*

$$\rho^2 \leq \inf_{r>0}\left(\frac{2}{r}\right)^{\beta_{12}-(\beta_{11}+\beta_{22})/2} \frac{\Gamma\left(\frac{\beta_{12}}{2}\right)^2}{\Gamma\left(\frac{\beta_{11}}{2}\right)\Gamma\left(\frac{\beta_{22}}{2}\right)} \frac{s_{12}^{n+\beta_{12}}}{s_{11}^{n/2+\beta_{11}/2}s_{22}^{n/2+\beta_{22}/2}} \frac{K_{\frac{\beta_{11}-n}{2}}\left(\frac{r}{s_{11}}\right)K_{\frac{\beta_{22}-n}{2}}\left(\frac{r}{s_{22}}\right)}{K_{\frac{\beta_{12}-n}{2}}\left(\frac{r}{s_{12}}\right)^2}$$

In particular, if $\beta_{12} < (\beta_{11}+\beta_{22})/2$ the model belongs to the class Φ_n^2, $n \in \mathbb{N}$ if and only if $\rho = 0$.

Proof. The spectral density of the correlation function $\psi(r) = (1+(sr)^2)^{\beta/2}$, $r \geq 0$, $s, \beta > 0$, is

$$f(r) = \frac{1}{\pi^{n/2}2^{n/2+\beta/2-1}\Gamma(\beta/2)s^n}\left(\frac{r}{s}\right)^{\beta/2-n/2}K_{\beta/2-n/2}\left(\frac{r}{s}\right).$$

Inequality (3.24) follows directly from inequality (3.1). □

Corollary 3.25
A matrix-valued function C given by equations (3.28) *and* (3.29) *with $\alpha_{ij} = 2$ and $\beta_{ij} = n + 1$ for all $i, j = 1, 2$, then*

(i) if $s_{12} \leq 2s_{11}s_{22}/(s_{11} + s_{22})$, the model belongs to the class Φ_n^2, $n \in \mathbb{N}$, if and only if

$$\rho^2 \leq \frac{s_{12}^{2n}}{s_{11}^n s_{22}^n},$$

(ii) $s_{12} > 2s_{11}s_{22}/(s_{11} + s_{22})$, the model belongs to the class Φ_n^2, $n \in \mathbb{N}$ if and only if $\rho = 0$.

Proof. For $\beta_{ij} = n + 1$, $i, j = 1, 2$, the inequality (3.24) becomes

$$\rho^2 \leq \inf_{r>0} \frac{s_{12}^{2n}}{s_{11}^n s_{22}^n} e^{r(\frac{2}{s_{12}} - \frac{1}{s_{11}} - \frac{1}{s_{22}})}. \tag{3.32}$$

Consider two cases:

1. $s_{12} \leq 2s_{11}s_{22}/(s_{11} + s_{22})$, then the exponent in (3.32) is nondecreasing in r and attains its minimum at zero, therefore
$$\rho^2 \leq \frac{s_{12}^{2n}}{s_{11}^n s_{22}^n}$$
2. $s_{12} > 2s_{11}s_{22}/(s_{11} + s_{22})$, then the exponent in (3.32) goes to zero as r goes to infinity and $\rho = 0$.

□

3.6 Discussion

This chapter presents several novel covariance models from class (3.19) for the bivariate Gaussian random fields. A parameter set of a valid bivariate covariance model possessing spectral densities with closed formulae can be fully characterized by Schoenberg's theorem. The examples of such models are collected in Section 3.1. We showed that the bivariate cardinal sine model and the bivariate spherical model from class (3.19) are valid covariance models in $\mathbb{R}^3$ only if the components are independent or share the same spatial correlation structure.

We discussed the necessary conditions for the positive definiteness of the models of class (3.19), which follow from Schoenberg's theorem combined with the Tauberian and the Abelian theorems. These conditions impose restrictions on the smoothness and long range dependence parameters and are common for all models of the class (3.19).

A sufficient conditions for positive definiteness proposed in Theorem 3.19 can be seen as a generalization of the criteria of Pólya type for radial positive definite functions in $\mathbb{R}$ and $\mathbb{R}^3$ (cf. Gneiting (2001); Gneiting et al. (2006) and Table 4.1) for multivariate fields. The bivariate powered exponential model and the bivariate generalized Cauchy model satisfy these conditions with certain sets of parameters. The bivariate generalized Cauchy model allows for distinct long range parameters and to the best of our knowledge it is the first bivariate model with such a property. Similarly to the criteria of Pólya type for univariate functions, our sufficient conditions impose some restrictions on the smoothness parameter. Thus, the question, how to characterize a parameter set of the valid bivariate powered exponential model and the bivariate

generalized Cauchy model with the smoothness parameter greater that one, remains open. The bounds for the correlation coefficient in both models are based on the sufficient conditions for positive definiteness, therefore identifying sharp bounds for ρ is left for future research.

Theorem 3.17 can be generalized to higher dimensions and higher number of field's components, however it requires the cumbersome calculations of higher order derivatives and verifying the positive definiteness of a larger matrix, respectively.

4 Simulation of univariate and bivariate fields

This chapter is mainly based on Moreva and Schlather (Moreva and Schlather).

4.1 Circulant embedding algorithm for compactly supported covariance functions

We describe here the idea of the circulant embedding algorithm for compactly supported covariance functions on $\mathbb{R}$. For technical details we refer the reader to the above mentioned papers. Following Daley et al. (2015) by compact support we mean the support that has a compact closure. We consider a univariate centered stationary Gaussian process Z on a grid $G = \{x_k = kh\}_{k=0}^{N}$ with a mesh size $h > 0$. Let C be a compactly supported covariance function, i.e. $C(x) = 0$ for all $|x| \geq d$ for some $d \geq 0$. We assume that $Nh \geq d$. Let Σ be the covariance matrix with entries $\Sigma_{ij} = C(|x_i - x_j|)$, $0 \leq i, j \leq N$. The matrix Σ is Toeplitz and it is uniquely determined by its first row

$$c = (C(0), C(x_1), \ldots, C(x_{N-1}), C(x_N)).$$

Consider now an embedding of Σ into a symmetric circulant matrix $S \in \mathbb{R}^{2N \times 2N}$ characterized by its first row s defined as follows:

$$s = (C(0), C(x_1), \ldots, C(x_{N-1}), C(x_N), C(x_{N-1}), \ldots, C(x_1)).$$

Each row of the circulant matrix S is composed of cyclically shifted versions of the preceding row. Figure 4.1 illustrates the case $N = 2$. Being circulant, S has the eigendecomposition

$$S = \frac{1}{2N} W \Lambda W^*,$$

where W is the one dimensional discrete Fourier transform matrix of size $2N \times 2N$ with entries $w_{pq} = e^{2\pi i pq/2N}$, $p, q, = 0, \ldots, 2N-1$ and W^* is the conjugate transpose of W. The eigenvalues in the diagonal matrix Λ form the vector $\lambda = Ws^T$. Because of the symmetry in the entries in s, the entries λ_j can also be written as

$$\lambda_j = C(0) + C(x_N)\cos(\pi j) + 2\sum_{k=1}^{N-1} C(x_k)\cos(\pi jk/N), \qquad j = 0, \ldots 2N-1. \tag{4.1}$$

$$\underset{\text{Toeplitz}}{\Sigma} = \begin{pmatrix} C(0) & C(h) & C(2h) \\ C(h) & C(0) & C(h) \\ C(2h) & C(h) & C(0) \end{pmatrix} \longrightarrow \underset{\text{Circulant}}{S} = \left(\begin{array}{ccc|c} C(0) & C(h) & C(2h) & C(h) \\ C(h) & C(0) & C(h) & C(2h) \\ C(2h) & C(h) & C(0) & C(h) \\ \hline C(h) & C(2h) & C(h) & C(0) \end{array}\right).$$

Figure 4.1: Toeplitz matrix and its circulant embedding matrix.

Now let $X = X_1 + iX_2$ be a complex-valued random vector of dimension $2N$, composed by $4N$ independent standard normal random variables. Furthermore, assume for the moment that all λ_j, $j = 0, \dots 2N-1$, are nonnegative. Then the real and the imaginary part of $\tilde{Z} = W\Lambda^{1/2}X/\sqrt{2N}$ form two independent vectors that are both $\mathcal{N}(0, S)$ distributed. Thus, a vector formed by any $N+1$ consecutive entries of $\tilde{Z}$ has the desired distribution.

Dietrich and Newsam (1997) showed that for a compactly supported univariate C there exists an N, such that all λ_j are nonnegative. They used a Poisson summation formula, see Chapter XIX in Feller (1971). We repeat their arguments, since their result can be extended for multivariate multidimensional processes. Our multivariate extension in Theorem 4.16 provides a sufficient condition for the positive semidefiniteness of the circulant (block circulant) embedding matrix which is much easier to check than the sufficient condition in Chan and Wood (1999)'s proposition. We denote by f the spectral density of C,

$$f(x) = \frac{1}{\pi}\int_0^\infty cos(ux)C(u)du, \qquad x \in \mathbb{R}.$$

Theorem 4.1 (Poisson summation formula)
Suppose that the continuous covariance function C on $\mathbb{R}$ is absolutely integrable, and hence the corresponding spectral density f is continuous. Then for $x, t \in \mathbb{R}$ and $\lambda > 0$ it holds that

$$\sum_{k=-\infty}^{\infty} C(x + 2k\lambda)e^{-it(2k\lambda+x)} = \frac{\pi}{\lambda}\sum_{n=-\infty}^{\infty} f\left(\frac{\pi}{\lambda}n + t\right)e^{in(\pi/\lambda)x}, \tag{4.2}$$

provided the series on the left converges to a continuous function.

The series on the left in equation (4.2) is finite for a compactly supported C, therefore it is continuous, as C is continuous. Let $x = 0$, $\lambda = h/2$, and $t = \pi j/(Nh)$. Since $C(kh) = 0$ for $k \geq N$ equation (4.2) reads

$$C(0) + 2\sum_{k=1}^{N-1} C(kh)\cos\left(\frac{\pi jk}{N}\right) = \frac{2\pi}{h}\sum_{n=-\infty}^{\infty} f\left(\frac{2\pi}{h}n + \frac{\pi j}{Nh}\right).$$

The non-negativity of the density f guarantees the non-negativity of the series on the left. Since $C(x_N) = 0$, we have shown that the eigenvalues λ_j of S in equation (4.1) are nonnegative.

The eigendecomposition of the circulant matrix S is calculated efficiently by the fast Fourier transform (FFT) provided that S is of an appropriate size $M \times M$, where M is highly composite, e.g., $M = 2^k$ for some integer k. This yields a substantial gain in computational speed, see Gneiting et al. (2006) for comparison with the Cholesky decomposition. If M is not highly composite, the vector s can be filled with auxiliary entries, see Wood and Chan (1994) for more details.

The idea of the algorithm for multivariate processes, that is $Z(x) = (Z_1(x), \dots, Z_m(x))$, $m \geq 2$, is intuitive: using circulant embedding algorithm for each $Z_1(x), \dots, Z_m(x)$ separately, we get independent $Z_1(x), \dots, Z_m(x)$, if the corresponding complex-valued vectors $X_1, \dots, X_m$ are independent. To have a certain covariance structure between $Z_1, \dots, Z_m$, correlated $X_1, \dots, X_m$ are used. The generalization of the circulant embedding for $n \geq 2$ exploits the block Toeplitz structure of Σ and the multidimensional FFT. The multivariate version of Bochner's theorem (Cramer, 1940) combined with the multidimensional generalizations of the Poisson summation formula (see Abate and Whitt (1992) and references therein) ensures the exact simulations for the matrix-valued function C with compactly supported components in complete analogy to the univariate case.

4.2 Cut-off circulant embedding algorithm for univariate fields

Let $\psi(r)$, $r \in [0,1]$, be a stationary and isotropic positive definite function for an n-dimensional ball $B_n(1)$ with diameter 1, and let $\chi(r)$ be of the form

$$\chi(r) = \begin{cases} \psi(r), & 0 \le r \le 1, \\ \phi(r), & 1 \le r \le R, \\ 0, & r \ge R. \end{cases}$$

Here, the radius R and the function ϕ are chosen such that χ is a covariance function in $\mathbb{R}^n$. In principle, ϕ can be any type of function, but for calculation brevity Gneiting et al. (2006) choose ϕ to be essentially a polynomial, see Figure 4.2 for the example with an exponential covariance function ψ. Let G be a rectangular grid in $[-1/\sqrt{4n}, 1/\sqrt{4n}]^n \in B_n(1)$, i.e. the grid has the diameter of length 1. The approach can be generalized to any arbitrary grid diameter. Since the function $\chi(r)$ has compact support, the corresponding circulant matrix is positive definite whenever the simulation window is larger than the support R. Hence a simulation on G can be obtained by extending the grid largely enough, applying the circulant embedding technique and restricting the obtained random field to G. This approach and an extension to an arbitrary simulation window diameter and geometric anisotropies are implemented in the R package **RandomFields** (Schlather et al., 2017).

We extend the cut-off approach by shifting the covariance ψ on G. More precisely, let $\psi(r) - C_0$ be a valid covariance function on G for some $C_0 > 0$, which depends on the function ψ. If a Gaussian random field Y has the covariance $\psi(r) - C_0$ on G and if $X \sim \mathcal{N}(0, C_0)$ is a spatially constant random variable independent of Y, then the field $Y + X$ has the covariance ψ on G. Indeed,

$$cov(Y(x) + X, Y(0) + X) = cov(Y(x), Y(0)) + cov(X, X) = \psi(r) - C_0 + C_0 = \psi(r),$$

where $r = \|x\|$ and $X \in \mathbb{R}^n$. This idea allows us to simulate fields with a smaller simulation window than in Gneiting et al. (2006). Thus, Theorems 1 and 2 in Gneiting et al. (2006) allow for the following far-reaching corollaries that guarantee the positive definiteness in $\mathbb{R}^n$, $n = 2, 3$, of functions obtained by a shift and a continuation with polynomials.

Note that although Theorem 2 in Gneiting et al. (2006) is formulated for $\mathbb{R}^2$, it is valid also in $\mathbb{R}^3$, see Theorem 1.1 in Gneiting (2001) with $k = 1$, $l = 1$ and $\alpha = 1/2$. For the reader's convenience we quote Theorems 1 and 2 from Gneiting et al. (2006) and then reformulate them for variograms in order to apply them later on for the bridging variogram model (Schlather and Moreva, 2017). These reformulations lead to the smaller cut-off radius R in a stationary case, see Remarks 4.6 and 4.8.

Theorem 4.2 (Gneiting et al. (2006))
Let ψ be a continuous function on $[0, d]$ such that $\psi(r^2)$ is positive and convex and $\psi'(d)$ is negative. Then the function

$$\chi(r) = \begin{cases} \psi(r), & 0 \le r \le d, \\ b(R^{1/2} - r^{1/2}), & d \le r \le R, \\ 0, & r \ge R, \end{cases}$$

$$R = d^{1/2} - \frac{\psi(d)}{2\psi'(d)d^{1/2}}, \qquad b = -2\psi'(d)d^{1/2},$$

is positive definite in $\mathbb{R}^2$.

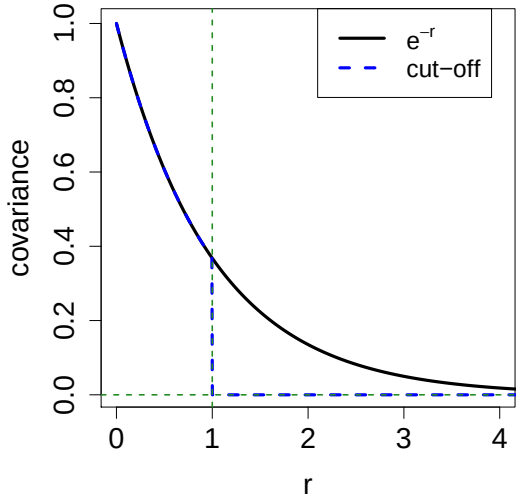

Figure 4.2: Exponential covariance function and its cut-off version. The two functions coincide on [0,1].

Theorem 4.3 (Gneiting et al. (2006))
Let ψ be a continuous function on $[0, d]$ such that $\psi'(r^{1/2})$ exists and is concave, $\psi(d)$ is positive, $\psi'(d)$ is negative, and

$$2\psi''(d)\psi(d) \geq (\psi'(d))^2. \tag{4.3}$$

Then the function

$$\chi(r) = \begin{cases} \psi(r), & 0 \leq r \leq d, \\ b(R-r)^2, & d \leq r \leq R, \\ 0, & r \geq R, \end{cases}$$

$$R = d - 2\frac{\psi(d)}{\psi'(d)}, \qquad b = \frac{(\psi'(d))^2}{4\psi(d)},$$

is positive definite in $\mathbb{R}^3$.

Lemma 4.4
Let f and g be two functions such that f is concave on $[0, d]$, g is concave on $[d, \infty)$, f has the left hand side derivative, g has the right hand side derivative, $f(d) = g(d) \leq 0$ and $0 \leq g'(d) \leq f'(d)$. Then the function

$$h(r) = \begin{cases} f(r), & 0 \leq r \leq d, \\ g(r), & r \geq d, \end{cases}$$

is concave.

Proof. First we note that for any r_1, r_2 such that $0 \leq r_1 \leq d \leq r_2$ it holds

$$g(r_2) \leq g(d) + g'(d)(r_2 - d),$$
$$f(r_1) \leq f(d) + f'(d)(r_1 - d) \leq 0,$$

which yields

$$g(r_2)(r_1 - d) - f(r_1)(r_2 - d) \geq f(d)(r_1 - r_2). \tag{4.4}$$

The function h is clearly concave on $[0, d]$ and $[d, \infty)$. Thus, we only need to show

$$h(tr_1 + (1-t)r_2) \geq th(r_1) + (1-t)h(r_2)$$

for $0 \leq r_1 \leq d \leq r_2$. We denote $l(t, r_1, r_2) = h(tr_1 + (1-t)r_2) - th(r_1) - (1-t)h(r_2)$. Consider the following cases

- $0 \leq tr_1 + (1-t)r_2 \leq d$. We note that

$$tr_1 + (1-t)r_2 = t^* r_1 + (1-t^*)d, \tag{4.5}$$

where $t^* = \frac{tr_1 + (1-t)r_2 - d}{r_1 - d}$, $t^* \in [0, 1]$. Then we have

$$t^* - t = \frac{tr_1 + (1-t)r_2 - d}{r_1 - d} - t = \frac{(1-t)(r_2 - d)}{r_1 - d} \leq 0, \tag{4.6}$$

$$1 - t^* = 1 - \frac{tr_1 + (1-t)r_2 - d}{r_1 - d} = \frac{(r_1 - r_2)(1-t)}{r_1 - d} \geq 0. \tag{4.7}$$

This yields

$$\begin{aligned}
l(t, r_1, r_2) &= f(tr_1 + (1-t)r_2) - tf(r_1) - (1-t)g(r_2) \\
&\overset{(4.5)}{=} f(t^* r_1 + (1-t^*)d) - tf(r_1) - (1-t)g(r_2) \\
&\geq t^* f(r_1) + (1-t^*)f(d) - tf(r_1) - (1-t)g(r_2) \\
&= (t^* - t)f(r_1) + (1-t^*)f(d) - (1-t)g(r_2) \\
&\overset{(4.6),(4.7)}{=} \frac{(1-t)(r_2 - d)}{r_1 - d} f(r_1) + \frac{(r_1 - r_2)(1-t)}{r_1 - d} f(d) - (1-t)g(r_2) \\
&= \frac{1-t}{r_1 - d} \left((r_2 - d)f(r_1) + (r_1 - r_2)f(d) - g(r_2)(r_1 - d) \right) \\
&\overset{(4.4)}{\geq} \frac{1-t}{r_1 - d} \left(f(d)(r_2 - r_1) + (r_1 - r_2)f(d) \right) \\
&= 0.
\end{aligned}$$

- $tr_1 + (1-t)r_2 \geq d$. We note that

$$tr_1 + (1-t)r_2 = t^{**} d + (1-t^{**})r_2$$

where $t^{**} = \frac{t(r_1 - r_2)}{d - r_2}$. Then we have

$$t^{**} - t = \frac{t(r_1 - r_2)}{d - r_2} - t = \frac{t(r_1 - r_2) - td + tr_2}{d - r_2} = \frac{t(r_1 - d)}{d - r_2} \geq 0. \tag{4.8}$$

This yields

$$\begin{aligned} l(t, r_1, r_2) &= g(tr_1 + (1-t)r_2) - tf(r_1) - (1-t)g(r_2) \\ &= g(t^{**}d + (1-t^{**})r_2) - tf(r_1) - (1-t)g(r_2) \\ &\geq t^{**}g(d) + (1-t^{**})g(r_2) - tf(r_1) - (1-t)g(r_2) \\ &= t^{**}g(d) + (t-t^{**})g(r_2) - tf(r_1) \\ &\overset{(4.8)}{=} \frac{t(r_1-r_2)}{d-r_2}g(d) - \frac{t(r_1-d)}{d-r_2}g(r_2) - tf(r_1) \\ &= \frac{t}{r_2-d}\left((r_2-r_1)g(d) + (r_1-d)g(r_2) - (r_2-d)f(r_1)\right) \\ &\overset{(4.4)}{\geq} \frac{t}{r_2-d}\left((r_2-r_1)g(d) + f(d)(r_1-r_2)\right) \\ &= 0. \end{aligned}$$

□

Recall that covariance ψ and variogram γ of a stationary random fields are linked by $\psi(r) = \psi(0) - \gamma(r)$. If the field is only intrinsically stationary, then there can exists a C_0 such that $\psi(r) = C_0 - \gamma(r)$ holds locally.

Corollary 4.5
Let γ be a continuous function on $[0, d]$, $d > 0$, such that $\gamma(r^2)$ is concave on $[0, \sqrt{d}]$ and $\gamma(d)$ and $\gamma'(d)$ are positive. Then the function χ on $[0, \infty)$ defined by

$$\chi(r) = \begin{cases} C_0 - \gamma(r), & 0 \leq r \leq d, \\ 0, & r \geq d, \end{cases} \tag{4.9}$$

where $C_0 = \gamma(d)$, is positive definite in $\mathbb{R}^2$.

Proof. The function $\chi(r^2)$ is convex by Lemma 4.4. From the concavity of $\gamma(r^2)$ it follows that

$$\gamma(r^2) \leq \gamma(d) + 2\sqrt{d}\gamma'(d)(r - \sqrt{d}) < \gamma(d), \qquad r \in [0, \sqrt{d})$$

This means that $\gamma(d) - \gamma(0) > 0$ and thus $\chi(0) > 0$. Then we apply the first criteria in Table 4.1. □

Remark 4.6
Let the function ψ satisfy the conditions of Theorem 4.2. Then the function $\gamma(r) = \psi(0) - \psi(r)$ satisfies the conditions of Theorem 4.5. A centered random field Y with the covariance function (4.9) can be simulated on G via the circulant embedding algorithm. Then we add a spatially constant random variable $X \sim \mathcal{N}(0, \psi(d))$ which is independent of Y. The field $Y + X$ has the covariance ψ on G. Thus, we can simulate a random field with the covariance function ψ without increasing the simulation window.

Corollary 4.7
Let γ be a continuous function on $[0, d]$ such that $\gamma'(r^{1/2})$ exists and is convex on $[0, d^2]$, $\gamma(0)$

is zero, $\gamma(d)$ is positive and $\gamma''(d)$ is negative. We set $C_0 = \gamma(d) - \frac{\gamma'(d)^2}{2\gamma''(d)}$. Then the function χ on $[0,\infty)$ defined by

$$\chi(r) = \begin{cases} C_0 - \gamma(r), & 0 \le r \le d, \\ b(R-r)^2, & d \le r \le R, \\ 0, & r \ge R, \end{cases} \tag{4.10}$$

where

$$R = d - \frac{\gamma'(d)}{\gamma''(d)}, \qquad b = -\frac{1}{2}\gamma''(d),$$

is positive definite in $\mathbb{R}^3$.

Proof. The result is proved by a reduction to the criteria of Pólya type in Table 4.1. The function $\chi'(r^{1/2})$ is concave on $[0, R^2]$ by Lemma 4.4, since $-\gamma'(r^{1/2})$ is concave on $[0, d^2]$ and $-2b(R - r^{1/2})^2$ is concave on $[d^2, R^2]$. Next we apply the same lemma to $\chi'(r^{1/2})$ on $[0, R^2]$ and zero on $[R^2, \infty)$. Thus, $\chi'(r^{1/2})$ is concave. The value $\chi(0)$ is positive, as $\gamma(0) = 0$ and $C_0 > 0$. □

Remark 4.8
Let the function ψ satisfy the conditions of Theorem 4.3. Then the function $\gamma(r) = \psi(0) - \psi(r)$ satisfies the conditions of Corollary 4.7. We compare the cut-off radius from Theorem 4.3, which we denote by R' and the cut-off radius R from Corollary 4.7.

$$\begin{aligned} R' - R &= d - 2\frac{\psi(d)}{\psi'(d)} - d + \frac{\gamma'(d)}{\gamma''(d)} \\ &= -2\frac{\psi(d)}{\psi'(d)} + \frac{\psi'(d)}{\psi''(d)} \\ &= \frac{-2\psi(d)\psi''(d) + (\psi'(d))^2}{\psi''(d)\psi'(d)} \\ &\ge 0, \end{aligned}$$

where the last inequality is due to the inequality (4.3) and the fact that $\psi'(d)$ is negative. Analogously to Remark 4.6, a centered random field Y with the the covariance function (4.10) can be simulated on G via the circulant embedding algorithm. Note that since

$$\psi(0) - C_0 = \psi(d) - \frac{(\psi'(d))^2}{2\psi''(d)} \ge 0$$

by the conditions of Theorem 4.3, we can take again X to be a spatially constant random variable independent of Y and $X \sim \mathcal{N}(0, \psi(0) - C_0)$. Then the field $Y + X$ has the covariance ψ on G. Thus, we can simulate a field with the covariance function ψ with a smaller simulation window than in Theorem 4.3.

Thus, in certain cases modifying covariance functions as in Corollaries 4.5 and 4.7 may increase the speed of circulant embedding by several times compared with Theorem 1 and 2 in Gneiting et al. (2006), respectively.

Corollaries 4.5 and 4.7 build upon functions χ that are once or twice differentiable outside the origin and require the fractal dimension of the corresponding field to be greater than or equal to $n + 3/4$ and $n + 1/2$, respectively, see Gneiting and Schlather (2004) and Table 4

Table 4.1: Criteria of the Pólya type for isotropic covariance functions in $\mathbb{R}^n$ (Gneiting et al., 2006), see also Theorem 1.1. in Gneiting (2001) with $k = 1$, $l = 1$ and $\alpha = 1/2$. A continuous function ψ on $[0, \infty)$ is a stationary and isotropic covariance function in $\mathbb{R}^n$, if $\psi(0)$ is positive, $\lim_{r\to\infty} \psi(r) = 0$, and if the convexity or the non-negativity condition in the table holds. Typographic errors have been corrected in the third criterion.

Convexity condition Non-negativity condition	Requires	n
$\psi(r^2)$ convex $\psi'(r) + 2r\psi''(r) \geq 0$	$\alpha \leq \frac{1}{2}$	2
$-\psi'(\sqrt{r})$ convex $\psi''(r) - r\psi'''(r) \geq 0$	$\alpha \leq 1$	3
$-r^{-2}\left(2\psi'(\sqrt{r}) - 2\sqrt{r}\psi''(\sqrt{r}) + r\psi'''(\sqrt{r})\right)$ convex $48\left(\psi''(r)r - \psi'(r)\right) - 24r^2\psi'''(r) + 7r^3\psi^{(iv)}(r) - r^4\psi^{(v)}(r) \geq 0$	$\alpha \leq 2$	3

in Gneiting et al. (2006). In order to generalize the cut-off approach to smoother functions (in the sense of fractal dimension of the corresponding field), we need an overall higher order differentiability. We consider the following construction of χ

$$\chi(r) = \begin{cases} C_0 - \gamma(r), & 0 \leq r \leq d, \\ \sum_{i=1}^{3} a_i (R - r)^{n_i}, & d \leq r \leq R, \\ 0, & r \geq R, \end{cases} \tag{4.11}$$

where $k \in \mathbb{N}$, $n_i \geq 4$, $n_i \in \mathbb{N}$, $i = 1, 2, 3$, $n_i \neq n_j, i \neq j$. For our purposes it suffices to choose $k = 3$. The radius R is the smallest solution of the cubic equation

$$\begin{aligned} \gamma^{(iv)}(d)(R-d)^3 + \gamma'''(d)\left(\sum_{i=1}^{3} n_i - 6\right)(R-d)^2 \\ + \gamma''(d)\left(\sum_{i\neq j}^{3} n_i n_j - 3\sum_{i=1}^{3} n_i + 7\right)(R-d) \\ + \gamma'(d)\prod_{i=1}^{3}(n_i - 1) = 0, \end{aligned} \tag{4.12}$$

that is greater than d and is assumed to exist. The coefficients $a_i, i = 1, 2, 3$, and the constant C_0 are

$$a_i = -\frac{\gamma'''(d)(R-d)^2 + \gamma''(d)(n_j + n_k - 3)(R-d) + \gamma'(d)(n_j - 1)(n_k - 1)}{n_i(n_j - n_i)(n_k - n_i)(R-d)^{n_i - 1}},$$

$$C_0 = \gamma(d) + \sum_{i=1}^{3} a_i (R-d)^{n_i},$$

respectively. Here $\{j, k\} = \{1, 2, 3\} \setminus \{i\}$.

Theorem 4.9
Let γ be a continuous function on $[0,d]$ such that $\gamma(0)=0$ and

$$r^{-2}(2\gamma'(r^{1/2})-2r^{1/2}\gamma''(r^{1/2})+r\gamma'''(r^{1/2})) \text{ is convex} \tag{4.13}$$

or

$$48\left(\gamma''(r)r-\gamma'(r)\right)-24r^2\gamma'''(r)+7r^3\gamma^{(iv)}(r)-r^4\gamma^{(v)}(r)\le 0. \tag{4.13*}$$

Assume furthermore that equation (4.12) has a root $R\ge d$. Then the function χ in (4.11) is a covariance function in $\mathbb{R}^3$, if $C_0>0$ and if for $r\in[d,R]$

$$\sum_{i=1}^{3} a_i f_{n_i}(r)\ge 0 \tag{4.14}$$

with

$$\begin{aligned} f_k(r) =& k\left[(k-2)(k-3)(k-5)(k-7)r^4+(k-3)(7k^2-69k+158)Rr^3\right.\\ &\left.+24(k-4)(k-5)R^2r^2+48(k-5)R^3r+48R^4\right](R-r)^{k-5}. \end{aligned}$$

Proof. We aim to show that the function $\chi(r)$ satisfies the following condition:

$$\zeta(r):=-r^{-2}(2\chi'(r^{1/2})-2r^{1/2}\chi''(r^{1/2})+r\chi'''(r^{1/2})) \text{ is convex,}$$

see the third condition in Table 4.1. Setting the polynomial in equation (4.11) and its derivatives up to the order 4 at the point $r=1$ to be equal to $C_0-\gamma(d)$, $-\gamma'(d)$, $-\gamma''(d)$, $-\gamma'''(d)$, $-\gamma^{(iv)}(d)$ respectively, we obtain the following system of equations

$$\begin{cases} \sum_{i=1}^3 a_i(R-d)^{n_i} & = C_0-\gamma(d),\\ \sum_{i=1}^3 a_i n_i(R-d)^{n_i-1} & = \gamma'(d),\\ \sum_{i=1}^3 a_i n_i(n_i-1)(R-d)^{n_i-2} & = -\gamma''(d),\\ \sum_{i=1}^3 a_i n_i(n_i-1)(n_i-2)(R-d)^{n_i-3} & = \gamma'''(d),\\ \sum_{i=1}^3 a_i n_i(n_i-1)(n_i-2)(n_i-3)(R-d)^{n_i-4} & = -\gamma^{(iv)}(d). \end{cases} \tag{4.15}$$

This system of equations reduces to the cubic equation (4.12) with respect to $R-d$. For the polynomial part on $[d,R]$ we check the non-negativity condition (4.13*), which after some tedious calculations reduces to the inequality (4.14). The function $\zeta(r)$ is now convex on $[0,d^2]$ and $[d^2,R^2]$. Because of the last equation in (4.15) the right derivative of ζ at point d^2 is equal to its left derivative and therefore ζ is convex on $[0,R^2]$ by Lemma 4.4. Next we apply again Lemma 4.4 to ζ is on $[0,R^2]$ and $[0,R^2]$ and get the convexity of ζ on $[0,\infty)$. By the third criteria in Table 4.1 it follows that χ is positive definite in $\mathbb{R}^3$. □

In practice the conditions in Theorem 4.9 can be checked numerically.

Remark 4.10
A solution $R\ge d$ of the equation (4.12) exists for any $n_1,n_2,n_3\ge 4$, whenever

$$\gamma^{(iv)}(d)\gamma'(d)<0. \tag{4.16}$$

Descartes' rule of signs states that the number of positive roots of the polynomial $g(y)=c_3y^3+c_2y^2+c_1y+c_0$, $y,c_i\in\mathbb{R}$, $i=0,\dots,3$, is either equal to the number of sign changes between consecutive nonzero coefficients, or is reduced by an even number. If $c_3c_0<0$, there are either one or three sign changes and therefore at least one positive root. Plugging in the expression for c_0 and c_3 from equation (4.12) leads to the inequality (4.16).

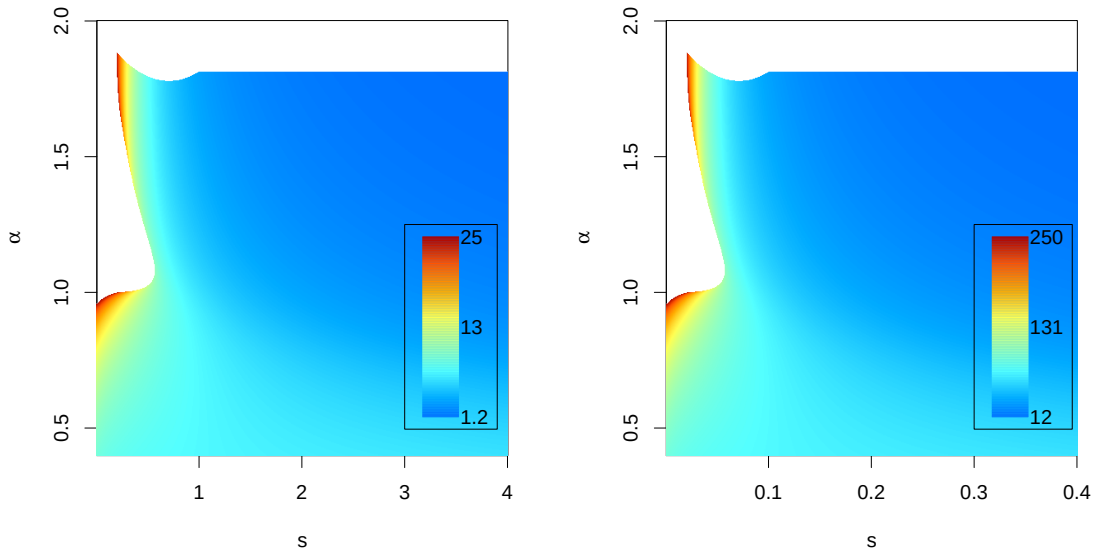

(a) The grid diameter is 1.

(b) The grid diameter is 10.

Figure 4.3: Univariate cut-off embedding for the powered exponential covariance model. The color scheme corresponds to the associated numerical value of the cut-of radius R. The white areas in both plots corresponds to the values of s and α in the powered exponential model, for which the conditions of Theorem 4.9 are not satisfied. This means that either there is no appropriate root of equation (4.12) or the construction (4.11) is not guaranteed to be positive definite. We also whiten the area, for which the radius R exceeds 25 times the grid diameter, since this requires increasing the simulation window at least by factor 625 and the simulating algorithm becomes computationally infeasible.

Remark 4.11
Let a random field Y have a covariance function $\chi(r)$ as in (4.11) such that the function $\gamma(r) = \psi(0) - \psi(r)$ satisfies the conditions of Theorem 4.9. Suppose that $0 < C_0 \leq \psi(0)$. Then, if $X \sim \mathcal{N}(0, \psi(0) - C_0)$ is a spatially constant random variable independent of Y, the field $Y + X$ has the covariance $\psi(r)$ on G. Note that Theorem 4.9 does not guarantee that $C_0 \in (0, \psi(0))$.

Example 4.12 (Powered exponential model)
Figures 4.3 (a) and (b) illustrate the cut-off radius R for $n_1 = 5$, $n_2 = 12$, $n_3 = 20$ and the powered exponential correlation function

$$\psi(r|\alpha, s) = \exp(-(sr)^\alpha),$$

where $s > 0$ and $\alpha \in (0, 2]$. The fractal dimension of the corresponding random field is $n + 1 - \alpha/2$. The convexity condition (4.13) holds true for $\alpha \leq 1.85$, which is a far larger bound than the bound 1.0 which has been known up to now (Gneiting et al., 2006). The white area in Figures 4.3 (a) for values $s < 1$ and $\alpha > 0.9$ corresponds to the case where equality (4.12) does not have an appropriate solution. This problem can be solved by increasing the grid diameter, see Figure 4.3 (b), where the diameter is 10. Figures 4.3 (a) and (b) are identical up to rescaling. In practice the diameter of the simulation window is typically several times larger than the inverse of the scale s, see for example Gneiting et al. (2010).

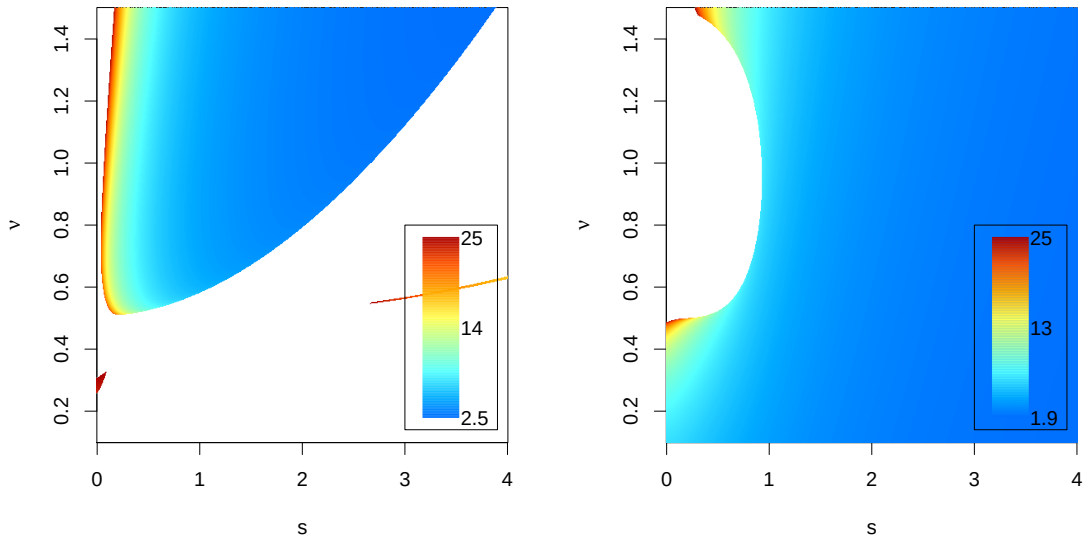

(a) $n_1 = 4$, $n_2 = 7$, $n_3 = 64$. (b) $n_1 = 4$, $n_2 = 12$, $n_3 = 15$.

Figure 4.4: Univariate cut-off embedding for the Matérn covariance model. The color scheme corresponds to the associated numerical value of the cut-off radius R. Analogously to Figure 4.3, the white areas corresponds to the values of s and ν for which the conditions of Theorem 4.9 are not satisfied. We also whiten the area, for which the radius R exceeds 25 times the grid diameter. The red spot and the line in the left plot are genuine.

Example 4.13 (Matérn model)
Figure 4.4 illustrates the cut-off radius R for the different n_1, n_2, n_3 and the Matérn correlation function

$$\psi(r|\nu, s) = \frac{2^{1-\nu}}{\Gamma(\nu)}(sr)^{\nu} K_{\nu}(sr).$$

Here $s > 0$, $\nu > 0$ and K_ν is a modified Bessel function of the second kind. The fractal dimension of the corresponding random field is $n + 1 - \min\{\nu, 1\}$. The convexity condition (4.13) holds true for $\nu \leq 1.5$ whereas Theorem 2 in Gneiting et al. (2006) holds only for $\nu \leq 1/2$.

4.3 Cut-off simulations for the parametric variogram model

We consider in detail the simulation of a random field with a bridging variogram model introduced in Schlather (2014), see also Schlather and Moreva (2017). For $0 < \alpha \leq 2$ and $-\infty < \beta \leq 2$ the isotropic variogram in $\mathbb{R}^n$ is defined as follows

$$\gamma_{\alpha,\beta}(r) = \frac{(1 + r^{\alpha})^{\beta/\alpha} - 1}{2^{\beta/\alpha} - 1}, \tag{4.17}$$

where, as $\beta \to 0$, the limiting function is $\log(1 + r^{\alpha})/\log 2$. The normalizing constant is chosen such that $\gamma_{\alpha,\beta}(1) = 1$.

The parameter α models the smoothness of both the variogram and the corresponding Gaussian random field (see Chapter 3 in Adler (1981) and Scheuerer (2010)), whereas β indicates

the long range behaviour. The variogram $\gamma_{\alpha,\beta}$ is bounded, if and only if $\beta < 0$, and has long memory for $\beta \in (-1, 0)$, see Gneiting and Schlather (2004). Up to some multiplicative constants, the function $\gamma_{\alpha,\beta}$ behaves like r^α at the origin and like r^β for large r and $\beta > 0$.

The model simplifies for $\beta = \alpha$ to the power model of a fractional Brownian random field (Mandelbrot and van Ness, 1968), i.e. $\gamma(r) = r^\alpha$, $\alpha \in (0, 2]$. For $0 < \beta \leq \alpha$ it is a generalization of the fractional Brownian model described in Schlather (2010), and for $\beta < 0$ it is the generalized Cauchy model (Gneiting, 2000; Gneiting and Schlather, 2004). As β tends to zero, the limiting model equals a modified version of the De Wijsian model (Wackernagel, 2003; Matheron, 1962). Thus, the main features of this model are that it separates behaviour at the origin and infinity and allows for a smooth transition between bounded and unbounded variograms.

We investigate which cut-off embedding techniques can be applied on $[0, d/\sqrt{2}]^n$, $n \leq 3$, to the model with an additional scale parameter $s > 0$, i.e.

$$\gamma_{\alpha,\beta,s}(r) = \frac{(1 + (sr)^\alpha)^{\beta/\alpha} - 1}{2^{\beta/\alpha} - 1}.$$

We will use the fact that for all derivatives of order $k \in \mathbb{N}$ it holds that:

$$\gamma^{(k)}_{\alpha,\beta,s}(r) = s^k \gamma^{(k)}_{\alpha,\beta}(sr). \tag{4.18}$$

We start with the limiting case, $\beta = 0$. For simplicity, we omit the normalization constant $\frac{1}{\log 2}$ and redefine $\gamma_{\alpha,0}(r) = \log(1 + r^\alpha)$. We will need the derivatives of $\gamma_{\alpha,0}(r)$, $r > 0$,

$$\begin{aligned}
\gamma'_{\alpha,0}(r) &= \frac{\alpha r^{\alpha-1}}{1 + r^\alpha} \geq 0,\\
\gamma''_{\alpha,0}(r) &= -\frac{\alpha r^{\alpha-2}(r^\alpha - \alpha + 1)}{(1 + r^\alpha)^2} \leq 0,\\
\gamma'''_{\alpha,0}(r) &= \frac{\alpha r^{\alpha-3}(2r^{2\alpha} - r^\alpha(\alpha - 1)(\alpha + 4) + (\alpha - 1)(\alpha - 2))}{(1 + r^\alpha)^3}.
\end{aligned}$$

Consider the following cases:

- $0 < \alpha \leq 1/2$. We apply Corollary 4.5, since $\gamma'_{\alpha,0}(d)$ is positive and $\gamma_{\alpha,0}(r^2)$ is a concave function,

$$\begin{aligned}
(\gamma_{\alpha,0}(r^2))''/2 &= \gamma'_{\alpha,0}(r^2) + 2r^2\gamma''_{\alpha,0}(r^2)\\
&= \frac{\alpha r^{2\alpha-2}}{1 + r^{2\alpha}} - 2r^2\frac{\alpha r^{2\alpha-4}(r^{2\alpha} - \alpha + 1)}{(1 + r^{2\alpha})^2}\\
&= \frac{\alpha r^{2\alpha-2}(1 + r^{2\alpha}) - 2\alpha r^{2\alpha-2}(r^{2\alpha} - \alpha + 1)}{(1 + r^{2\alpha})^2}\\
&= \frac{\alpha r^{2\alpha-2} + \alpha r^{4\alpha-2} - 2\alpha r^{4\alpha-2} + 2\alpha^2 r^{2\alpha-2} - 2\alpha r^{2\alpha-2}}{(1 + r^{2\alpha})^2}\\
&= \frac{-\alpha r^{4\alpha-2} + 2\alpha^2 r^{2\alpha-2} - \alpha r^{2\alpha-2}}{(1 + r^{2\alpha})^2}\\
&= -\alpha r^{2\alpha-2}\frac{r^{2\alpha} + 1 - 2\alpha}{(1 + r^{2\alpha})^2}\\
&\leq 0.
\end{aligned}$$

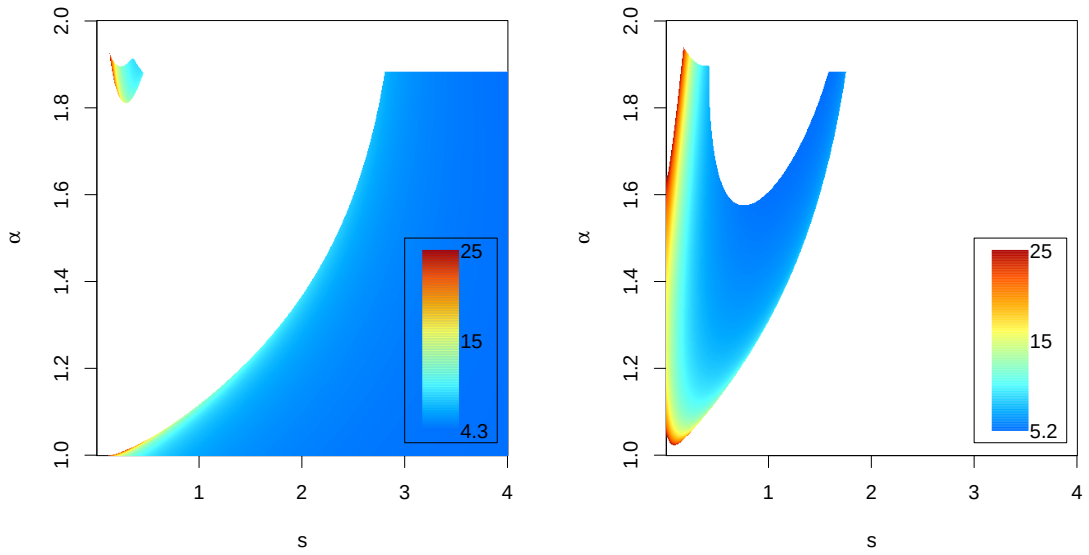

(a) $n_1 = 4$, $n_2 = 6$, $n_3 = 7$. (b) $n_1 = 4$, $n_2 = 5$, $n_3 = 128$.

Figure 4.5: Univariate cut-off embedding for the modified De Wijsian variogram model. The color scheme corresponds to the associated numerical value of the cut-of radius R. Analogously to Figure 4.3, the white areas corresponds to s, α in the De Wijsian model, for which the conditions of Theorem 4.9 are not satisfied. We also whiten the area, for which the radius R exceeds 25 times the grid diameter.

In this case the circulant embedding works in $\mathbb{R}^2$ and simulation window does not need to be increased. The same method can be applied to the modified De Wijsian model with an additional scale parameter $s > 0$, namely $\gamma_{\alpha,0,s}(r) = \log(1 + (sr)^\alpha)$. The scale parameter s does not affect the positive definiteness of the cut-off function due to the equation (4.18).

- $0 < \alpha \leq 1$. We apply Corollary 4.7, since $\gamma''_{\alpha,0}(d)$ is negative and the function $\gamma'_{\alpha,0}(r^{1/2})$ is convex:

$$\begin{aligned}(\gamma'_{\alpha,0}(r^{1/2}))'' &= \frac{1}{2}(\gamma''_{\alpha,0}(r^{1/2})r^{-1/2})' \\ &= \frac{1}{4}\gamma'''_{\alpha,0}(r^{1/2})r^{-1} - \frac{1}{2}r^{-3/2}\gamma''_{\alpha,0}(r^{1/2}) \\ &= \frac{1}{4}r^{-3/2}(\gamma'''_{\alpha,0}(r^{1/2})r^{1/2} - 2\gamma''_{\alpha,0}(r^{1/2})).\end{aligned}$$

Then, note that

$$\begin{aligned}r\gamma'''_{\alpha,0}(r) - \gamma''_{\alpha,0}(r) &= \frac{\alpha r^{\alpha-2}(2r^{2\alpha} - r^\alpha(\alpha-1)(\alpha+4) + (\alpha-1)(\alpha-2))}{(1+r^\alpha)^3} \\ &\quad + \frac{\alpha r^{\alpha-2}(r^\alpha - \alpha + 1)}{(1+r^\alpha)^2} \\ &= \frac{\alpha r^{\alpha-2}}{(1+r^\alpha)^3}\left(3r^{2\alpha} - r^\alpha(\alpha^2+4\alpha-6) + \alpha^2 - 4\alpha + 2\right)\end{aligned}$$

$$= \frac{\alpha r^{\alpha-2}}{(1+r^\alpha)^3}\left(3r^{2\alpha} + r^\alpha(1-(\alpha-1)(\alpha+5)) + (\alpha-2)^2\right)$$
$$\geq 0,$$

for $r \geq 0$. Similarly to the previous case, introducing the scale parameter s does not affect the positive definiteness of the cut-off function in $\mathbb{R}^3$ due to the equation (4.18).

- $1 < \alpha \leq 2$. We apply Theorem 4.9 and continue the covariance function with the polynomial. The positive definiteness of the cut-off function in $\mathbb{R}^3$ depends on the scale parameter s and the degree of polynomial. Numerical results show that the modified de Wijsian variogram satisfies the conditions (4.13*) for $d = 1$ if $1 < \alpha \leq 1.88$ and $s \in (0, 4]$. Figure 4.5 illustrates the cut-off radius R for the different n_1, n_2, n_3.

Remark 4.14
If we take in the definition of χ (4.11) *four instead of three summands, the equations* (4.12) *becomes*

$$\begin{aligned}\gamma^{(iv)}(d)(R-d)^3 + \gamma'''(d)\left(\sum_{i=1}^{3} n_i - 6\right)(R-d)^2 \\ + \gamma''(d)\left(\sum_{i\neq j}^{3} n_i n_j - 3\sum_{i=1}^{3} n_i + 7\right)(R-d) \\ + \gamma'(d)\prod_{i=1}^{3}(n_i - 1) \\ + a_4 n_4\left(\prod_{i=1}^{3}(n_4 - n_i)\right)(R-d)^{(n_4-1)} = 0. \end{aligned} \tag{4.19}$$

Numerical experiments for the De Wijsian model show that for $a_4 < 0$ *and some* $n_4 > \max_i n_i$ *the radius* R *is smaller than for* $a_4 = 0$*, but then the condition* (4.14) *is not fulfilled. For* $a_4 > 0$ *we could not find any combination of* n_i *such that the equation* (4.19) *has a real root* $R \geq d$*.*

Now we exclude the case $\beta = 0$. Again, we need the derivatives of $\gamma_{\alpha,\beta}(r)$, $r \geq 0$,

$$\gamma'_{\alpha,\beta}(r) = \frac{\beta r^{\alpha-1}(1+r^\alpha)^{\beta/\alpha-1}}{2^{\beta/\alpha}-1} \geq 0,$$
$$\gamma''_{\alpha,\beta}(r) = \frac{\beta r^{\alpha-2}(1+r^\alpha)^{\beta/\alpha-2}((\beta-1)r^\alpha + \alpha - 1)}{2^{\beta/\alpha}-1},$$
$$\gamma'''_{\alpha,\beta}(r) = \frac{\beta r^{\alpha-3}(1+r^\alpha)^{\beta/\alpha-3}((\beta-2)(\beta-1)r^{2\alpha} - (\alpha-1)(\alpha-3\beta+4)r^\alpha + \alpha^2 - 3\alpha + 2)}{2^{\beta/\alpha}-1}.$$

Consider the following cases:

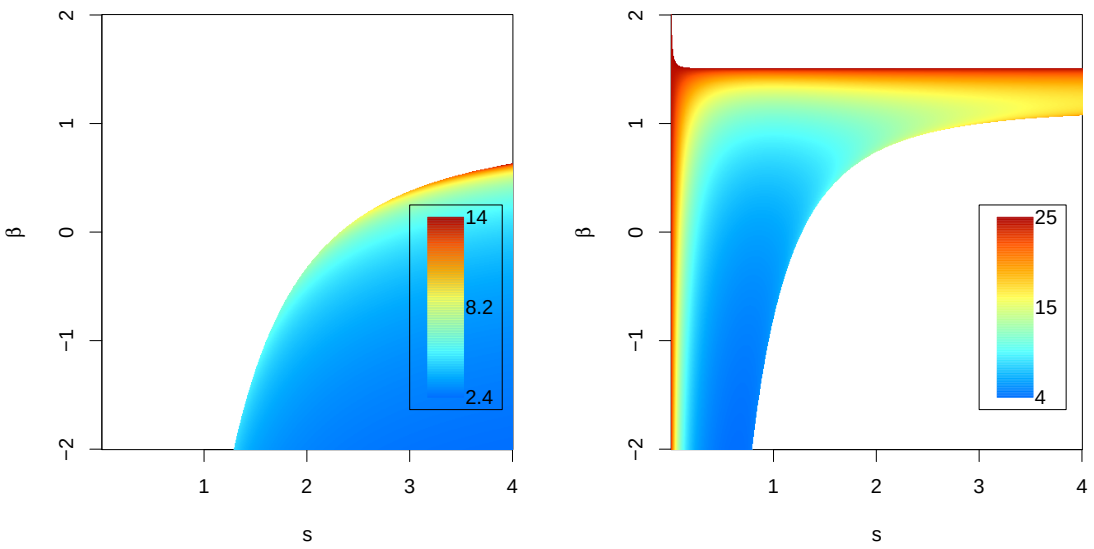

(a) $n_1 = 4$, $n_2 = 6$, $n_3 = 7$. (b) $n_1 = 4$, $n_2 = 5$, $n_3 = 80$.

Figure 4.6: Univariate cut-off embedding for the variogram model (4.17) with $\alpha = 1.5$. The color scheme corresponds to the associated numerical value of the cut-of radius R. Analogously to Figure 4.3, the white areas corresponds to s, β, for which the conditions of Theorem 4.9 are not satisfied. We also whiten the area, for which the radius R exceeds 25 times the grid diameter.

- $\beta \leq (1+(1-2\alpha)/(sd)^\alpha)/2$, $0 < \alpha \leq 1/2$. We apply Corollary 4.5, since $\gamma'_{\alpha,\beta}(d)$ is positive and $\gamma_{\alpha,\beta}(r^2)$ is a concave function,

$$\begin{aligned}(\gamma_{\alpha,\beta}(r^2))''/2 &= \gamma'_{\alpha,\beta}(r^2) + 2r^2\gamma''_{\alpha,\beta}(r^2)\\ &= \frac{\beta r^{2\alpha-2}(1+r^{2\alpha})^{\beta/\alpha-1}}{2^{\beta/\alpha}-1} + \frac{2\beta r^{2\alpha-2}(1+r^{2\alpha})^{\beta/\alpha-2}((\beta-1)r^{2\alpha}+\alpha-1)}{2^{\beta/\alpha}-1}\\ &= \frac{\beta r^{2\alpha-2}(1+r^{2\alpha})^{\beta/\alpha-2}}{2^{\beta/\alpha}-1}\left((2\beta-1)r^{2\alpha}+2\alpha-1\right)\\ &\leq 0.\end{aligned}$$

  Introducing an additional scale parameter $s > 0$ influences only the boundary for β, which comes from the equation (4.18). The upper boundary for β tends to $1/2$ as the diameter goes to infinity. The cut-off function is positive definite in $\mathbb{R}^3$.

- $\beta \leq 1$, $1/2 < \alpha \leq 1$. We apply Corollary 4.7, since $\gamma''_{\alpha,\beta}(d)$ is negative and $\gamma'(r^{1/2})$ is convex,

$$\begin{aligned}r\gamma'''(r) - \gamma''(r) = \frac{\beta r^{\alpha-2}(1+r^\alpha)^{\beta/\alpha-3}}{2^{\beta/\alpha}-1}&\left[(\beta-2)(\beta-1)r^{2\alpha} - (\alpha-1)(\alpha-3\beta+4)r^\alpha\right.\\ &\left.+\alpha^2-3\alpha+2-(1+r^\alpha)((\beta-1)r^\alpha+\alpha-1)\right]\\ = \frac{\beta r^{\alpha-2}(1+r^\alpha)^{\beta/\alpha-3}}{2^{\beta/\alpha}-1}&\left[(\beta-2)(\beta-1)r^{2\alpha} - (\alpha-1)(\alpha-3\beta+4)r^\alpha\right.\end{aligned}$$

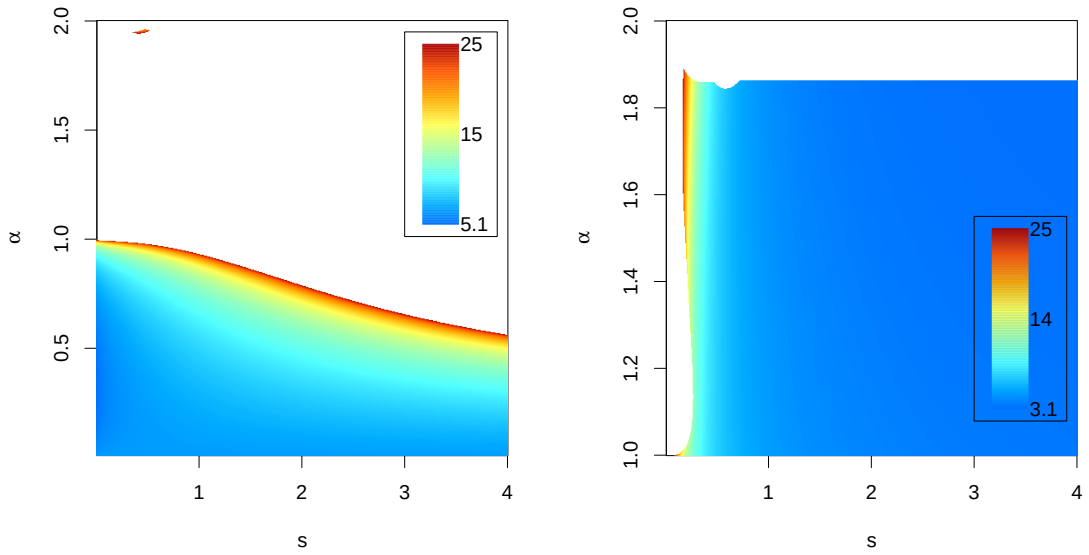

(a) $n_1 = 4$, $n_2 = 6$, $n_3 = 7$, $\beta = 1.5$ (b) $n_1 = 4$, $n_2 = 14$, $n_3 = 30$, $\beta = -1.5$

Figure 4.7: Univariate cut-off embedding for the variogram model (4.17). The color scheme corresponds to the associated numerical value of the cut-of radius R. Analogously to Figure 4.3, the white areas corresponds to s, α, for which the conditions of Theorem 4.9 are not satisfied. We also whiten color the area, for which the radius R exceeds 25 times the grid diameter.

$$
\begin{aligned}
&\quad +\alpha^2 - 3\alpha + 2 - (\beta-1)r^\alpha - \alpha + 1 - (\beta-1)r^{2\alpha} - \alpha r^\alpha + r^\alpha\big] \\
&= \frac{\beta r^{\alpha-2}(1+r^\alpha)^{\beta/\alpha-3}}{2^{\beta/\alpha}-1}\big[(\beta-3)(\beta-1)r^{2\alpha} - (\alpha^2 - 3\alpha\beta + 4\alpha + 4\beta - 6)r^\alpha \\
&\quad +(\alpha-3)(\alpha-1)\big] \\
&= \frac{\beta r^{\alpha-2}(1+r^\alpha)^{\beta/\alpha-3}}{2^{\beta/\alpha}-1}\big[(\beta-3)(\beta-1)r^{2\alpha} \\
&\quad -((\alpha-1)(\alpha-2) + (3\alpha-4)(1-\beta))r^\alpha + (\alpha-3)(\alpha-1)\big] \\
&\geq 0.
\end{aligned}
$$

In this case the scale parameter s does not affect the positive definiteness of the cut-off function in $\mathbb{R}^3$ due to the equation (4.18).

- Theorem 4.9 can be applied for some α, β and s for simulations in $\mathbb{R}^3$. Figure 4.6 illustrates the cut-off radius R depending on $s \in [0.01, 4]$, $\beta \in [-2, 2]$ and two different choices of n_1, n_2, n_3. The parameter $\alpha = 1.5$ is fixed. Figures 4.7 (a) and (b) illustrate the dependence of the cut-off radius R on α and s for the fixed $\beta = 1.5$ and $\beta = -1.5$ respectively.

4.4 Cut-off techniques for bivariate fields

We extend the univariate cut-off circulant embedding method to the case of a bivariate field $Z(x) = (Z_1(x), Z_2(x))$, $x \in \mathbb{R}^n$, $n = 1$ or $n = 3$, so that our modified covariance function is the following

$$\begin{bmatrix} \sigma_1^2\chi_{11}(r) & \rho\sigma_1\sigma_2\chi_{12}(r) \\ \rho\sigma_1\sigma_2\chi_{12}(r) & \sigma_2^2\chi_{22}(r) \end{bmatrix}, \tag{4.20}$$

with

$$\chi_{ij}(r) = \begin{cases} \psi_{ij}(r) - C_{0,ij}, & 0 \le r \le 1, \\ \phi_{ij}(r), & 1 \le r \le R_{ij}, \\ 0, & r \ge R_{ij}, \end{cases} \tag{4.21}$$

where $i, j = 1, 2$. The functions ϕ_{ij}, the constants $C_{0,ij}$ and $R_{ij}, i, j = 1, 2$ must be chosen such that the function (4.20) is a matrix-valued covariance function in $\mathbb{R}^n$. Then, as discussed in Section 4.1, we can apply the circulant embedding algorithm to the function (4.20).

For a bivariate stationary Gaussian process in $\mathbb{R}^3$ we take $\phi_{ij}(r)$ to be a polynomial of degree four in order to get twice continuously differentiable $\chi_{ij}(r)$,

$$\phi_{ij}(r) = b_{ij}(R_{ij} - r)^4, \tag{4.22}$$

and

$$R_{ij} = 1 - \frac{3\psi'_{ij}(1)}{\psi''_{ij}(1)}, \qquad b_{ij} = \frac{\psi''_{ij}(1)^3}{108\psi'_{ij}(1)^2}, \qquad C_{0,ij} = \psi_{ij}(1) - \frac{3\psi'_{ij}(1)^2}{4\psi''_{ij}(1)}. \tag{4.23}$$

Note that in $\mathbb{R}$ and in $\mathbb{R}^3$ we shift each element of the multivariate covariance by $C_{0,ij}$, $i, j = 1, 2$, see also Figure 4.8. Remark 4.17 below shows how to correct this in case of positive $C_{0,ij}$ by adding spatially constant random variables.

Theorem 4.15
Let ψ_{ij}, $i, j = 1, 2$, satisfy the conditions of Theorem 3.17 in $\mathbb{R}$. Additionally assume that each ψ_{ij} satisfy the conditions of Theorem 4.3. Then the matrix-valued function (4.20) *defined by* (4.21)- (4.23) *is positive definite in $\mathbb{R}$ if*

$$R_{12} \le \min\{R_{11}, R_{22}\}$$

Proof. First we note that each $\chi_{ij}(r)$, $i, j = 1, 2$ is a positive definite function in $\mathbb{R}^3$, so that (2.3) is well defined. The proof of this fact purely repeats the proof of Theorem 2 in Gneiting et al. (2006), adding a constant. Then we apply Theorem 3.17 in $\mathbb{R}$ to the function (4.20). The conditions (i)-(ii) in Theorem 3.17 in $\mathbb{R}$ are obviously satisfied. It remains to check the positive semidefiniteness of the matrix (3.11) for almost all $r \ge 0$. Clearly, it holds in $(0, 1)$ by the construction of (4.20) and the conditions of the theorem. We assume without loss of generality that $R_{12} \le R_{11} \le R_{22}$. For the positive definiteness of the matrix (3.11) in $(1, R_{12})$ we need the following inequality to hold

$$\rho^2 \le \inf_{1<r<R_{12}} \frac{\chi''_{11}(r)\chi''_{22}(r)}{(\chi''_{12}(r))^2} = \frac{b_{11}b_{22}}{b_{12}^2} = \frac{\psi''_{11}(d)\psi''_{22}(d)}{(\psi''_{12}(d))^2}.$$

This inequality holds automatically by the conditions of the theorem. Since $b_{ij} > 0$ and inequality (4.24) holds, the matrix (3.11) is positive semidefinite for $R_{12} < r < R_{11}$. Inequality (4.24) guarantees that the matrix (3.11) is identically zero for $r > R_{11}$. □

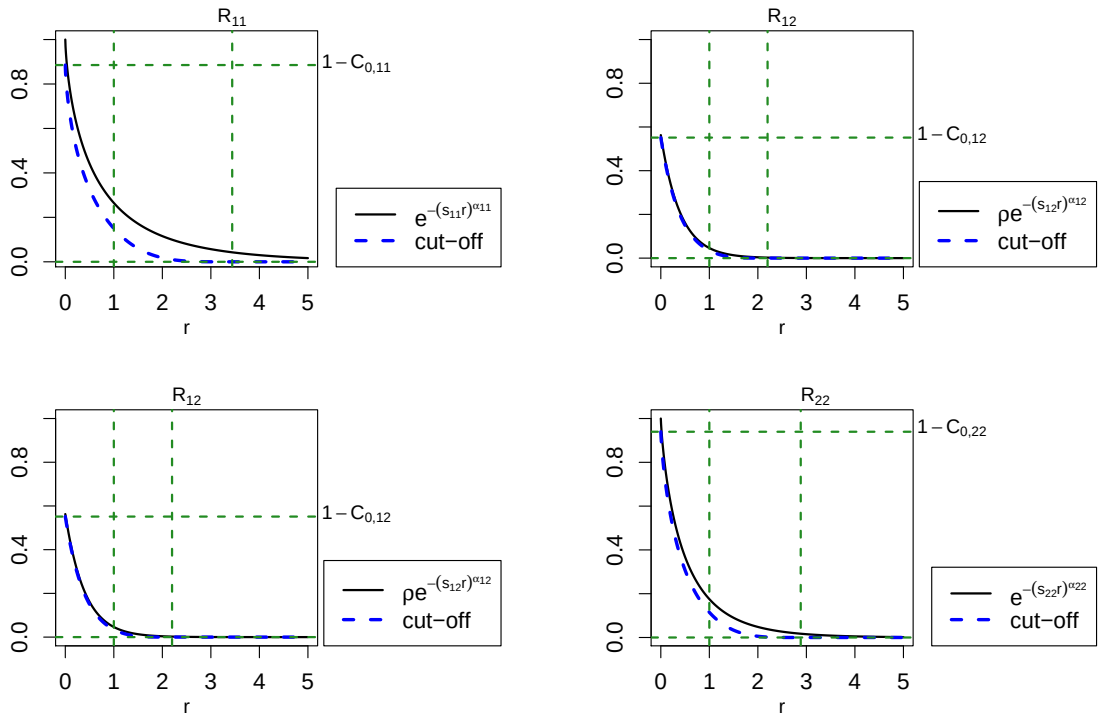

Figure 4.8: Bivariate powered exponential covariance function and its cut-off version. The parameters are $\alpha_{11} = 0.7$, $\alpha_{12} = 1$, $\alpha_{22} = 0.8$, $s_{11} = 1.5, s_{12} = 2.5, s_{22} = 2$, $\sigma_1 = \sigma_2 = 1$, and $\rho = 0.56$. The dashed blue line and the solid black line are identical on $[0, 1]$ up to a shifting constant.

Theorem 4.16
Let ψ_{ij}, $i, j = 1, 2$, satisfy the conditions of Theorem 3.17 in $\mathbb{R}^3$. Additionally assume that each ψ_{ij} satisfy the conditions of Theorem 4.3. Then the matrix-valued function (4.20) *defined by* (4.21), (4.22), *and* (4.23) *is positive definite in $\mathbb{R}^3$ if*

$$R_{12} \leq \min\{R_{11}, R_{22}\} \tag{4.24}$$

and

$$\rho^2 \leq \frac{b_{11}b_{22}}{b_{12}^2} \frac{(R_{11}^2 - 1)(R_{22}^2 - 1)}{(R_{12}^2 - 1)^2}. \tag{4.25}$$

Proof. The proof is analogous to the proof of Theorem 4.15. First we note that each $\chi_{ij}(r)$, $i, j = 1, 2$ is a positive definite function in $\mathbb{R}^3$, so that (2.3) is well defined. The proof of this fact purely repeats the proof of Theorem 2 in Gneiting et al. (2006), replacing the polynomial of degree 2 by the polynomial of degree 4 and adding a constant. Then we apply Theorem 3.17 in $\mathbb{R}^3$ to the function (4.20). The conditions (i)-(ii) in Theorem 3.17 in $\mathbb{R}$ are obviously satisfied. It remains to check the positive semidefiniteness of the matrix (3.12) for almost all $r \geq 0$. Clearly, it holds in $(0, 1)$ by the construction of (4.20) and the conditions of the theorem. We assume without loss of generality that $R_{12} \leq R_{11} \leq R_{22}$. For the positive definiteness of

the matrix (3.12) in $(1, R_{12})$ we need the following inequality to hold

$$\begin{aligned}\rho^2 &\leq \inf_{1<r<R_{12}} \frac{(\chi_{11}''(r) - r\chi_{11}'''(r))(\chi_{22}''(r) - r\chi_{22}'''(r))}{(\chi_{12}''(r) - r\chi_{12}'''(r))^2} \\ &= \frac{b_{11}b_{22}}{b_{12}^2} \inf_{1<r<R_{12}^2} \frac{(R_{11}^2 - r)(R_{22}^2 - r)}{(R_{12}^2 - r)^2}.\end{aligned}$$

Taking the derivative of $g(r) = (r - R_{11}^2)(r - R_{22}^2)/(r - R_{12}^2)^2$, we obtain that g is increasing on $[1, R_{12}^2)$ and takes its minimum at the left endpoint $r = 1$. Thus, the inequality (4.25) ensures the positive definiteness of the matrix (3.12) in $(1, R_{12})$. The proof of the positive definiteness of the matrix (3.12) in $(R_{12}, R_{11}) \cup (R_{11}, \infty)$ is similar to the proof of this fact in Theorem 4.15. □

Remark 4.17
Let $Y(x) = (Y_1(x), Y_2(x))$ be a centered bivariate Gaussian random field with a covariance matrix given by equations (4.20) to (4.22) and such that $0 \leq C_{0,ij} < 1$, $i, j = 1, 2$, and $\rho^2 C_{0,12}^2 \leq C_{0,11}C_{0,22}$. Let X_1, X_2 be spatially constant random variables, which are independent of $Y_1(x)$ and $Y_2(x)$ and have a bivariate normal distribution with zero mean and the following covariance matrix

$$\begin{bmatrix} C_{0,11} & \rho C_{0,12} \\ \rho C_{0,12} & C_{0,22} \end{bmatrix}.$$

Then on the grid G we have

$$\begin{aligned}cov\left(Y_1(x) + X_1, Y_2(0) + X_2\right) &= cov\left(Y_1(x), Y_2(0)\right) + cov(X_1, X_2) \\ &= \rho\psi_{12}(r) - \rho C_{0,12} + \rho C_{0,12} \\ &= \rho\psi_{12}(r),\end{aligned}$$

where $r = \|x\|$. Note that Theorem 4.16 neither guarantees $C_0 \in [0, 1)$ nor $\rho^2 C_{0,12}^2 \leq C_{0,11}C_{0,22}$. However, in our numerical simulations, we could not find any counterexamples.

The two upper plots in Movies 4.1 and 4.2 illustrate simulations from the bivariate powered exponential covariance model and bivariate Matérn covariance model, respectively, using cut-off circulant embedding technique for the bivariate fields. The covariance functions are shown in the three lower plots. The simulations were performed in R (R Core Team, 2018) with the **RandomFields** package (Schlather et al., 2017).

4.5 Discussion

In this chapter we improved and extended the cut-off circulant embedding technique for the univariate and multivariate Gaussian random fields. The idea of shifting the covariance function by subtracting a constant allows us to simulate univariate fields with a smaller simulation window than in the original cut-off embedding. Cut-off circulant embedding, originally formulated for simulating stationary fields on a grid, can be also applied to locally stationary fields, since it requires only certain convexity conditions to hold. We reformulate the cut-off embedding techniques for variograms and apply them to the new parametric variogram model, proposed by Schlather (2014). The model allows for the smooth parametrization between the bounded and unbounded variograms. Our modified cut-off technique allows us to exploit the circulant

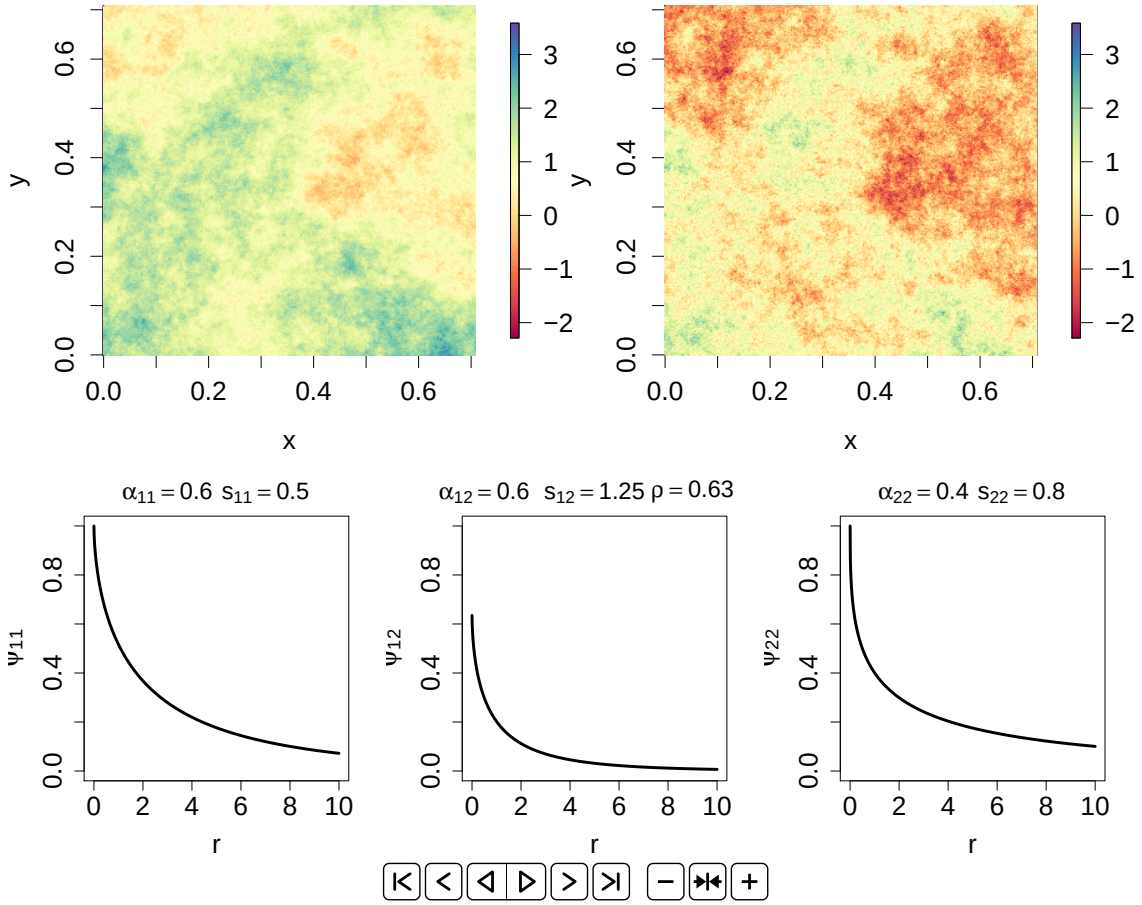

Movie 4.1: Simulations from the bivariate powered exponential model by means of the bivariate cut-off circulant embedding techniqueand the corresponding covariance structure.

embedding method to simulate the fields with the bounded and unbounded variograms for a certain parameter set. By means of the extended cut-off technique based on Theorem 4.9 we can simulate smoother fields than in Gneiting et al. (2006). However, when α in the powered exponential or the generalized Cauchy covariance approaches to two, the construction 4.11 is not guaranteed to be positive definite and the circulant embedding algorithm fails. The improvement of the cut-off algorithm is left for further research.

In the bivariate cut-off method the additional shifting constants allow us to continue the covariance functions with polynomials of degree four outside the grid smoothly enough, so that we can prove the positive definiteness of the modified function by Theorem 3.17 and the criteria of the Pólya type. Therefore, the smoothness of the simulated bivariate fields is limited. The smoothness parameters in the bivariate powered exponential and the bivariate generalized Cauchy models cannot exceed one. Finding a construction permitting smoother covariance functions is left for future research.

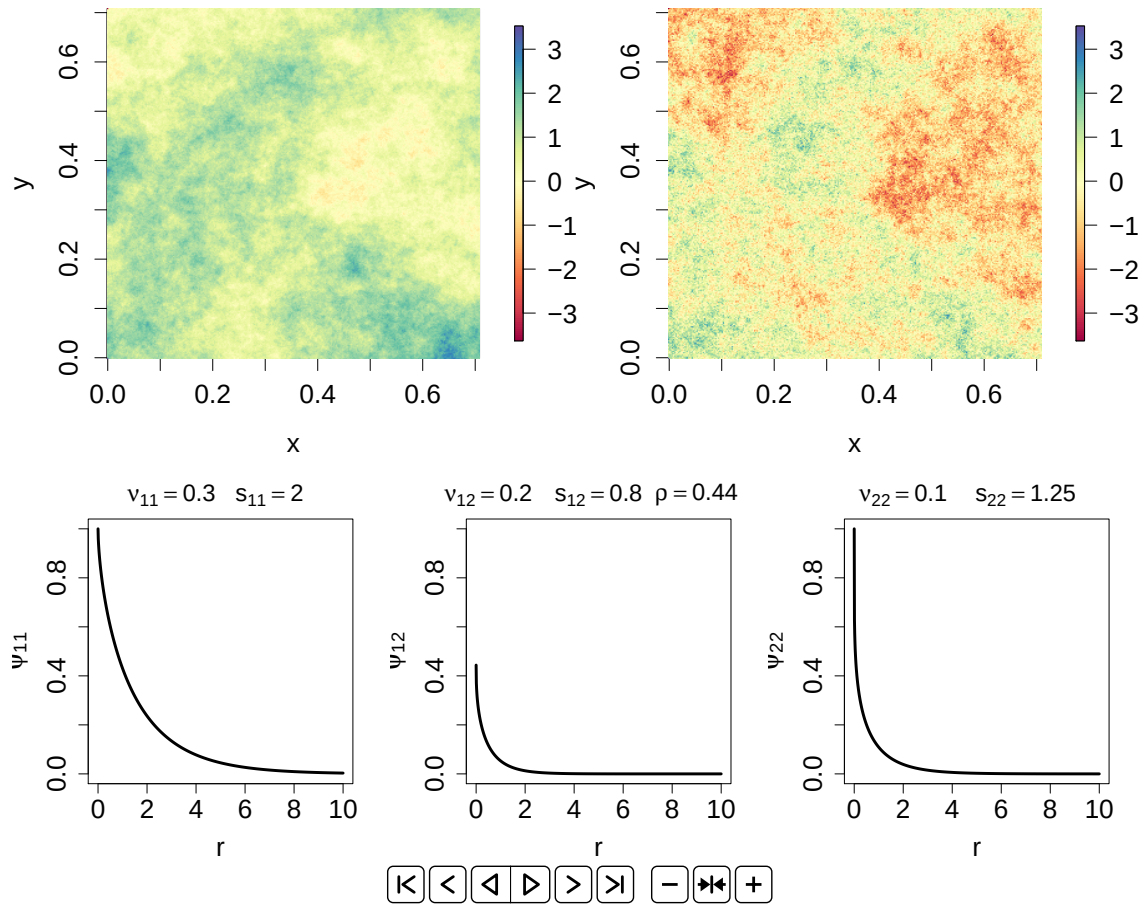

Movie 4.2: Simulations from the bivariate Matérn model by means of the bivariate cut-off circulant embedding techniqueand the corresponding covariance structure.

5 Data analysis with bivariate covariance models

5.1 Data example: content of copper and zinc in Swiss Jura

The classical geostatistical dataset Jura from Pierre Goovaerts' book (Goovaerts and Goovaerts, 1997) is provided by the package **gstat** (Pebesma (2004), Gräler et al. (2016)). It contains concentrations of seven heavy metals (cadmium, cobalt, chromium, copper, nickel, lead and zinc) in the topsoil. In this section we analyze the measurements of copper and zinc. The topsoil of the 14.5 km^2 region in Swiss Jura was sampled on a square grid at 250 m intervals with additional nesting with distances of 100 m, 40 m, 16 m and 6 m (Webster et al., 1994). The basic grid consists of 207 nodes, out of which 38 nodes were selected for nesting. Starting from each of these 38 nodes, the first location was chosen 100 m away in a random direction. The second location was chosen 40 m away from the first one again in a random direction. In a similar way the third and the forth locations were picked out, see Figure 5.1 for the points layout. For more details on the sampling scheme and its statistical impact see Atteia et al. (1994), Webster et al. (1994) and Chapters 2.3.1 and 4.1.1 in Goovaerts and Goovaerts (1997). The content of zinc and copper is measured in parts per million (ppm), which means that the data are compositional, i.e. contain only relative information and range from 0 to 10^6. However, since the concentrations of copper and zinc are low (maxiumum 166.4 ppm for copper and 259.8 ppm for zinc), we analyze the dataset in a non-compositional way, following Pebesma (2017) and Goovaerts and Goovaerts (1997), rather then employ a compositional approach (Aitchison (1982), Pawlowsky-Glahn and Buccianti (2011), and Pawlowsky-Glahn and Egozcue (2006)).

The measurements at 359 locations are divided into a training set (259 locations) and a validation set (100 locations). The training set consists of the grid points and the nested points, while the validation set contains only the grid points. We fit several bivariate covariance models to the training set and compare the models performance on the validation set.

Following Webster et al. (1994) we first take the log-transform of the metals concentration and then subtract the mean values of the logarithms. Figure 5.1 shows the transformed concentrations of copper and zinc. To asses the normality of the data, we examine one and two dimensional distributions. Shapiro-Wilk test does not reject the hypothesis that marginal distributions of zinc and copper are univariate normal at significance level 0.05. QQ-plots in Figures 5.2 and 5.3 for marginal distributions of copper and zinc also suggest that they are close to normal. The chi-squared QQ-plot in Figure 5.4 does not go against the bivariate normal distribution of the colocated data, neither rejects the Royston's test the bivariate normality at significance level 0.05. Further we assume that the data stem from a bivariate Gaussian process with zero mean.

The colocated empirical correlation of the data is 0.62, therefore it is reasonable to fit a bivariate covariance model. Covariance functions, which are not differentiable at the origin, are often used in geostatistics, see for example Goovaerts (1999), Journel (1974), Lark et al. (2006), Oliver and Webster (2014). Before fitting bivariate covariance models to the data, we

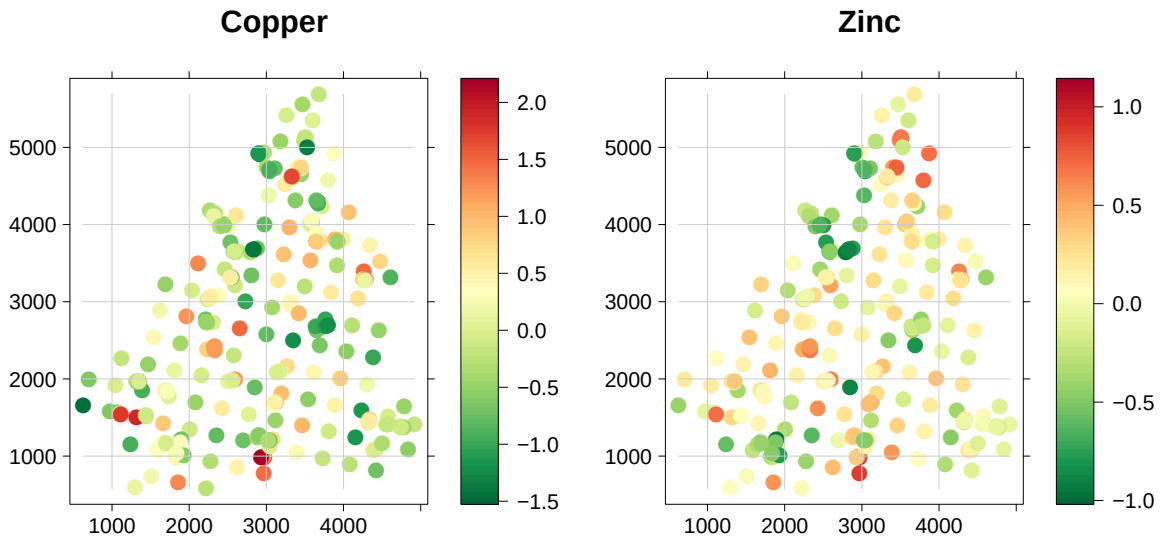

Figure 5.1: Concentration of copper and zinc in the topsoil.

fit a univariate exponential model to copper and zinc observations separately in order to see if the condition $\alpha_{ii} \in (0, 1]$, $i = 1, 2$ in the bivariate powered exponential covariance model is restrictive for this dataset. To account for measurement error we add the nugget effects to the univariate powered exponential models

$$C_C(r) = \sigma_C^2 e^{-(s_C r)^{\alpha_C}} + \tau_C^2 \mathbb{1}(r = 0),$$
$$C_Z(r) = \sigma_Z^2 e^{-(s_Z r)^{\alpha_Z}} + \tau_Z^2 \mathbb{1}(r = 0),$$

where $r > 0$, $\alpha_C, \alpha_Z \in (0, 2]$, and $\sigma_C, \sigma_Z, \tau_C, \tau_Z, s_C, s_Z > 0$. Subscripts C and Z refer for copper and zinc, respectively. The maximum likelihood estimates of parameters for the univariate powered exponential model applied to the copper and zinc data are shown in the first line of Table 5.1. The fit suggests that the smoothness parameters α_C and α_Z for copper and zinc, respectively, are less than one. Copper and zinc have different scale parameters, $1/s_C = 94.8$ and $1/s_{s_Z} = 188.6$, therefore a flexible bivariate model is needed. Our full bivariate powered exponential covariance model is defined by

$$C_C(r) = \sigma_C^2 e^{-(s_C r)^{\alpha_C}} + \tau_C^2 \mathbb{1}(r = 0),$$
$$C_Z(r) = \sigma_Z^2 e^{-(s_Z r)^{\alpha_Z}} + \tau_Z^2 \mathbb{1}(r = 0),$$

and

$$C_{CZ}(r) = C_{ZC}(r) = \rho_{CZ} \sigma_C \sigma_Z e^{-(s_{CZ} r)^{\alpha_{CZ}}},$$

where $\alpha_C, \alpha_Z \in (0, 1]$, $\alpha_{CZ} \in (0, 2]$, $s_C, s_Z, s_{CZ} > 0$ and $|\rho_{CZ}| < 1$ satisfy the conditions of Theorem 3.20 and $\sigma_C, \sigma_Z, \tau_C, \tau_Z > 0$. The maximum likelihood estimates of the full bivariate powered exponential model agree with the independent univariate estimates, see Table 5.1. The copper and zinc standard deviations are $\sigma_C = 0.70$ and $\sigma_Z = 0.36$ respectively. There are nugget effects for copper ($\tau_C = 0.04$) and for zinc ($\tau_C = 0.07$). The values of estimated smoothness parameters $\alpha_C = 0.74$ and $\alpha_C = 0.77$ are closer to each other than in the independent

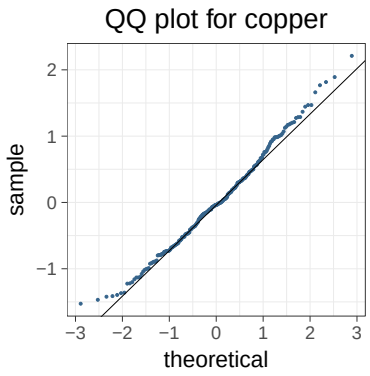

Figure 5.2: QQ plot for copper concentrations

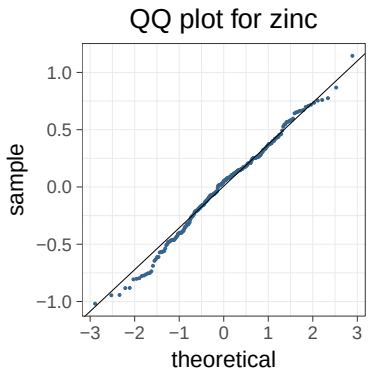

Figure 5.3: QQ plot for zinc concentrations

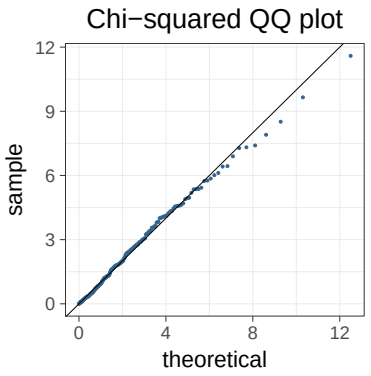

Figure 5.4: Chi-squared QQ-plot for copper and zinc concentrations

Table 5.1: Maximum likelihood estimates of parameters for bivariate powered exponential model applied to the copper and zinc data.

Model	σ_C	σ_Z	α_C	α_Z	α_{CZ}	$1/s_C$	$1/s_Z$	$1/s_{CZ}$	ρ_{CZ}	τ_C	τ_Z
Independent	0.69	0.35	0.77	0.90	-	94.8	188.6	-	-	0.09	0.1
Full	0.7	0.36	0.74	0.77	0.77	90.4	188.5	114.6	0.63	0.04	0.07
Parsimonious	0.7	0.36	0.76	0.76	0.76	91.0	197.5	117.6	0.62	0.07	0.07

model. This is probably due to the positive definiteness restrictions in Theorem 3.20, which exclude some parameter combinations with very distinct scale and smoothness parameters and a high correlation, which is estimated as $\rho_{LC} = 0.63$. The estimate of ρ_{LC} agrees well with the colocated empirical correlation.

In order to assess a typical finite sample variability in the estimation of the bivariate powered exponential model we perform a small simulation study. Specifically, we generate 500 realizations from the full bivariate powered exponential model with parameter values of Table 5.1. The simulations are done on a 50 by 50 square grid of the area 14.6 km^2. For each realization, we choose randomly 259 points of the grid and fit the bivariate powered exponential model by maximum likelihood. The fitted covariance functions are shown in Figure 5.5. The average of all 500 covariances (red dashed line) is close to the original model (solid green line). The parameters estimates are summarized by the boxplots in Figure 5.6. The medians of estimates of σ_C, σ_Z, α_C, α_Z, ρ_{CZ}, s_C, s_Z, s_{CZ} are very close to their true values.

Following Gneiting et al. (2010), we extend these finite sample results with a view towards the infill and increasing domain spatial asymptotics. For infill asymptotics, we but doubled the number of sample locations (to 518) in the same grid. For increasing domain asymptotics, we extended the domain in both coordinate directions by a factor of $\sqrt{2}$ and doubled the number of sample locations (to 518), so that the sampling density does not change. For simplicity we did not include nesting locations. Fitted covariance functions and the boxplots of the corresponding estimates are also included in Figures 5.5 and 5.6, respectively. Generally speaking, parameter estimates are seen to be tighter under both asymptotic frameworks.

Since there is no strong evidence that α_C, α_Z, α_{CZ} are distinct for the full bivariate powered exponential model, we fit a parsimonious bivariate powered exponential model with $\alpha_C = \alpha_L =$

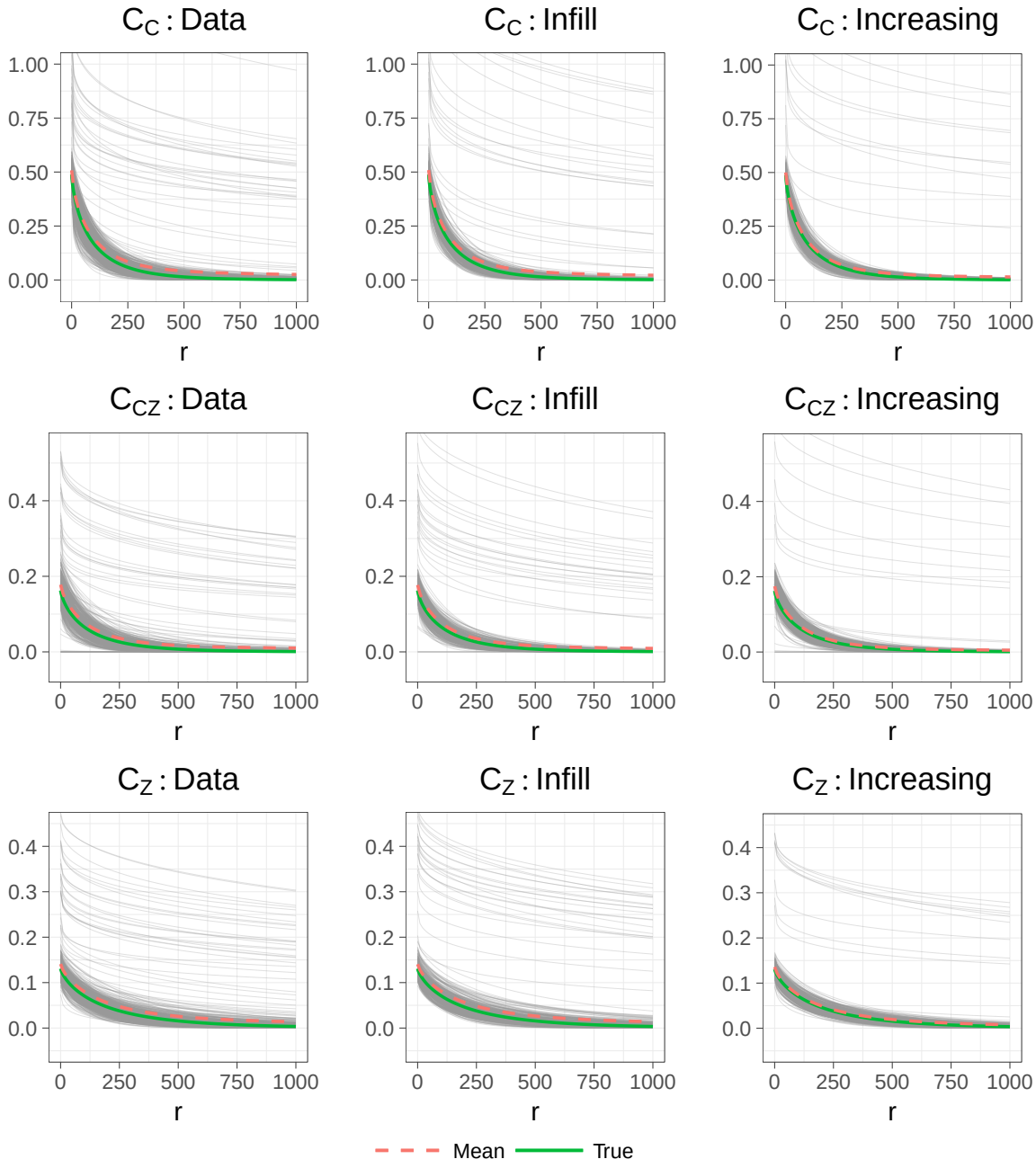

Figure 5.5: Fitted bivariate powered exponential covariance models for 500 simulated bivariate random fields. The bold solid line is the original covariance model, with which the fields were simulated, the dashed line is the average of 500 fitted bivariate powered exponential models.

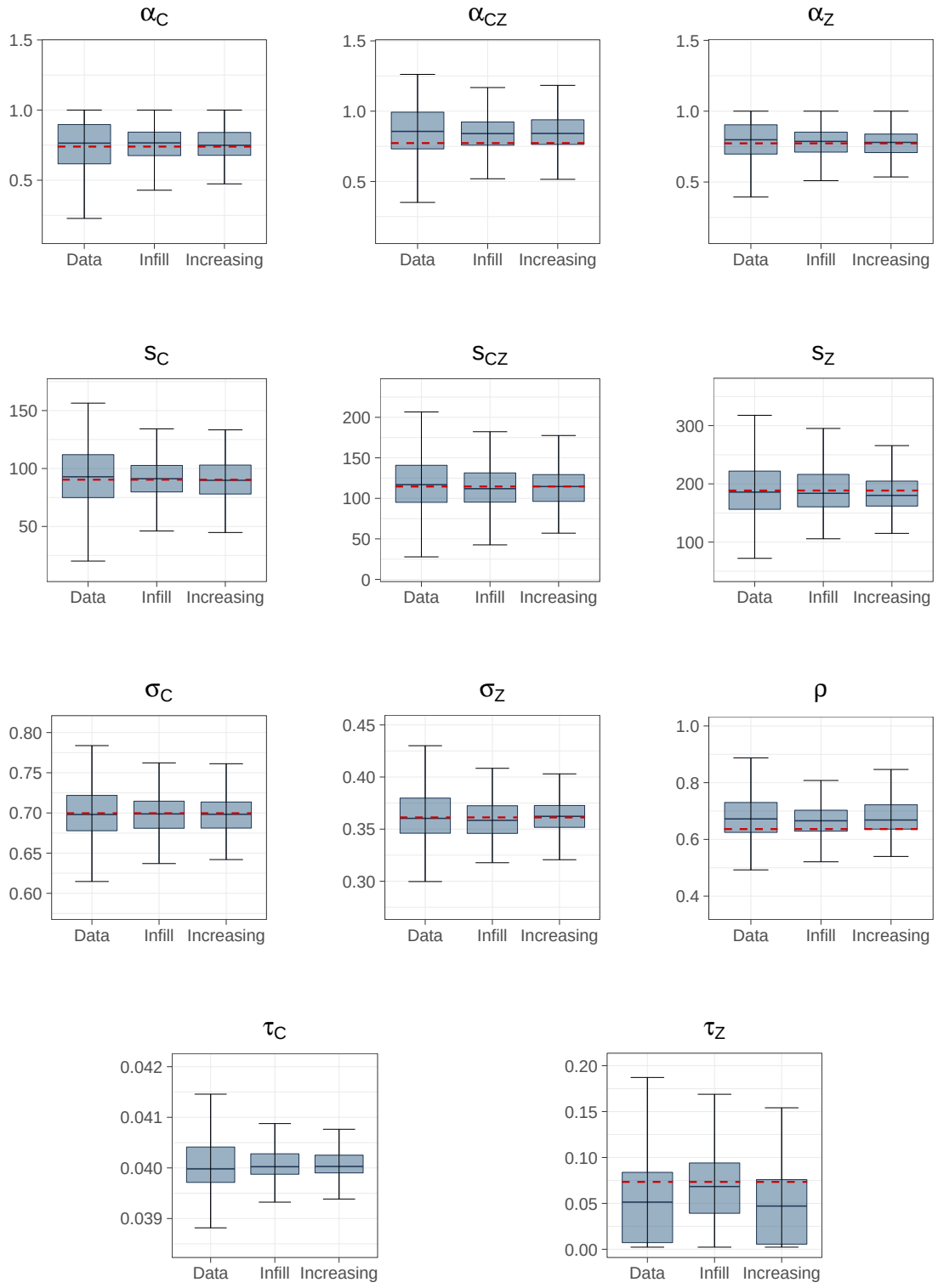

Figure 5.6: Results of the simulation study for the bivariate powered exponential model, summarized by boxplots of the ML estimates for σ_C, σ_Z, ρ_{CZ}, α_C, α_{CZ}, α_Z, s_C, s_Z, s_{CZ}, τ_C, τ_Z. The boxes range from the lower to the upper quartile, and the whiskers extend to the most extreme data point that is no more than 1.5 times the interquartile range from the box. The red dashed horizontal lines are at the true values.

Table 5.2: Maximum likelihood estimates of parameters for the bivariate Matérn model applied to the copper and zinc data.

Model	σ_C	σ_Z	ν_C	ν_Z	ν_{CZ}	$1/s_C$	$1/s_Z$	$1/s_{CZ}$	ρ_{CZ}	τ_C	τ_Z
Full	0.7	0.37	0.3	0.28	0.32	155.1	337.8	185.7	0.66	0.02	0.01

$\alpha_{LC} = \alpha$. In addition, we set $\tau_C = \tau_L = \tau$, since the medians of their estimates close to each other. Thus, our parsimonious bivariate powered exponential model becomes

$$C_C(r) = \sigma_C^2 e^{-(s_C r)^\alpha} + \tau^2 \mathbb{1}(r = 0),$$
$$C_Z(r) = \sigma_Z^2 e^{-(s_Z r)^\alpha} + \tau^2 \mathbb{1}(r = 0),$$

and

$$C_{CZ}(r) = C_{ZC}(r) = \rho_{CZ}\sigma_C\sigma_Z e^{-(s_{CZ} r)^\alpha},$$

where $\alpha \in (0, 1]$, $s_C, s_Z, s_{CZ} > 0$ and $|\rho_{CZ}| < 1$ satisfy the conditions of Theorem 3.20 and $\sigma_C, \sigma_Z, \tau > 0$. The parameter estimates of the parsimonious bivariate powered exponential model agree well with those of the full bivariate powered exponential model, see Table 5.1. The likelihood of the parsimonious model is only 0.05 smaller than the likelihood of the full model, see Table 5.4.

Next, we fit the full bivariate Matérn model, i.e.

$$C_C(r) = \sigma_C^2 M_{\nu_C}(s_C r) + \tau_C^2 \mathbb{1}(r = 0),$$
$$C_Z(r) = \sigma_Z^2 M_{\nu_Z}(s_Z r) + \tau_Z^2 \mathbb{1}(r = 0),$$

and

$$C_{CZ}(r) = C_{ZC}(r) = \rho_{CZ}\sigma_C\sigma_Z M_{\nu_{CZ}}(s_{CZ} r),$$

where $\nu_L, \nu_C, \nu_{CZ}, s_C, s_Z, s_{CZ}, \sigma_C, \sigma_Z, \tau > 0$, $|\rho_{CZ}| \leq 1$, $M_\nu(sr) = \frac{2^{1-\nu}}{\Gamma(\nu)}(sr)^\nu K_\nu(sr)$, $K_\nu(r)$ is the modified Bessel function of the second kind and Γ is the gamma function. The ML estimates are displayed in Table 5.2. The estimates of the variance are close to those in the bivariate powered exponential model, whereas the estimated nugget effects are smaller than those in the bivariate powered exponential model. From the estimates of the smoothness parameters $\nu_C = 0.3$ and $\nu_{CZ} = 0.28$ we get the estimates of the fractal dimensions of zinc and copper fields, which are 2.7 and 2.72. The corresponding estimates of fractal dimension in the bivariate powered exponential models are 2.63 for copper and 2.62 for zinc in the full model and 2.62 in the parsimonious.

The last model that we fit is the linear model of coregionalization with two latent powered exponential fields. As in the previous cases, we augment the model with nugget effects. We choose two latent fields in order to have a comparable number of parameters to estimate. The covariance function thus becomes

$$C_C(r) = b_{11}^2 e^{-(s_1 r)^{\alpha_1}} + b_{12}^2 e^{-(s_2 r)^{\alpha_2}} + \tau_C^2 \mathbb{1}(r = 0),$$
$$C_Z(r) = b_{21}^2 e^{-(s_1 r)^{\alpha_1}} + b_{22}^2 e^{-(s_2 r)^{\alpha_2}} + \tau_Z^2 \mathbb{1}(r = 0),$$

and

$$C_{CZ}(r) = C_{ZC}(r) = b_{11}b_{21} e^{-(s_1 r)^{\alpha_1}} + b_{12}b_{22} e^{-(s_2 r)^{\alpha_2}}$$

Table 5.3: Maximum likelihood estimates of parameters for the LMC model applied to the copper and zinc data.

Model	b_{11}	b_{12}	b_{21}	b_{22}	α_1	α_2	$1/s_1$	$1/s_2$	τ_L	τ_C
LMC	0.68	0.1	0.18	0.31	0.78	0.79	91.32	240.04	0.1	0.07

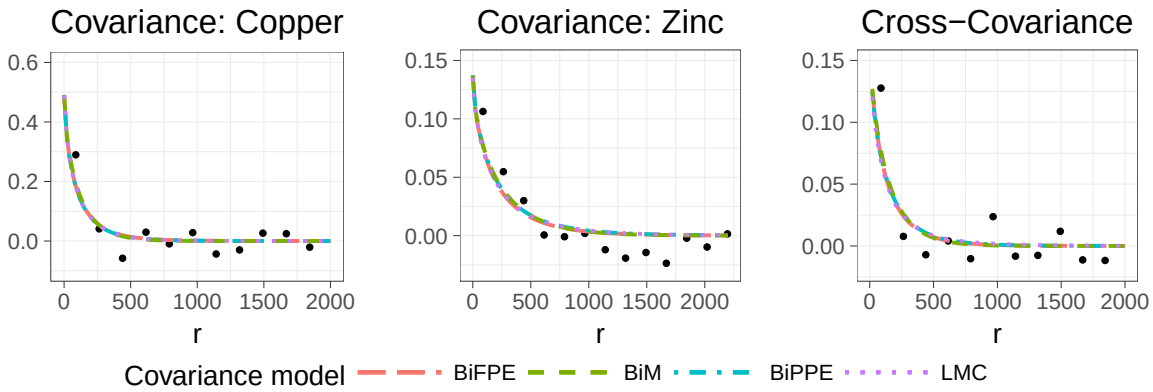

Figure 5.7: Empirical covariance and bivariate covariance functions for the copper and zinc data, with maximum likelihood fits under the full bivariate powered exponential model, (BiFPE; red long dashed line), the bivariate Matérn (BiW; green dashed line) , the parsimonious bivariate powered exponential model, (BiPPE; blue dashed dotted line), and the linear model of coregionalization (LMC; violet dotted line).

with $b_{11}, b_{21}, b_{12}, b_{22}, s_1, s_2 > 0$, $\alpha_1, \alpha_2 \in (0, 2]$. The ML estimates of the LMC model are displayed in the Table 5.3. Similarly to the previous models, the estimated smoothness parameters are close to each other, $\alpha_1 = 0.78$ and $\alpha_2 = 0.79$, whereas the scale parameters are clearly distinct, $1/s_1 = 91.32$, $1/s_2 = 240.04$. The estimated variances, which are defined by $\sqrt{b_{11}^2 + b_{12}^2} = 0.69$ for copper and $\sqrt{b_{21}^2 + b_{22}^2} = 0.35$ for zinc, agree well with the estimates in the bivariate powered exponential model and the bivariate Matérn model and so do the estimates of nugget effects.

Table 5.4 contains the comparison between the bivariate powered exponential, the bivariate Matérn, the independent powered exponential and the LMC fits. The full bivariate Matérn model achieves the highest likelihood. The parsimonious bivariate powered exponential model has the smallest value of AIC. Having the same number of parameters as the LMC, the parsimonious bivariate powered exponential model has a higher likelihood value. All bivariate models have higher likelihood and smaller value of AIC than the independent powered exponential model.

We compare predictive performance of the models on the validation set. First we take the logarithm of copper and zinc in the test set and then subtract the mean of logarithms of copper and zinc from the training set. At the test set locations we perform co-kriging to predict the values for copper and zinc. Then we calculate the mean absolute error (MAE), i.e. the average absolute error between the realization and the co-kriging point predictor. When we do not use the measurements of zinc from the test set for copper prediction, there is no gain in exploiting the bivariate models. The same holds for the zinc prediction without using copper values. Smaller MAE is achieved when the measurements of zinc concentrations is included for copper

Table 5.4: Comparison of the bivariate powered exponential, the bivariate Matérn, the independent powered exponential and the LMC models for copper and zinc data.

Model	Number of parameters	Log likelihood	AIC	MAE (copper)	MAE (zinc)
Full bivariate powered exponential	11	-181.42	384.84	0.5543	0.2315
Parsimonious powered exponential	8	-181.47	378.93	0.5550	0.2318
Full bivariate Matérn	11	-181.21	384.42	0.5593	0.2347
LMC	10	-181.59	383.19	0.5534	0.2292
Independent powered exponential	8	-245.6	507.22	0.5764	0.2742

prediction and vice versa. The results are summarized in Table 5.4. The bivariate models clearly outperform the independent model both in copper and zinc.

5.2 Implementation details

Theorem 3.20 in Section 3.4 determines the conditions on the parameter set of the bivariate powered exponential model which guarantee the positive definiteness in $\mathbb{R}^n$, $n \in \{1, 3\}$. These conditions set the boundaries for ρ_{LC} depending on given α_{11}, α_{22}, α_{12}, s_{11}, s_{22}, s_{12}. Moreover, parts (i)-(iv) of Theorem 3.20 state that the infimum in (3.22) can be positive only if $\alpha_{12} \geq \max\{\alpha_{11}, \alpha_{22}\}$. These restrictions lead to the correlated maximum likelihood estimates. In order to reduce the correlation of estimates and increase the speed of the parameters search, we reparametrise the model inside the **RandomFields** package, following the approach for the bivariate Matérn model. We introduce auxiliary parameters β_{red}, ρ_{red} and ρ_{max} such that

$$\alpha_{12} = \max\{\alpha_{11}, \alpha_{22}\} + \beta_{red}(2 - \max\{\alpha_{11}, \alpha_{22}\}),$$

where $\beta_{red} \in [0, 1]$ and

$$\rho = \rho_{red}\rho_{max},$$

where $|\rho_{red}| \in [0, 1]$ and $\rho_{max} = \alpha_{11}\alpha_{22}s_{11}^{\alpha_{11}}s_{22}^{\alpha_{22}}/(\alpha_{12}^2 s_{12}^{2\alpha_{12}}) \inf_{r>0} g(r)$ with

$$g(r) = \left[r^{\alpha_{11}+\alpha_{22}-2\alpha_{12}} e^{2(s_{12}r)^{\alpha_{12}} - (s_{11}r)^{\alpha_{11}} - (s_{22}r)^{\alpha_{22}}} \frac{q^{(n)}_{\alpha_{11},s_{11}}(r) q^{(n)}_{\alpha_{22},s_{22}}(r)}{(q^{(n)}_{\alpha_{12},s_{12}}(r))^2} \right].$$

When performing loglikelihood optimization we vary the parameters α_{11}, α_{22}, β_{red}, ρ_{red}, s_{11}, s_{22}, s_{12} and based on their values compute α_{12} and ρ. The parameters β_{red} and ρ_{red} are chosen independently of α_{11}, α_{22}, α_{12}, s_{11}, s_{22}, s_{12}. With this reparametrization any combination of values of $\alpha_{11} \in (0, 1]$, $\alpha_{22} \in (0, 1]$, $\beta_{red} \in [0, 1]$, $s_{11}, s_{22}, s_{12} > 0$, $\rho_{red} \in [-1, 1]$ leads to the valid bivariate powered exponential covariance model.

The calculation of ρ_{max} requires finding an infimum of the function $g(r)$. We are interested in positive values of ρ_{max} or, in other words, in cases (i)-(iv) of Theorem 3.20. Consider the behaviour of the function $g(r)$ at zero and at infinity provided that the conditions (i)-(iv) in Theorem 3.20 hold true. Then we have

$$\lim_{r\to\infty} g(r) = \infty.$$

Under condition (i) of Theorem 3.20 we have

$$\lim_{r\to 0} g(r) = 1.$$

Conditions (ii) - (iv) of Theorem 3.20 yield

$$\lim_{r\to 0} g(r) = \infty.$$

Thus, if the one of the conditions (ii) - (iv) of Theorem 3.20 holds, the function g attains its minimum in $(0, \infty)$ and if the conditions (i) of Theorem 3.20 holds, g attains its minimum in $[0, \infty)$. In general g is not unimodal on $[0, \infty)$, therefore we use the following heuristic algorithm to find the minimum. First we locate an interval which is likely to contain a global minimum. To do so we choose the starting points $r_m = 10^k$, $k \in \{-10, -9, \ldots, 10\}$, and repeat Algorithm 1 for each k or until $g_{min} = 0$ for some k. If for some $k \in \{-10, -9, \ldots, 10\}$ Algorithm 1 returned $g_{min} = 0$, we stop and set $\rho_{max} = 0$. If $g_{min} = -1$, we located an interval with a local maximum. We run again Algorithm 1 with a new starting point $r_m/2$. If $g_{min} > 0$ for several $k \in \{-10, -9, \ldots, 10\}$, we apply the golden-section search algorithm (Press et al., 1982) to the corresponding intervals in order to find the minimum. Then the smallest minimum is the value of ρ_{max}. We noticed that in the intervals, where g takes values less than 0.05, the algorithm often stops before finding a minimum. This happens when the function does not decrease fast enough in the neighborhood of the true minimum and the golden-section search algorithm fails to locate it, since its precision is limited, see Press et al. (1982) for more details. To avoid these situations, we set $\rho_{max} = 0$ if we came across a point r which guarantees that $\rho_{max} \leq 0.05$ while running Algorithm 1 or the golden-section search algorithm. From a practical perspective this is not a strict restriction, since the use of the bivariate model with such a low cross-correlation parameter is superfluous. For the sake of consistency, we choose $\varepsilon = 0.05$ in Algorithm 1.

Compute $r_l = r_m/2$, $r_r = 2r_m$. $g_{min} = 0$.
while $g(r_m) \geq \min\{g(r_r), g(r_l)\}$ **and** $\min\{g(r_m), g(r_l), g(r_r)\} > \varepsilon$ **do**
  if $g(r_m) \geq \max\{g(r_r), g(r_l)\}$ **then**
    $r_m = r_l$;
    $g_{min} = -1$;
    break;
  end
  if $g(r_l) \leq g(r_m)$ **then**
    $r_m = r_l$;
    $g_{min} = g(r_m) = g(r_l)$;
    $r_l = r_l/2$;
  end
  if $g(r_r) \leq g(r_m)$ **then**
    $r_m = r_r$;
    $g_{min} = g(r_m) = g(r_r)$;
    $r_r = 2r_r$;
  end
  if $\min\{g(r_m), g(r_l), g(r_r)\} \leq \varepsilon$ **then**
    $r_r = r_l = 0$;
    $g_{min} = 0$;
  end
end
return g_{min}, r_l, r_r;

Algorithm 1: Search for an interval which contains a local minimum

6 Bibliography

Abate, J. and W. Whitt (1992). The Fourier-series method for inverting transforms of probability distributions. *Queueing systems 10*(1-2), 5–87.

Adler, R. (1981). *The Geometry of Random Fields*. Chichester: John Wiley & Sons.

Aitchison, J. (1982). The statistical analysis of compositional data. *Journal of the Royal Statistical Society. Series B (Methodological)*, 139–177.

Apanasovich, T., M. Genton, and Y. Sun (2012). A valid Matérn class of cross-covariance functions for multivariate random fields with any number of components. *Journal of the American Statistical Association 107*(497), 180–193.

Apostol, T. (1974). *Mathematical Analysis*. Addison-Wesley series in mathematics. Addison-Wesley.

Arroyo, D. and X. Emery (2017). Spectral simulation of vector random fields with stationary Gaussian increments in d-dimensional Euclidean spaces. *Stochastic Environmental Research and Risk Assessment 31*(7), 1583–1592.

Atkinson, P., R. Webster, and P. Curran (1992). Cokriging with ground-based radiometry. *Remote Sensing of Environment 41*(1), 45–60.

Atteia, O., J. Dubois, and R. Webster (1994). Geostatistical analysis of soil contamination in the Swiss Jura. *Environmental Pollution 86*(3), 315–327.

Berrocal, V. J., A. E. Raftery, and T. Gneiting (2007). Combining spatial statistical and ensemble information in probabilistic weather forecasts. *Monthly Weather Review 135*(4), 1386–1402.

Bingham, N. H. (1972). A Tauberian theorem for integral transforms of Hankel type. *Journal of the London Mathematical Society. Second series 2*(3), 493–503.

Bochner, S. (1955). *Harmonic Analysis and the Theory of Probability*. Berkeley and Los Angeles: University of California Press.

Chan, G. and A. T. A. Wood (1999). Simulation of stationary Gaussian vector fields. *Statistics and computing 9*(4), 265–268.

Chilès, J. and P. Delfiner (1999). *Geostatistics: modeling spatial uncertainty*. Wiley series in probability and statistics. Wiley.

Cramer, H. (1940). On the theory of stationary random processes. *Annals of Mathematics 41*(1), 215–230.

Cressie, N. (1993). *Statistics for Spatial Data*. Wiley.

Cressie, N. and A. Zammit-Mangion (2016). Multivariate spatial covariance models: a conditional approach. *Biometrika 103*(4), 915–935.

Daley, D. J., E. Porcu, and M. Bevilacqua (2015). Classes of compactly supported covariance functions for multivariate random fields. *Stochastic Environmental Research and Risk Assessment 29*(4), 1249–1263.

Dietrich, C. R. and G. N. Newsam (1997). Fast and exact simulation of stationary Gaussian processes through circulant embedding of the covariance matrix. *SIAM Journal on Scientific Computing 18*(4), 1088–1107.

Du, J. and C. Ma (2013). Vector random fields with compactly supported covariance matrix functions. *Journal of Statistical Planning and Inference 143*(3), 457–467.

Emery, X., D. Arroyo, and E. Porcu (2016). An improved spectral turning-bands algorithm for simulating stationary vector Gaussian random fields. *Stochastic environmental research and risk assessment 30*(7), 1863–1873.

Feldmann, K., M. Scheuerer, and T. L. Thorarinsdottir (2015). Spatial postprocessing of ensemble forecasts for temperature using nonhomogeneous Gaussian regression. *Monthly Weather Review 143*(3), 955–971.

Feller, W. (1971). *An Introduction to Probability Theory and Its Applications. Vol 2.* Wiley.

Gaspari, G. and S. E. Cohn (1999). Construction of correlation functions in two and three dimensions. *Quarterly Journal of the Royal Meteorological Society 125*(554), 723–757.

Gel, Y., A. E. Raftery, and T. Gneiting (2004). Calibrated probabilistic mesoscale weather field forecasting: the geostatistical output perturbation method. *Journal of the American Statistical Association 99*(467), 575–583.

Genton, M. G. and W. Kleiber (2015). Cross-covariance functions for multivariate geostatistics. *Statistical Science 30*(2), 147–163.

Gikhman, I. I. and A. V. Skorokhod (2004). *The Theory of Stochastic Processes: I.* Springer Berlin Heidelberg.

Gneiting, T. (1999). Radial positive definite functions generated by Euclid's hat. *Journal of Multivariate Analysis 69*(1), 88–119.

Gneiting, T. (2000). Power-law correlations, related models for long-range dependence and fast simulation. *Journal of Applied Probability 37*, 1104–1109.

Gneiting, T. (2001). Criteria of Pólya type for radial positive definite functions. *Proceedings of the American Mathematical Society 129*(8), 2309–2318.

Gneiting, T. (2002). Compactly supported correlation functions. *Journal of Multivariate Analysis 83*(2), 493–508.

Gneiting, T., W. Kleiber, and M. Schlather (2010). Matérn cross-covariance functions for multivariate random fields. *Journal of the American Statistical Association 105*(491), 1167–1177.

Gneiting, T., Z. Sasvári, and M. Schlather (2001). Analogies and correspondences between variograms and covariance functions. *Advances in Applied Probability 33*, 617–630.

Gneiting, T. and M. Schlather (2004). Stochastic models that separate fractal dimension and the Hurst effect. *SIAM review 46*, 269–282. MR2114455.

Gneiting, T., H. Ševčíková, D. B. Percival, M. Schlather, and Y. Jiang (2006). Fast and exact simulation of large Gaussian lattice systems in $\mathbb{R}^2$: exploring the limits. *Journal of Computational and Graphical Statistics 15*(3), 483–501.

Goovaerts, P. (1999). Geostatistics in soil science: state-of-the-art and perspectives. *Geoderma 89*(1), 1–45.

Goovaerts, P. and D. Goovaerts (1997). *Geostatistics for Natural Resources Evaluation*. Applied geostatistics series. Oxford University Press.

Goulard, M. and M. Voltz (1992). Linear coregionalization model: tools for estimation and choice of cross-variogram matrix. *Mathematical Geology 24*(3), 269–286.

Gräler, B., E. Pebesma, and G. Heuvelink (2016). Spatio-temporal interpolation using gstat. *The R Journal 8*, 204–218.

Guillot, G. and F. Santos (2009). A computer program to simulate multilocus genotype data with spatially autocorrelated allele frequencies. *Molecular Ecology Resources 9*(4), 1112–1120.

Hansen, N. (2018). Asymmetrische Kreuzkovarianzfunktionen. Master's thesis, Universität Mannheim.

Helgason, H., V. Pipiras, and P. Abry (2011). Fast and exact synthesis of stationary multivariate Gaussian time series using circulant embedding. *Signal Processing 91*(5), 1123–1133.

Henderson, R., S. Shimakura, and D. Gorst (2002). Modeling spatial variation in leukemia survival data. *Journal of the American Statistical Association 97*(460), 965–972.

Hewer, R., P. Friederichs, A. Hense, and M. Schlather (2017). A Matérn-based multivariate Gaussian random process for a consistent model of the horizontal wind components and related variables. *Journal of the Atmospheric Sciences 74*(11), 3833–3845.

Journel, A. (1974). Geostatistics for conditional simulation of ore bodies. *Economic Geology 69*(5), 673–687.

Kent, J. and A. Wood (1997). Estimating the fractal dimension of a locally self-similar Gaussian process by using increments. *Journal of the Royal Statistical Society. Series B (Methodological)*, 679–699.

Kleiber, W. (2017). Coherence for multivariate random fields. *Statistica Sinica 27*, 1675–1697.

Koutsoyiannis, D. (2005). Uncertainty, entropy, scaling and hydrological stochastics. 2. Time dependence of hydrological processes and time scaling. *Hydrological Sciences Journal 50*(3).

Lantuejoul, C. (2001). *Geostatistical Simulation: Models and Algorithms*. Collezione legale Pirola. Springer Berlin Heidelberg.

Lark, R., B. Cullis, and S. Welham (2006). On spatial prediction of soil properties in the presence of a spatial trend: the empirical best linear unbiased predictor (E-BLUP) with REML. *European Journal of Soil Science 57*(6), 787–799.

Lark, R. and A. Papritz (2003). Fitting a linear model of coregionalization for soil properties using simulated annealing. *Geoderma 115*(3-4), 245–260.

Leonenko, N. (1999). *Limit Theorems for Random Fields with Singular Spectrum*. Mathematics and Its Applications. Springer Netherlands.

Li, M. and S. Lim (2008). Modeling network traffic using generalized Cauchy process. *Physica A: Statistical Mechanics and its Applications 387*(11), 2584–2594.

Lim, S. C. and L. P. Teo (2009). Gaussian fields and Gaussian sheets with generalized Cauchy covariance structure. *Stochastic Processes and their Applications 119*(4), 1325–1356.

Mandelbrot, B. and J. van Ness (1968). Fractional Brownian motions, fractional noises and applications. *SIAM review 10*, 422–437.

Mardia, K. and C. Goodall (1993). Spatial-temporal analysis of multivariate environmental monitoring data. *Multivariate environmental statistics 6*(76), 347–385.

Matheron, G. (1962). *Traité de Géostatistique Appliquée*, Volume 1. Paris: Technip.

Mery, N., X. Emery, A. Cáceres, D. Ribeiro, and E. Cunha (2017). Geostatistical modeling of the geological uncertainty in an iron ore deposit. *Ore Geology Reviews 88*, 336–351.

Moreva, O. and M. Schlather. Fast and exact simulation of univariate and bivariate Gaussian random fields. *Stat 7*(1), e188.

Moreva, O. and M. Schlather (2017). Covariance functions for bivariate Gaussian random fields. *arXiv preprint arXiv:1609.06561*.

Muniandy, S. and J. Stanslas (2008). Modelling of chromatin morphologies in breast cancer cells undergoing apoptosis using generalized Cauchy field. *Computerized Medical Imaging and Graphics 32*(7), 631–637.

Nolan, J. P. (2005). Multivariate stable densities and distribution functions: general and elliptical case. In *Deutsche Bundesbank's 2005 annual fall conference*.

Oliver, M. and R. Webster (2014). A tutorial guide to geostatistics: Computing and modelling variograms and kriging. *Catena 113*, 56–69.

Pawlowsky-Glahn, V. and A. Buccianti (2011). *Compositional Data Analysis: Theory and Applications*. Wiley.

Pawlowsky-Glahn, V. and J. Egozcue (2006). Compositional data and their analysis: an introduction. *Geological Society, London, Special Publications 264*(1), 1–10.

Pebesma, E. (2017). The meuse data set: a brief tutorial for the gstat R package.

Pebesma, E. J. (2004). Multivariable geostatistics in S: the gstat package. *Computers & Geosciences 30*, 683–691.

Pelletier, B., P. Dutilleul, G. Larocque, and J. W. Fyles (2009). Coregionalization analysis with a drift for multi-scale assessment of spatial relationships between ecological variables 2. Estimation of correlations and coefficients of determination. *Environmental and ecological statistics 16*(4), 467–494.

Porcu, E., D. J. Daley, M. Buhmann, and M. Bevilacqua (2013). Radial basis functions with compact support for multivariate geostatistics. *Stochastic environmental research and risk assessment 27*(4), 909–922.

Porcu, E. and V. Zastavnyi (2011). Characterization theorems for some classes of covariance functions associated to vector valued random fields. *Journal of Multivariate Analysis 102*(9), 1293–1301.

Press, W., S. Teukolsky, W. T. Vetterling, and B. Flannery (1982). *Numerical recipes in C*. Cambridge Univ Press.

R Core Team (2018). *R: A Language and Environment for Statistical Computing*. Vienna, Austria: R Foundation for Statistical Computing.

Rundel, C. W., M. B. Wunder, A. Alvarado, K. Ruegg, R. Harrigan, A. Schuh, J. Kelly, R. Siegel, D. DeSante, T. Smith, et al. (2013). Novel statistical methods for integrating genetic and stable isotope data to infer individual-level migratory connectivity. *Molecular ecology 22*(16), 4163–4176.

Scheuerer, M. (2010). Regularity of the sample paths of a general second order random field. *Stochastic Processes and their Applications 120*, 1879–1897.

Schlather, M. (2010). Some covariance models based on normal scale mixtures. *Bernoulli 16*(3), 780–797.

Schlather, M. (2014). A parametric variogram model bridging between stationary and intrinsically stationary processes. *arXiv preprint arXiv:1412.1914*.

Schlather, M., A. Malinowski, P. J. Menck, M. Oesting, and K. Strokorb (2015). Analysis, simulation and prediction of multivariate random fields with package RandomFields. *Journal of Statistical Software 63*(8), 1–25.

Schlather, M., A. Malinowski, M. Oesting, D. Boecker, K. Strokorb, S. Engelke, J. Martini, F. Ballani, and O. Moreva (2017). *RandomFields: Simulation and Analysis of Random Fields*. R package version 3.1.50.

Schlather, M. and O. Moreva (2017). A parametric model bridging between bounded and unbounded variograms. *Stat 6*(1), 47–52.

Schoenberg, I. J. (1938). Metric spaces and completely monotone functions. *Annals of Mathematics*, 811–841.

Sironvalle, M. A. (1980). The random coin method: Solution of the problem of the simulation of a random function in the plane. *Mathematical Geology 12*(1), 25–32.

Stein, M. L. (1999). *Interpolation of Spatial Data: Some Theory for Kriging*. Springer Series in Statistics. Springer New York.

Ver Hoef, J. M. and R. P. Barry (1998). Constructing and fitting models for cokriging and multivariable spatial prediction. *Journal of Statistical Planning and Inference 69*(2), 275–294.

Wackernagel, H. (2003). *Multivariate Geostatistics: An Introduction with Applications*. Springer Berlin Heidelberg.

Webster, R., O. Atteia, and J.-P. Dubois (1994). Coregionalization of trace metals in the soil in the Swiss Jura. *European Journal of Soil Science 45*(2), 205–218.

Wood, A. T. A. and G. Chan (1994). Simulation of stationary Gaussian processes in $[0, 1]^d$. *Journal of Computational and Graphical Statistics 3*(4), 409–432.

Yaglom, A. M. (1987). *Correlation Theory of Stationary and Related Random Runctions I, Basic Results*. Springer.

Zawadzki, J., P. Fabijańczyk, and H. Badura (2013). Estimation of methane content in coal mines using supplementary physical measurements and multivariable geostatistics. *International Journal of Coal Geology 118*, 33–44.

Hiermit erkläre ich, dass ich die vorliegende Arbeit mit dem Titel “Bivariate Gaussian random fields: models, simulation, and inference“ selbstständig angefertigt und keine anderen als die angegebenen Hilfsmittel verwendet habe.

Mannheim, den 28.05.2018 .....

Olga Moreva